PERCEPTUAL AUDIO CODING

THAT SCALES TO LOW BITRATES

BY

SRIVATSAN A KANDADAI, B.E., M.S.

A dissertation submitted to the Graduate School

in partial fulfillment of the requirements

for the degree

Doctor of Philosophy

Major Subject: Electrical Engineering

New Mexico State University

Las Cruces New Mexico

May 2007

"Scalable Audio Coding that Scales to Low Bitrates," a dissertation prepared by Srivatsan A. Kandadai in partial fulfillment of the requirements for the degree, Doctor of Philosophy, has been approved and accepted by the following:

Linda Lacey
Dean of the Graduate School

Charles D. Creusere
Chair of the Examining Committee

Date

Committee in charge:

Dr. Charles D. Creusere, Chair

Dr. Phillip De Leon

Dr. Deva K. Borah

Dr. Joseph Lakey

DEDICATION

I dedicate this work to my wife Ashwini for her understanding and my sister Madhu, I wish I could be as focused and meticulous as you guys.

ACKNOWLEDGMENTS

I would like to thank my advisor, Charles D. Creusere, for his encouragement, guidance and knowledge. Also, I wish to thank professors Phillip DeLeon and Deva Borah, who have taught me all my basics.

My thanks to all the NMSU students who helped in the subjective evaluations. Kumar Kallakuri and Rahul Vanam, their work on the objective metrics was a great help in this work. Vimal Thilak, for the long chats in the hallway. Finally, my family for supporting me through everything.

VITA

February 22, 1979	Born at Srirangam, Tamil Nadu, India
1996-2000	B.E., Bharathidasan University, Trichy, India
2001-2002	M.S., New Mexico State University Las Cruces, New Mexico
2003-2006	Ph.D., New Mexico State University Las Cruces, New Mexico

PROFESSIONAL AND HONORARY SOCIETIES

Institute of Electrical and Electronic Engineers (IEEE)

PUBLICATIONS [or Papers Presented]

1. Srivatsan Kandadai and Charles D. Creusere,"Scalable Audio Compression at Low Bitrates,"Submitted to IEEE Transations on Audio, Speech and Signal Processing

2. Srivatsan Kandadai and Charles D. Creusere,"Reverse Engineering and Repartitioning of Vector Quantizers Using Training Set Synthesis," Submitted to IEEE Transactions on Signal Processing

3. Srivatsan Kandadai and Charles D. Creusere,"Perceptually -Weighted Audio Coding that Scales to Extremely Low Bitrates," Proceedings of the Data Compression Conference DCC- 2006, Snowbird, UT, Mar. 2006, pp. 382-391

4. Srivatsan Kandadai and Charles D. Creusere, "Reverse Engineering Vector Quantizers for Repartitioned Vector Spaces," 39th Asilomar Conference on Signals Systems and Computers, Asilomar, CA, Nov. 2005

5. Srivatsan Kandadai,"Directional Multiresolutional Image Analysis," Mathematical Modeling and Analysis, T-7 LANL Summer Projects, Aug. 2004

6. Srivatsan Kandadai and Charles D. Creusere,"Reverse Engineering Vector Quantizers by Training Set Synthesis," 12th European Signal Processing Conference, EUSIPCO 2004, Vienna

7. Srivatsan Kandadai and Charles D. Creusere,"An Experimental Study of Object Detection in the Wavelet Domain," 37th Asilomar Conference on Signals, Systems and Computers, November 2003, Pacific Grove, CA

8. Srivatsan Kandadai,"Object Detection and Localization in The Wavelet Domain," 38th International Telemetering Conference, October 2002, San Diego, CA

FIELD OF STUDY

Major Field: Electrical Engineering

Signal Processing

ABSTRACT

SCALABLE AUDIO CODING THAT SCALES TO LOW BITRATES

BY

SRIVATSAN A. KANDADAI, B.S., M.S.

Doctor of Philosophy

New Mexico State University

Las Cruces, New Mexico, 2007

Dr. Charles D. Creusere, Chair

A perceptually scalable audio coder generates a bit-stream that contains layers of audio fidelity and is encoded in such a way that adding one of these layers enhances the reconstructed audio by an amount that is just noticeable by the listener. Such algorithms have applications like music on demand at variable levels of fidelity for 3G and 4G cellular radio since these standards support operation at different bit rates. While the MPEG-4 (Motion Picture Experts Group) natural audio coder can create scalable bit streams, its perceptual quality at low bit rates is poor. On the other hand, the nonscaleable transform domain weighted interleaved vector quantization (Twin VQ) performs well at low bit rates. As part

of this research, we present a technique to modify the Twin VQ algorithm such that it generates a perceptually scalable bit-stream with many fine-grained layers of audio fidelity. Using Twin VQ as our base ensures good perceptual quality at low bit rates (8 16k bits/second) unlike the bit slice arithmetic coding (BSAC) used in MPEG-4.

In this thesis, we first present the Twin VQ algorithm along with our technique of reverse engineering it. From the reverse engineered Twin VQ information, we build a scalable audio coder that performs as well as Twin VQ at low bitrates in human subjective testing. The residual signals generated by the successive quantization strategy developed here are shown to have statistical properties similar to independent Laplacian random variables, so we can therefore apply a lattice VQ that takes advantage of the spherically invariant random vectors (SIRV) generated by such random variables. In particular, the lattice VQ allows us more control over the layering of the bitstream at higher rates.

We also note that the layers of audio fidelity in the compressed representation must be stored and transmitted in a perceptually optimal fashion. To accomplish this, we make use of an objective metric that takes advantage of subjective test results and psychoacoustic principles to quantify audio quality. This objective metric is used to optimize the ordering of audio fidelity layers to provide a perceptually seamless transition from lower to higher bit rates.

CONTENTS

LIST OF TABLES

LIST OF FIGURES

1 INTRODUCTION

Scalable audio coding has many uses. One major application is real time audio streaming over non-stationary communication channels or in multicast environments. Services like music-on-demand could be facilitated over systems that support different bitrates to each user such as the recently developed 3G and 4G cellular systems. Digital radio systems might also use such scalable bit-rate formats to facilitate graceful degradation of audio quality over changing transmission channels rather than the sudden loss of signal that occurs with current systems when the signal power drops below some threshold. Furthermore, scalable bit streams might also be used to smooth quality fluctuations in audio that is broadcast over the internet: specifically, higher fidelity layers could be selectively removed by transport nodes as needed when congestion occurs so as to retain the best possible quality. The other advantage to having a scalable bit stream is in transmission of audio over wireless channels having a fixed digital bandwidth. Traditional (non-scalable) perceptually-transparent audio encoders have output bit rates that change with time, requiring that a sophisticated rate buffer with a feedback mechanism be used to control quantization in order to prevent rate buffer over or under flows. This complex rate buffer can be avoided altogether when using a finely scalable bit stream by simply transmitting as many layers of fidelity as fit the available channel capacity.

Many scalable audio coding schemes have been proposed [1]–[18]. Scalable audio compression schemes can be compared using three basic criteria; granularity, (i.e., minimum increase in bitrate to achieve the next fidility level), the minimum bitrate that can be supported, and seamless transition between successive bitrates. Commercial audio coders like Real 8.5 and WMA scale down to only 24 kbits/s and do not have much granularity. For example, WMA 8.0 scales down from 32 kbits/s to 16 kbits/s in a single step [15][16].

Some algorithms are designed to be efficient channel representations for scalable audio files, and does not study the problem of fidelity layering [4][12][13][14][18]. A new development in the field of scalable audio compression is the embedded audio coder (EAC) [11]. In this work the author combines psychoacoustic principles with entropy coding to create a technique called *implicit auditory masking*. Implicit auditory masking relies on a bit plane coding scheme and layers each bit plane by using a threshold calculated from the spectral envelope of the transform domain coefficients; it is similar to the embedded zero tree wavelet compression method used for images [19]. This method could not be used to compare with our technique because code for the algorithm is not publicly available.

Recently, a lot of attention has been given to audio coding algorithms that operate from scalable lossy to lossless audio quality [2][3][6]. These coding algorithms operate on bitstreams that range from 92 – 128 kb/s whereas, the research presented here deals with perceptually scalable audio compression at low bitrates

of 8 – 85 kb/s.

Despite the wide variety of coding schemes available, the MPEG-4 natural audio coder still represents the current state-of-the-art [20]. The MPEG-4 audio coder is a collection of different audio coding algorithms and can create scalable bit streams. Many rigorous core experiments and evaluations have been performed in the course of developing the MPEG-4 standard and it is the only framework for which detailed information is available. In the following work we draw comparisons with and apply some of the coding tools provided in the MPEG-4 standard. The MPEG-4 audio coder uses different techniques to achieve scalability, the simplest of which is to use a low rate coder to generate the first bit stream layer, and then compress the resulting error residuals using some other algorithm to generate layers of higher fidelity. This system, however, cannot generate more than two or three layers of audio fidelity [21]. Fine grained scalability is achieved within the MPEG-4 framework by using BSAC, either with the MPEG-4 scalable sampling rate (SSR) scheme or with the MPEG-2 advanced audio coder (AAC) [9][22] [20]. The SSR algorithm first applies a uniform 4-band cosine modulated filter bank with maximally decimated outputs to the input audio sequence [23]. Each rate-altered stream is then transformed by a modified discrete cosine transform (MDCT), and the resulting coefficients are encoded in different layers. This allows scalable reconstruction using the four different frequency bands with bit stream scalability within each subband.

The scalability of MPEG4 however, is not psychoacoustically motivated. To achieve psychoacoustic scalability, one must first decompose the signal so that adding a single subband to those already reconstructed by the decoder increases the fidelity of the reproduced audio in a way that is just discernable by a human listener. This can only be achieved if the audio signal is decomposed into critical bands or Barks [24], and then encoded in a perceptually embedded fashion. Furthermore, from a perceptual standpoint, it will almost certainly be optimal to initially quantize some critical bands coarsely and then later to add additional bits to improve the audio fidelity. In contrast to this idea, the MPEG-4 encoder uses a 4-band filter bank that does not approximate the critical band filtering well and only at the highest level of fidelity is each band psychoacoustically optimized. Thus, perceptual optimality cannot be guaranteed for the lower fidelity layers generated from these finely quantized coefficients.

TWIN-VQ has a scalable version [10][1] that uses residual vector quantization (RVQ) to obtain a scalable bitstream. This technique splits the MDCT coefficients within a frame into subvectors with some overlap between successive subvectors. The codec then creates different bit-streams by quantizing the subvectors separately from lower to higher frequencies assuming the lower frequencies to be more significant than higher frequencies. However, this residual quantization scheme does not perform any perceptual optimization in layering the different bit streams. The different subvectors and their overlap is chosen based on heuristic

assumptions.

Experiments have been performed in this research that show scalable MPEG AAC-BSAC performs poorly at low bit rates compared to high performance, non-scalable coders like the TWIN-VQ and nonscalable AAC [25]. Nonscalable TWIN-VQ performs almost 73% better in human subjective tests compared to scalable AAC-BSAC at a rate of 16 kb/s (based on a comparison category rating scale). Here, we develop a perceptually scalable audio coding algorithm based on the TWIN-VQ format. We chose the TWIN-VQ as our starting point because it is the best algorithm available for encoding bit rates below 16 kb/s – the most difficult region for audio coding.

The conventional TWIN-VQ and its original scalable version quantizes the flattened MDCT spectrum using interleave vector quantization and does not support the critical band specific quantization that is required to achieve optimal fidelity layering [26][10]. In our work, however, we apply residual vector quantization separately to each critical band of human hearing. Doing so relates the quantization error to its corresponding perceptual relevance, bringing us closer to perceptually optimality.

To further improve perceptual optimality, we also develop a new method to layer the residual bits based on perceptual relevance. This perceptual relevance is calculated using certain objective metrics developed specifically for this purpose [25]. Rigorous human subjective test results show that the scalable coder devel-

oped in this work performs 64-173% better than AAC-BSAC in the range of 16 to 24 kb/s and performs close to the nonscalable TWIN-VQ at the rates of 8 to 16 kb/s.

In the course of developing the residual VQs for our method we have also developed a novel way to reverse engineer vector quantizers [27] [28]. To design VQ codebook, we require a training set. In literature, the non-uniform bin histogram method described by Fukunaga in [29] comes closest to estimating the source pdf from a VQ codebook. The original TWIN-VQ used by the MPEG-4 standard was developed by NTT, Japan, and the training data used by the original developers is not available. This fact motivates our need for such an algorithm here. One could always construct a training set by combining a large number of audio sequences, but the resulting VQ might not be as good as the original, highly optimized one. Instead, we synthesize new training data from the information embedded within the TWIN-VQ codebook. The training data thus obtained was then used to design the VQ codebooks for the sub-vectors representing the critical bands.

This thesis is organized as follows. Chapter 2 discusses the foundations of perceptual audio coding, specifically introducing audio coding algorithms like the AAC and AAC-BSAC. Chapter 3 explains non scalable TWIN-VQ while chapter 4 develops a method for reverse engineering vector quantizers and applies it to TWIN-VQ to create a scalable compression algorithm. The modified, scalable TWIN-VQ algorithm is presented in Chapter 5. An improvement on this algo-

rithm which uses scalable lattice vector quantization in many of the higher critical bands to improve efficiency is also included in Chapter 5. In Chapter 6, we describe an objective metric for subjective audio quality, and we use it to determine the bit layering for perceptually optimal fidelity control. Experimental results and analysis are discussed in Chapter 7 while conclusions and future research are presented in Chapter 8.

2 HUMAN AUDIO PERCEPTION

To compress a particular type of data it helps to have an accurate engineering model of its source. For example, understanding of the human vocal tract and its interaction with sound has been critical in developing efficient methods of compressing human speech [30][31]. In the case of general audio signals, however, good source models do not exist. Thus, to efficiently compress audio, we have available only a generalized model for the receiver-i.e., the human ear.

The science of psychoacoustics characterizes human auditory perception. It models the inner ear, characterizing its time-frequency analysis capabilities. Based on this model, "irrelevant" signal information is classified as that which cannot be detected by even the most sensitive listener. Irrelevant information is identified during signal analysis by incorporating into the coder several psychoacoustic principles. The different psychoacoustic redundancies are: absolute threshold of hearing, simultaneous masking, the spread of masking and temporal masking. Combining these psychoacoustic principles, lossy compression can be performed in such a way that the noise generated by it is not perceivable by human listeners [32][33].

Most sound-related measurements are done using the *sound pressure level*(SPL) units measured in dB. SPL is a standard metric that quantifies the intensity of

an acoustical stimulus [34]. It is a relative measure defined as follows

$$L_{SPL} = 20 \log_{10} \left(\frac{p}{p_0} \right)$$

where L_{SPL} is the SPL of a stimulus, p is the pressure level of the stimulus in Pascals (1 Pa = 1 N/m^2), and p_0 is the standard reference level of 20μ Pa. The dynamic range of intensity for the human auditory system is from 0 dB SPL, limits of detection for low-intensity, to 150 dB SPL the threshold of pain.

2.1 Absolute Threshold of Hearing

The absolute threshold of hearing represents the amount of energy in a pure tonal signal that can be detected by a listener in a noiseless environment [35]. The threshold is represented as a function of frequency over the range of audible frequencies. This function is approximated by the following equation

$$\begin{aligned} T_q(f) = 3.64(f/1000)^{-0.8} - 6.5 \exp -0.6(f/1000 - 3.3)^2 \\ +10^{-3}(f/1000)^4 \text{ (dB SPL)}. \end{aligned} \tag{1}$$

Figure 1 represents the absolute threshold of hearing for a young listener with acute hearing. In an audio compression system, the function $T_q(f)$ is used to limit the quantization noise in the frequency domain. There are two things that prevent us from using the absolute threshold of hearing directly, however. First, the threshold represented by (1) is associated with pure tonal stimuli, whereas the quantization noise generated by a compression system has a more complex spectrum. Second, the threshold represents a relative measure of the stimuli with

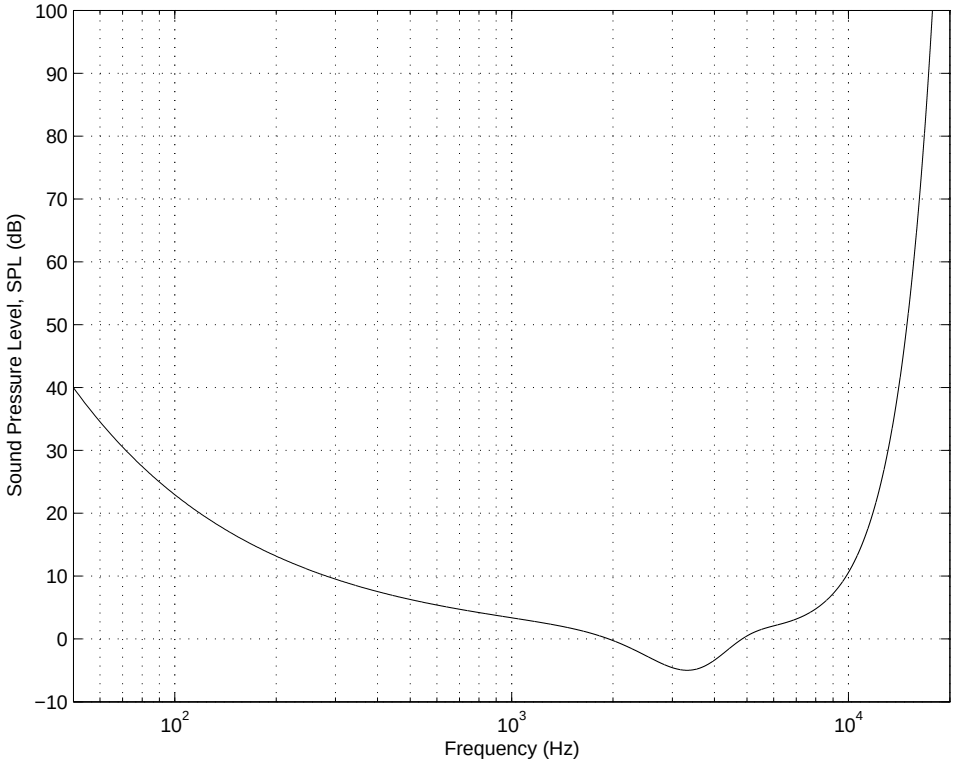

Figure 1: The absolute threshold of hearing in dB SPL, across the audio spectrum. It quantifies the SPL required at each frequency such that an average listener will detect a pure tone stimulus in a noiseless environment.

respect to a standard reference level. Most audio compression algorithms have no a priori knowledge of actual play back levels and thus no information about the reference level. We can overcome this problem by equating the lowest point (i.e., near 4 kHz) to the energy in ± 1 bit of signal amplitude.

Another commonly used acoustical metric is the *sensation level* (SL) measured in dB. The SL quantifies the difference between a stimulus and a listener's threshold of hearing for that particular stimulus. Signals with equal SL measurements may have different absolute SPL, but each SL component will have the same supra threshold margin.

2.2 Critical Bands

Shaping the coding noise spectrum using the absolute threshold of hearing is a first step in perceptual audio coding. The quantization distortion is not tonal in nature, however, and has a more complex spectrum. The detection threshold for spectrally complex quantization noise is a modified version of the absolute threshold, with its shape determined by the stimuli in the signal present at any given time. Auditory stimuli is time varying, which implies that the detection threshold is also a time-varying function of the input signal. In order to understand this threshold, we must first understand how the ear performs spectral analysis.

Within the ear, an acoustic stimulus moves the eardrum and the attached ossicular bones, which, in turn, transfer mechanical vibrations to the cochlea, a spiral

fluid-filled structure which contains a coiled tissue called the basilar membrane. A frequency-to-place transformation takes place in the cochlea (inner ear), along the basilar membrane [34]. Once excited by mechanical vibrations at its oval window (the input), the cochlear structure induces traveling waves along the length of the basilar membrane. The traveling waves generate peak responses at frequency specific positions on the basilar membrane, and along the basilar membrane there are hair-tipped neural receptors that convert the mechanical vibrations into chemical and electric signals.

For sinusoidal signals, the traveling wave moves along the basilar membrane until it reaches a point where the resonant frequency of the basilar membrane matches that of the stimuli frequency. The wave then slows, the magnitude increases to a peak and the wave decays rapidly beyond the peak. The location where the input signal peaks is referred to as the "characteristic place" for the stimulus frequency [36]. This frequency dependent transformation can be compared, from a signal processing perspective, to a bank of highly overlapping bandpass filters. Experiments have shown that these filters have asymmetric and nonlinear magnitude responses. Also, the cochlear filter frequency bands are of non-uniform widths which increase with frequency.

The width of cochlear passbands or "critical bands" can be represented as a function of frequency. We consider two examples by which the critical bandwidth can be characterized. In one scenario, a constant SPL, narrow-band noise signal

is introduced in a noiseless environment. The loudness (perceived intensity) of this noise is then monitored while varying the signal's bandwidth. The loudness remains constant till the bandwidth is increased up to the critical bandwidth, beyond which the loudness increases. Thus, when the noise is forced into adjacent critical bands the perceived intensity increases, while it remains constant within the critical band.

Critical bandwidth can also be viewed as the result of auditory detection with respect to a signal-to-noise ratio (SNR) criteria. For a listener the masked threshold of detection occurs at a constant, listener-specific SNR as assumed by the power spectrum model presented in [37]. Given two masking tones, the detection threshold of a narrowband noise source inserted between them remains constant as long as both the tonal signals, and the frequency separation between the tones remains within the critical bandwidth. If the narrowband noise is moved beyond the critical bandwidth the detection threshold rapidly decreases. Thus, from an SNR perspective, as long as the masking tones are introduced within the passband of the auditory filter (critical band) that is tuned to the probe noise, the SNR presented to the auditory system remains constant, i.e.– the detection threshold does not change. However, as the tones spread further apart and forced outside the critical band filter the SNR improves. For the power spectral model, therefore, to keep the SNR constant at the threshold for a particular listener, the probe noise has to be reduced with respect to the reduction of energy in the masking

tones as they move out of the critical band filter passband. Thus, beyond the critical bandwidth, the detection threshold for the probe tones decreases, and the threshold SNR remains constant.

Critical bandwidth tends to remain constant (about 100 Hz) up to 500 Hz, and increases to approximately 20% of the center frequency above 500 Hz. For an average listener the critical bandwidth centered at a frequency f is given approximately by

$$BW_c(f) = 25 + 75(1 + 1.4(f/1000)^2)^{0.69} \tag{2}$$

Although (2) is a continuous function of f, for practical purposes the ear is considered as a discrete set of bandpass filters corresponding to (2). The band gap of one critical band is commonly referred to as "one Bark". To convert from frequency in hertz to the Bark scale the following formula is used.

$$z(f) = 13 \arctan(0.00076f) + 3.5 \arctan\left[\left(\frac{f}{7500}\right)^2\right] \text{ (Bark)} \tag{3}$$

Another model used in audio coding is the equivalent rectangular bandwidth (ERB) scale. ERB emerged from research directed toward measurement of auditory filter shapes. To measure the ERB, human subjective experiments are performed with notched noise masker and probe signals to collect relevant data. Spectral shape of the critical bands are then estimated by fitting parametric weighting functions to the masking data [37]. Most commonly used models are rounded exponential functions with one or two free parameters. For example, the single-

parameter roex(p) model is given by

$$W(g) = (1 + pg)\exp(-pg) \tag{4}$$

where $g = |f - f_0|/f_0$ is the normalized frequency, f_0 is the center frequency and f is the input frequency in hertz. The roex(p,r), a two parameter model is also used to gain additional degrees of freedom which iproves the accuracy of the estimated filter shape. After curve fitting, an ERB estimate is obtained directly from the parametric filter shape. For the roex(p) model, it can be shown that the equivalent rectangular bandwidth is given by

$$ERB_{roex(p)} = \frac{4f_0}{p}. \tag{5}$$

Combining a collection of ERB measurements on center frequencies across the audio spectrum and curve fitting yields and expression for the ERB as a function of center frequency, this formula is given by

$$ERB(f) = 24.7(4.37(f/1000) + 1). \tag{6}$$

The critical bandwidth and ERB functions are plotted in Figure 2 and Figure 3 respectively.

Either the critical bandwidth or the ERB can be used to perform time-frequency analysis on an audio signal. However, the perceptually relevant information in the frequency domain is, in most cases, determined by the frequency resolution of the filter banks. The auditory time frequency analysis that occurs in the in the critical

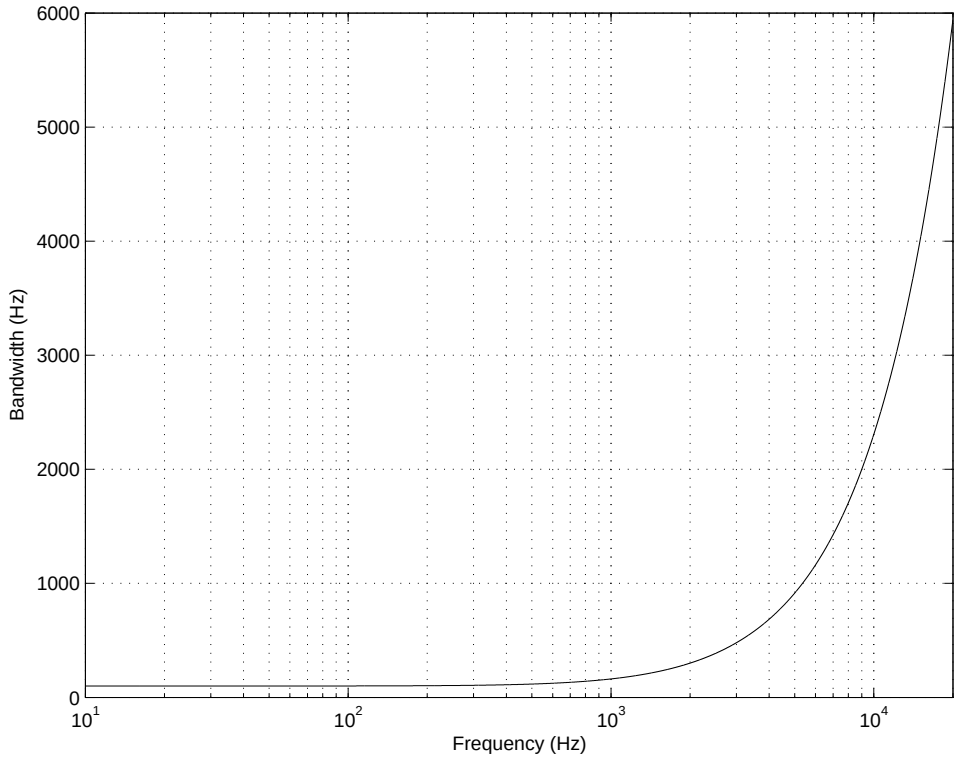

Figure 2: Critical bandwidth $BW_c(f)$ as a function of center frequency

band filter bank induces simultaneous and nonsimultaneous masking phenomena that are used by modern audio coders to shape the quantization noise spectrum. The shaping is done by adaptively allocating bits to signal components depending on their perceptual relevance.

2.3 Simultaneous masking

A sound stimulus, also known as the maskee, is said to be masked if it is rendered inaudible by the presence of another sound or masker. Simultaneous masking is said to occur if the human auditory system is presented with two or more signals

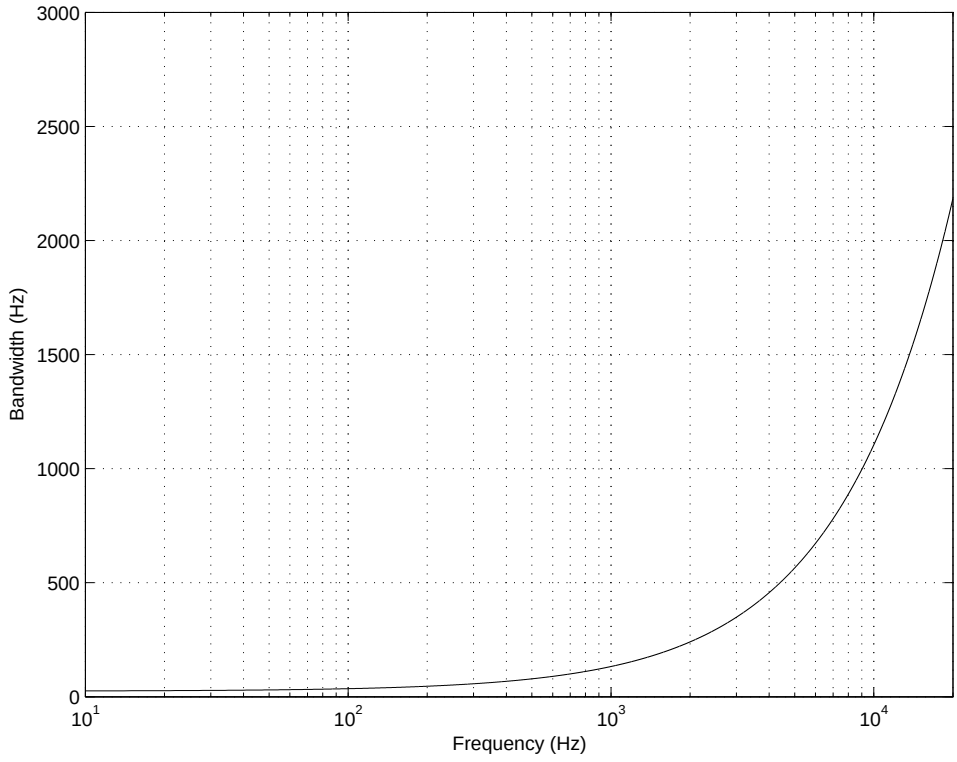

Figure 3: $ERB(f)$ as a function of center frequency.

at the same instant of time. In the frequency domain, the shape of the magnitude spectrum determines which frequency components will be masked and which will be perceived by the listener. In the time-domain, phase relationships between different stimuli can affect masking outcomes. An explanation of masking is that the presence of strong noise or tone masker creates an excitation of sufficient strength on the basilar membrane at the critical band location that the detection of a weaker signal in nearby locations are blocked.

Audio spectra may consist of several complex simultaneous masking scenarios. However, for the purpose of shaping quantization distortion it is convenient to use three types of simultaneous masking: (1) noise-masking-tone (NMT) [38], (2) tone-masking-noise (TMN) [39] and (3) noise-masking-noise (NMN) [40].

2.3.1 Noise-Masking-Tone (NMT)

In the NMT scenario of Figure 4, a narrow band noise with a bandwidth of one bark, masks a tone within the same critical band. Where the intensity of the masked tone is below a predictable threshold directly related to the intensity and the center frequency of the masking noise.

A lot of experiments have been done to characterize the NMT for random noise and pure tonal stimuli [41][42]. We first define the signal-to-mask ratio (SMR) as the minimum difference between the intensity of the masking noise and the intensity of the masked tone at the threshold of detection for the tone. The SMR

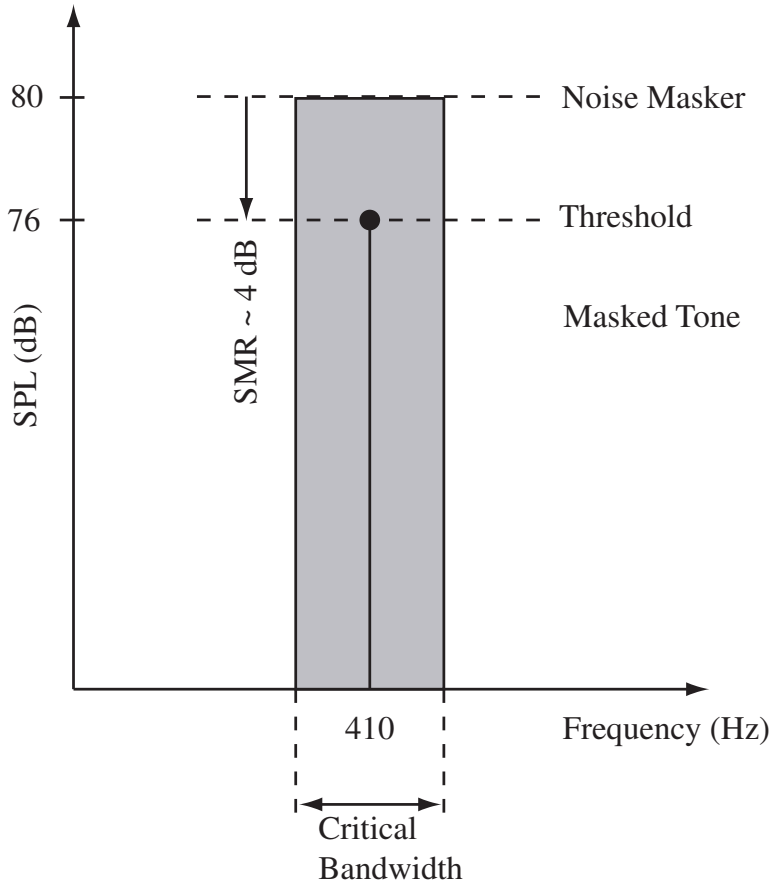

Figure 4: Noise-masking-tone – at the threshold of detection, a 410 Hz pure tone presented at 76 dB SPL masked by a narrow-band noise signal (1 Bark bandwidth) with overall intensity of 80 dB.

is measured in dB SPL. Minimum SMR occurs when the masked tone is close to the center frequency of the masking noise and lies between -5 and $+5$ dB for most cases. Figure 4 represents a sample result from a NMT experiment. The critical band noise masker is centered at 410 Hz with an intensity of 80 dB SPL. A tonal masked signal with a frequency of 410 Hz is used and the resulting SMR at the threshold of detection is obtained at 4 dB. The SMR increases if the probe tone frequency is above or below the central frequency.

2.3.2 Tone-Masking-Noise (TMN)

In the case of TMN as shown in Figure 5, a pure tone occurring at the center of a critical band masks a narrow band noise signal of arbitrary shape and lying within the critical band, if the noise spectrum is below a predictable threshold directly related to intensity and frequency of the masking tone. Similar to NMT, at the threshold of detection for a noise-band masked by a pure tone, the minimum SMR happens when the center frequency of the masked noise is close to the frequency of the masking tone. This minimum SMR lies in the range of 21-28 dB which is much greater than that for the NMT case. Figure 5 shows a narrow band noise signal (1 Bark), with center frequency 1 kHz, being masked by a tone of frequency 1 kHz. The SMR at the threshold of detection for the noise is 24 dB. As with the NMT, TMN masking power decreases for critical bandwidth probe noises centered above and below the minimum SMR noise.

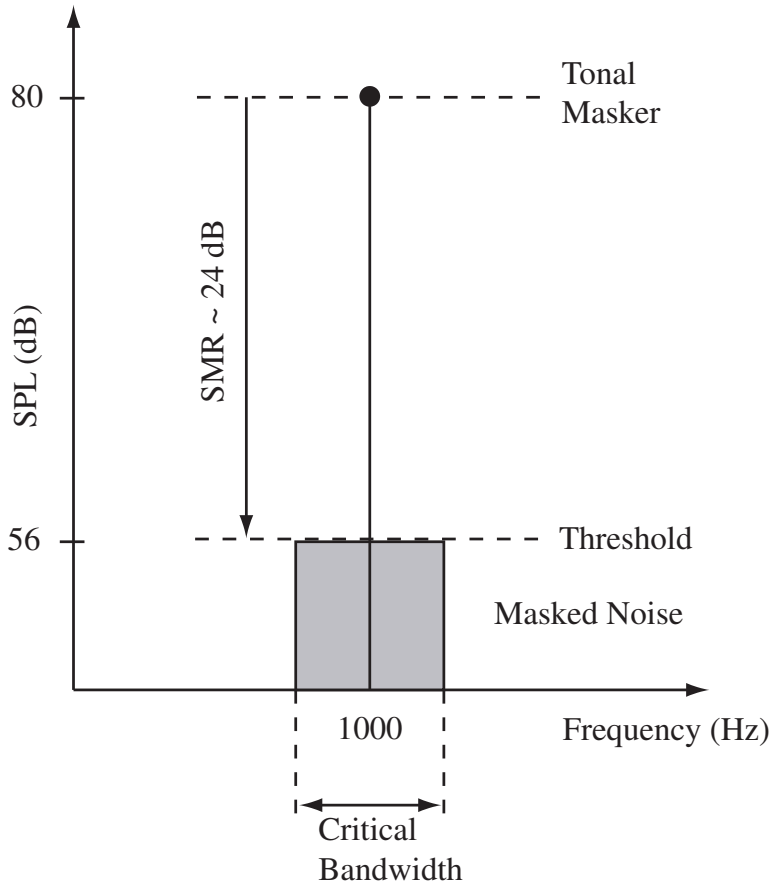

Figure 5: Tone-masking-noise – at the threshold of detection, a 1 kHz pure tone at 80-dB SPL masks a narrow band noise signal of overall intensity 56 dB.

2.3.3 Noise-Masking-Noise (NMN)

In the NMN scenario, a narrow-band noise masks another narrow-band noise. This type of masking is more difficult to characterize than either the NMT or TMN because of phase relationships between the masker and maskee [40]. Different relative phases between the two components can lead to inconsistent threshold SMR. A threshold SMR of about 26 dB was reported of NMN using an intensity difference based threshold detection methodology [43].

2.3.4 Asymmetry of Masking

For both the NMT and TMN cases of Figures 4 and 5, we note an asymmetry in the masking thresholds, even though both the maskers are presented at 80 dB(SPL). The difference between the thresholds is 20 dB. To shape the coding distortion so that it is not perceived by the human ear, we study the asymmetry in the masking threshold for the NMT and TMN scenarios. For each temporal analysis interval, the perceptual model for coding should identify noise-like and tone-like components across the frequency spectrum. These components occur in both the audio and quantization noise spectra. It has been shown that masking asymmetry can be explained in terms of relative masker/maskee bandwidths, and not necessarily exclusively in terms of absolute masker properties [44]. This implies that the standard energy-based schemes for masking power estimation among perceptual codecs may be valid only so long as the masker bandwidth equals or ex-

ceeds maskee bandwidth. In cases where the probe bandwidth exceeds the masker bandwidth, an envelope-based measure is embedded in the masking calculation [44].

2.3.5 The Spread of Masking

The simultaneous masking effects described above are not band limited to within the limits of a single critical band. Interband masking also occurs – i.e., a masker centered within one critical band affects the detection thresholds in adjacent critical bands. This effect is also known as the spread of masking, it is often modeled in coding applications by a triangular spreading function that has slopes of +25 and -10 dB per Bark. An expression for the spread of masking is given by

$$SF_{dB}(x) = 15.81 + 7.5(x + 0.474) - 17.5\sqrt{1 + (x + 0.474)^2} \tag{7}$$

where x is frequency in Barks and $SF_{dB}(x)$ is measured in dB. After critical band analysis is done and the spread of masking has been accounted for, masking thresholds in perceptual coders are often established by the decibel relations

$$TN_N = E_T = 14.5 - B \tag{8}$$

and

$$TH_T = E_N - K \tag{9}$$

where TH_N and TH_T are the noise and tone masking thresholds due to TMN and NMT respectively. E_N and E_T are critical band noise and tone masker energy

levels, respectively. Finally, B is the critical band number.

Depending on the algorithm, the parameter K is typically set to between 3 and 5 dB. However, the thresholds of (8) and (9) capture only the contributions of individual tone-like and noise-like maskers. In the actual coding scenario, each frame typically contains a collection of both masker types. One can see easily that (8) and (9) capture the masking asymmetry described previously. After they have been identified, these individual masking thresholds are combined to form a global masking threshold. The global masking threshold comprises of one final estimate beyond which the quantization noise becomes just noticeable also known as *just noticeable distortion* (JND). In most perceptual coding algorithms, the masking signals are classified as either noise or tone and then the appropriate thresholds are calculated by using this information to shape the noise spectrum beneath JND. The absolute threshold of hearing is also considered when shaping the noise spectra, and the maximum of the T_q and JND is generally used as the permissible distortion threshold. Figure 6 illustrates a general critical bandwidth and simultaneous masking threshold for a single masking tone occurring at the center of a critical band. All levels in the figure are given in terms of dB SPL.

2.4 Nonsimultaneous Masking

In the above paragraphs we have shown the effects of masking within the spectrum of a temporal frame. We have not, however, taken into consideration the effects

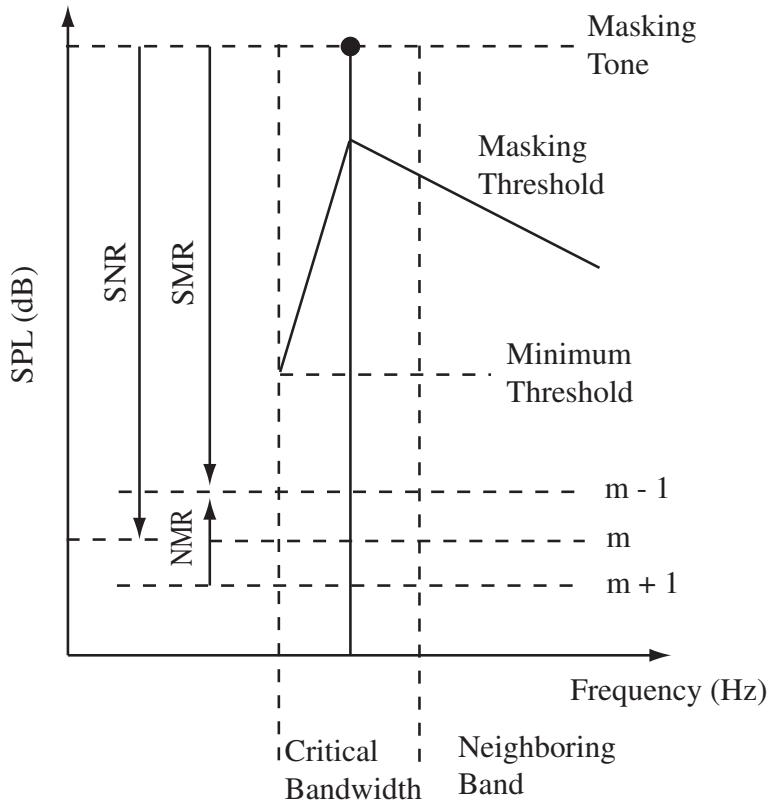

Figure 6: Schematic representation of simultaneous masking.

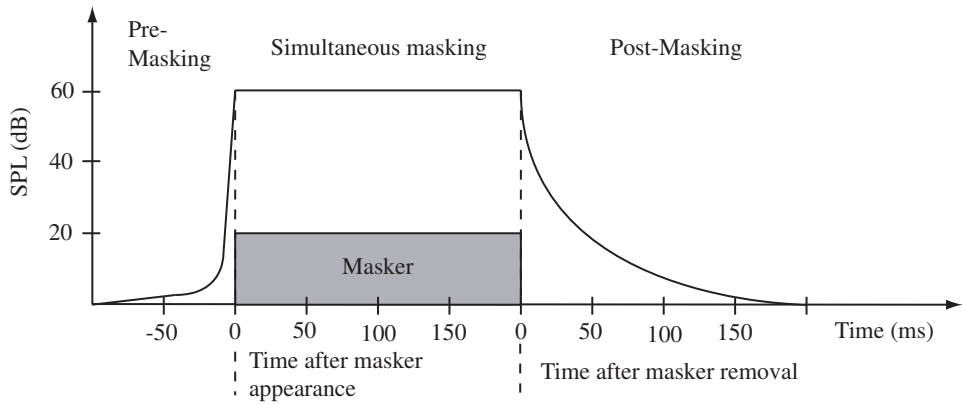

Figure 7: Nonsimultaneous maksing properties of the human ear. Backward (pre) masking occurs prior to masker onset and lasts only a few milliseconds whereas post masking may persist for more than 100 ms after removal of masker.

of masking over time. Figure 7 depicts the effects of temporal or nonsimultaneous masking. This type of masking effect occurs both prior to and after the appearance of the masking signal. The skirts on both regions are schematically represented in Figure 7. Essentially, absolute audibility thresholds for masked signals increase prior to, during and following the occurrence of the masker. Pre-masking ranges from about 1–2 ms before the onset of the masker while post-masking can range from between 50 to 300 ms after the masker ends, depending on the strength and duration of the masking signal [34].

There have been tutorial treatments of nonsimultaneous masking [37][40]. Here, we consider temporal masking properties that can be embedded within au-

dio coding systems. Of the two temporal masking modes, post-masking is better understood. For masker and probe of the same frequency, experimental studies have shown that the amount of post-masking depends in a predictable way on stimulus frequency, masker intensity and masker duration [45]. Forward masking also exhibits frequency-dependent behavior similar to that of simultaneous masking which can be observed when masker and probe frequencies are changed [46]. Although pre-masking has also been studied, it is not as well understood as post masking. Pre-masking clearly decays much rapidly than post masking. For example, only 2 ms prior to masker onset, the masked threshold is already 25 dB below that of simultaneous masking [47]. There is no consistent agreement on the maximum time limit for pre-masking – it appears to be dependent on the training given to the experimental subjects used to study the phenomenon.

2.5 Perceptual Entropy

Perceptual entropy (PE) refers to the amount of perceptually relevant information contained in an audio signal. Psychoacoustic masking and signal quantization principles were combined by Johnston to perform PE measurements [33][48]. PE, represented in bits per sample, is a theoretical limit on the compressibility of an audio signal. A wide variety of CD-quality audio signals can be compressed transparently at about 2.1 bits per sample. The PE estimation is done as follows. The audio signal is split into time frames and each of the time frame is transformed

into the frequency domain. Masking thresholds are then calculated based on the perceptual rules described in previous sections of this chapter. Finally, the PE is calculated as the number of bits needed to reconstruct the audio without injecting perceptible noise.

The audio signal is first split into time-frames with 1024-2048 samples each. These time frames are then weighted by a Hann window to take care of Gibbs ringing effects which is then followed by a fast Fourier transform (FFT). Masking thresholds are calculated by performing critical band analysis (with spreading), determining tone-like and noise-like spectral components, applying thresholding rules for the signal quantity, then accounting for the absolute hearing threshold. First, real and imaginary transform components are converted to power spectral components

$$P(\omega) = \Re^2(\omega) + \Im^2(\omega) \tag{10}$$

then a discrete Bark spectrum is formed by summing the energy in each critical band

$$B_i = \sum_{\omega=bl_i}^{bh_i} P(\omega) \tag{11}$$

where bl_i and bh_i are the critical band boundaries. The range of index i is sample-rate dependent, and in particular $1 \leq i \leq 27$ for CD-quality audio. A spreading function as in (7) is convolved with the discrete bark spectrum

$$C_i = B_i * SF_i \tag{12}$$

to account for the spread of masking. An estimation of the tone-like or noise like quality for C_i is then obtained using a spectral flatness measure (SFM) [64]

$$SFM = \frac{\mu_g}{\mu_a} \tag{13}$$

where μ_g and μ_a are the geometric and arithmetic averages of the spectral components of the power spectral density (PSD) within a critical band. The SFM ranges between 0 and 1, where values close to 1 indicate noise like components and values near 0 are more tonal in nature. A coefficient of tonality α is derived from the SFM measurement on the dB scale,

$$\alpha = \min\left(\frac{SFM_{dB}}{-60}, 1\right) \tag{14}$$

this coefficient is used to weight the threshold values calculated in (8) and (9) for each band which results in an offset

$$O_i = \alpha(14.5 + i) + (1 - \alpha)5.5 \text{ dB}. \tag{15}$$

A set of JND estimates in the frequency power domain are then formed by subtracting the offsets from the Bark spectral components

$$T_i = 10^{\log_1 0(C_i) - (O_i/10)}. \tag{16}$$

These estimates are scaled by a correction factor to simulate deconvolution of spreading funcion, and each T_i is then checked against the absolute threshold of hearing and replaced by $\max(T_i, T_q(i))$. The playback level is configured such

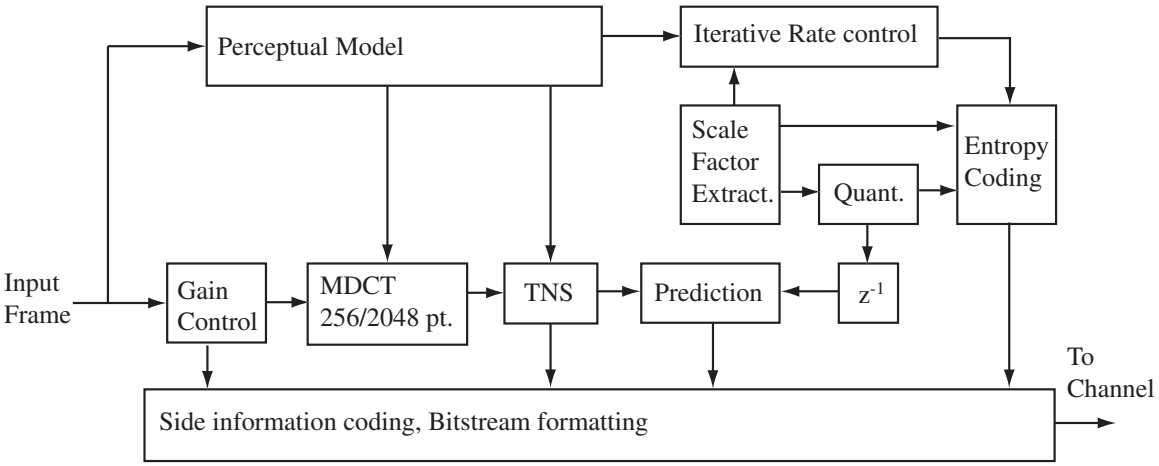

Figure 8: MPEG-4 Advanced audio coder (AAC).

that the smallest possible signal amplitude is associated with an SPL equal to the minimum absolute threshold. Applying uniform quantization principles to the signal and the associated JND estimates, it is possible to estimate a lower bound on the number of bits required to achieve transparent coding. In fact, it can be shown that the perceptual entropy in bits per sample is given by

$$\mathrm{PE} = \sum_{i=1}^{27} \sum_{\omega=bl_i}^{bh_i} \log_2 \left(2 \left\lfloor \frac{\Re(\omega)}{\sqrt{6T_i/k_i}} \right\rfloor + 1 \right) + \log_2 \left(2 \left\lfloor \frac{\Im(\omega)}{\sqrt{6T_i/k_i}} \right\rfloor + 1 \right) \quad \text{(bits/sample)} \tag{17}$$

where i is the index of the critical band, bl_i and bh_i are the lower and upper bounds of the critical band, k_i is the number of spectral components in band i and finally T_i is the masking threshold in the band. The masking threshold and PE computations as shown above form the basis for most perceptual audio coding.

2.6 Advanced Audio Coder (AAC)

The AAC algorithm as shown in Figure 8 is a collection of coding tools. We first describe the MPEG-2 AAC in this section and then briefly describe the modifications done to it in the MPEG-4 standard. The AAC has three complexity profiles, main, low (LC) and scalable sample rate (SSR) and each complexity uses a specific combination of coding tools. Here, we describe the complete set of tools used in the AAC algorithm [20].

First, a high resolution MDCT filter bank is used to obtain spectral representation of the input. The MDCT used for AAC is signal adaptive. Stationary signals are analyzed by a 2048-point window, while transients are analyzed with a block of eight 256-point windows to maintain time synchronization for multichannel operations. For a sampling frequency of 48 kHz the frequency and time resolutions obtained are 23 Hz and 2.5 ms respectively. The AAC filter bank also can change between two different MDCT analysis window shapes. Window shape adaptation is used to optimize filter bank frequency selectivity to localize masking thresholds, thereby increasing perceptual coding gain. Both windows satisfy the perfect reconstruction and alias cancelation requirements of the MDCT and they offer different spectral analysis properties. A sine window is selected when narrow passband selectivity is more beneficial than strong stopband attenuation, as in the case of inputs characterized by dense harmonic structure (less than 140-Hz

spacing). On the other hand a Keiser-Bessell derived (KBD) window is selected in cases for which stronger stopband attenuation is required, or when strong spectral components are separated by more than 220 Hz [64][65]. The AAC also has an embedded temporal noise shaping (TNS) module for pre-echo control (See Chapter 5).

The AAC algorithm realizes improved coding efficiency by applying prediction over time to the transform coefficients below 16 kHz [49][50]. The bit allocation and quantization in the AAC follows an iterative procedure. Psychoacoustic masking thresholds are first obtained as shown in the previous section. Both lossy and lossless coding blocks are integrated into a rate-control loop structure. This rate-control loop removes redundancy and reduces irrelevancy in one single analysis-by-synthesis process. The AAC coefficients are grouped into 49 scale-factor bands that mimic the auditory system's frequency resolution, similar to MPEG-1, Layer III [51][52]. A bit-reservoir is maintained to compensate for time-varying perceptual bit-rate requirements.

Within the entropy coding block [53], 12 Huffman codebooks are available for two- and four-tuple blocks of quantized coefficients. Sectioning and merging techniques are applied to maximize redundancy reduction. Individual codebooks are applied to time-varying sections of scale-factor bands, and the sections are defined on each frame through a greedy merge algorithm that minimizes the bitrate. Grouping across time and intraframe frequency interleaving of coefficients

prior to codebook application are also applied to maximize zero coefficient runs and further reduce bitrates.

For the MPEG-4 framework, the MPEG-2 AAC reference model was selected as the "time-frequency" audio coding core. Further, the perceptual noise substitution (PNS) scheme was included in the MPEG-4 AAC reference model. PNS exploits the fact that a random noise process can be used to model efficiently, the transform coefficients in noise-like frequency subbands, provided the noise vector has an appropriate temporal fine structure [54]. Bit-rate reduction is realized since only a compact, parametric representation is required for each PNS subband rather than requiring full quantization and coding of subband transform coefficients.

2.7 Bit-slice Scalable Arithmetic Coding

The concept of bit-sliced scalable arithmetic coding (BSAC) was introduced for audio coding in [55] and is standardized as a part of MPEG-4 [20]. BSAC plays the role of an alternative lossless coding kernel for MPEG-4 AAC, utilizing the MDCT and applying a perceptually controlled bandwise quantization to the spectral values. The main difference between BSAC and the standard AAC lossless coding kernel is that the quantized values are not Huffman coded, but arithmetically coded in bitslices. This allows a fine grain scalability by omitting some of the lower bitslices while maintaining a compression efficiency comparable to

the Huffman coding approach for the quantized spectral values. In the MPEG-4 AAC/BSAC codec the bitslices of the perceptually quantized spectral values are already ordered in a perceptual hierarchy. In this way more perceptually shaped noise is introduced as more and more bitslices are omitted.

3 TRANSFORM DOMAIN WEIGHTED INTERLEAVED VECTOR QUANTIZATION

Transform-domain weighted interleave vector quantization (TWIN-VQ) is a method used for compressing audio signals which has been found to be particularly effective at low bit rates [56] [26]. Figure 9 shows block diagrams describing the TWIN-VQ encoder and decoder. The input signal is first split into time frames of 1024 samples. This frame is then transformed into the frequency domain using

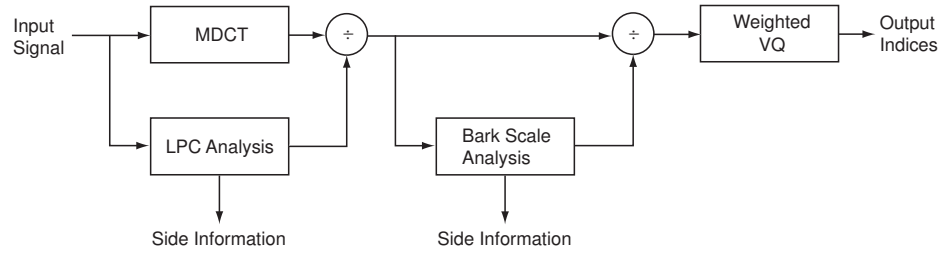

(a) Encoder

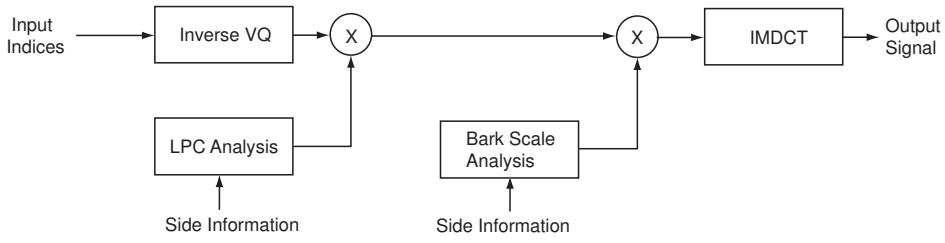

(b) Decoder

Figure 9: TWIN-VQ block diagram (a) Encoder (b) Decoder.

a 1024-point modified discrete cosine-transform (MDCT) while at the same time the linear predictive coding (LPC) spectrum is calculated directly from the input. The LPC spectrum provides a rough representation of the spectral envelope of the MDCT coefficients, and it is used to normalize the MDCT coefficients to obtain a flat spectrum by division in the MDCT domain. This is equivalent to performing linear predictive filtering and subtraction in the time domain to obtain the residual error signal (i.e., the signal with the predictable portions removed). Further normalization of the MDCT spectrum is done using the bark scale envelope. Bark-scale envelope normalization is performed mainly to improve quantization performance of signals with a lot of harmonic structure. Finally, quantization of the final flattened spectrum is accomplished by using weighted interleave vector quantization. The linear prediction coefficients and the power envelope from the second flattening operation are also quantized and transmitted to the decoder as side information.

The decoder simply inverts the steps of the encoder as illustrated in Figure 9. The flattened spectrum is reconstructed from the VQ indices and the reconstructed bark scale coefficients and linear predictive coefficients multiply this spectrum to obtain an approximation of the original spectrum. A single frame of the time domain audio signal is then reproduced by applying the inverse MDCT transform to the reconstructed MDCT coefficients.

In the introduction, we stated that our intention is to modify the TWIN-VQ

algorithm to create a perceptually scalable audio coder. Note that it is only in the quantization and encoding stage that psychoacoustic and statistical redundancy are truly removed. Virtually all of the information removed by the prediction stages in the encoder is added back to the signal in the decoder. It is thus this stage that we must modify in the conventional TWIN-VQ algorithm to generate a scalable bit stream. The quantizer in TWIN-VQ uses three main concepts: (1) weighted vector quantization, (2) vector interleaving and (3) two-channel conjugate VQ [57] [58] [59]. We will discuss each of these in the following sections.

3.1 Weighted Vector Quantization

Weighted vector quantization (WVQ) is a VQ equivalent of adaptive bit allocation. Adaptive bit allocation determines an optimal bit allocation scheme for a given collection of random variables (the MDCT coefficients, in our case), based on the variance of each random variable. The coding advantage or SNR improvement obtained by using adaptive bit allocation is given by

$$G = \frac{\sum_{i=1}^{m} \lambda_i}{m \prod_{i=i}^{m} (\lambda_i)^{\frac{1}{m}}} \tag{18}$$

where λ_i^2 is the variance of the ith variable. Optimal bit allocation works by allocating bits to random variables proportional to their variances, but for *perceptually* optimal bit allocation the variances must be modified to take into account the masking properties of the human ear.

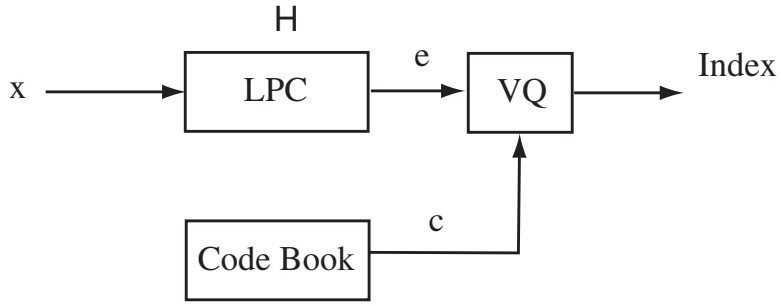

Figure 10: Vector quantization scheme for LPC residue.

A linear predictive coder (LPC) decorrelates successive samples in a signal. For a vector $\mathbf{x}$ of successive samples $[x[1], x[2], \ldots, x[N]]^T$, a linear predictor is an FIR filter with coefficients $\mathbf{h}^T = [h_1, h_2, \ldots, h_N]$. The filter coefficients can be obtained by spectral factorization of the autocorrelation matrix $\mathbf{R} = E(\mathbf{x}\mathbf{x}^T)$ [21].

As shown in Figure 10, quantization is performed by finding the best code vector $\mathbf{c}$ so as to minimize the distortion d between the input residual $\mathbf{x}$ and the vector $\mathbf{Hc}$, determined by synthesizing the residual codebook vector $\mathbf{c}$. Here, $\mathbf{H}$ denotes the impulse response matrix of the LPC synthesis filter: i.e.,

$$\mathbf{H} = \begin{bmatrix} 1 & 0 & \cdots & 0 & 0 \\ h_1 & 1 & \cdots & 0 & 0 \\ h_2 & h_1 & \cdots & 0 & 0 \\ \vdots & \vdots & \cdots & \vdots & \vdots \\ h_{m-1} & h_{m-2} & \cdots & h_1 & 1 \end{bmatrix},$$

and we use $\mathbf{H}^T$ to denote its transpose. If Euclidean distance is used, then distortion is given by

$$d = \|\mathbf{x} - \mathbf{Hc}\|^2. \tag{19}$$

Assuming the power of the input vector $\mathbf{x}$ is normalized so that the residual

power is unity, we can write $\mathbf{x}$ as

$$\mathbf{x} = \mathbf{He} \tag{20}$$

where $\mathbf{e}$ is the LPC residual vector. Replacing $\mathbf{x}$ in equation (19) with (20) we get

$$d = \|\mathbf{He} - \mathbf{Hc}\|^2 = (\mathbf{e} - \mathbf{c})^T \mathbf{H}^T \mathbf{H} (\mathbf{e} - \mathbf{c}). \tag{21}$$

Since $\mathbf{H}$ is a factor of the correlation matrix $\mathbf{R}$ of the vector $\mathbf{x}$ we can say

$$d = (\mathbf{e} - \mathbf{c})^T \mathbf{R} (\mathbf{e} - \mathbf{c}). \tag{22}$$

Because $\mathbf{R}$ is a positive definite matrix, we can diagonalize it with a unitary matrix $\mathbf{U}$ that is composed of the eigenvectors of $\mathbf{R}$

$$\mathbf{\Lambda} = \mathbf{U}^T \mathbf{R} \mathbf{U} = \mathrm{diag}[\lambda_1, \cdots, \lambda_m]. \tag{23}$$

The eigenvalues λ_i are all non-negative and represent the variance of each random variable in $\mathbf{x}$. Rewriting the distortion d using (23), we have

$$\begin{aligned} d &= (\mathbf{e} - \mathbf{c})^T \mathbf{U} \mathbf{\Lambda} \mathbf{U}^T (\mathbf{e} - \mathbf{c}) \\ &= \textstyle\sum_{i=1}^{m} \lambda_i (E_i - C_i)^2 \end{aligned} \tag{24}$$

Equation (24) now represents the distortion as a weighted sum of the quantization error between the transformed residual vector $\mathbf{E}$ and the transformed codevector $\mathbf{C}$: i.e.,

$$\mathbf{E} = \mathbf{U}^T \mathbf{e} = [E_1, E_2, \ldots, E_m]^T$$

$$\mathbf{C} = \mathbf{U}^T \mathbf{c} = [C_1, C_2, \ldots, C_m]^T.$$

The transformation $\mathbf{U}^T$ is the Karhunen-Loeve transformation (KLT) for an autoregressive random process. Clearly, the quantization error in the transformed domain, as computed in (24), is the same as that in the time domain as found in (19). Thus, linear predictive quantization in the time domain can be represented as a weighted vector quantization in KLT domain.

In this section, we want to quantify the quantization gain achieved by using weighted vector quantization (WVQ). To do so, we first show that if a source is uniformly distributed, the SNR gain due to WVQ matches the SNR gain for adaptive bit allocation in (18). Let $\mathbf{x} = [x_1, \ldots, x_m]^T$ be a m dimensional, uniformly distributed vector with variances $\lambda_1, \ldots, \lambda_m$. Now, we introduce two vector quantizer code books $\mathbf{C}_u$ and $\mathbf{C}_w$ that both contain the same number of codewords and thus operate at the same bitrate of $\overline{b}$. Codebook $\mathbf{C}_u$ is designed as a lattice formed by uniform scalar quantization of each component x_i of the vector $\mathbf{x}$. If the vector $\mathbf{x}$ is uniformly distributed over a hyper-rectangle of edge length L_i with respect to the component x_i, then all of the VQ bins are hyper-rectangles of edge size $L_i/\overline{N}$, where $\overline{N} = 2^{\overline{b}}$, and the centroid is the corresponding codeword $\mathbf{c}_u$. The average distortion for this case is given by

$$d_u = \int_0^{L_1/\overline{N}} \cdots \int_0^{L_m/\overline{N}} \sum_{i=0}^{m} (x_i - c_{ui})^2 dx_1 \cdots dx_m. \tag{25}$$

Equation (25) is nothing more than the variance of the VQ bin normalized by the total volume. The average distortion can also be written in relation to the

individual variances λ_i as

$$d_u = k \sum_{i=1}^{m} \lambda_i \tag{26}$$

where

$$k = \frac{1}{3} \prod_{i=1}^{m} \lambda_i^{1/2}. \tag{27}$$

Now, we construct the codebook for the weighted VQ $\mathbf{C}_w$ in a similar fashion. In this case we use a lattice of uniform scalar quantizers with b_i bits per dimensional component x_i. The optimal value of b_i [21] is given by

$$b_i = \overline{b} + \frac{1}{2} \log_2 \frac{\lambda_i}{\left(\prod_{i=1}^{m} \lambda_i^{\frac{1}{m}} \right)} \tag{28}$$

and N_i the number of levels for the ith variable is given by $N_i = 2^{b_i}$. Using the uniform quantization assumption and noting that the number of quantization levels for index i is given by $N_i = 2^{b_i}$, the edge size of the ith VQ bin becomes

$$\frac{L_i}{N_i} = 2^{-\overline{b}} L_i \frac{\prod_{j=1}^{m} \lambda_j^{\frac{1}{2m}}}{\lambda_i^{\frac{1}{2}}}. \tag{29}$$

Here, we use the weighted distortion integral to calculate the distortion instead of the simple Euclidean distance-based distortion. Thus, the weighted distortion is given by

$$d_w = \int_0^{L_1/N_1} \cdots \int_0^{L_m/N_m} \sum_{i=0}^{m} \lambda_i (x_i - c_{wi})^2 dx_1 \cdots dx_m. \tag{30}$$

which on simplification yields

$$d_w = km \left(\prod_{i=1}^{m} \lambda_i^{\frac{1}{m}} \right) \tag{31}$$

Thus, dividing (26) by (31) we can see that the coding gain for weighted VQ is the same as that given for adaptive bit allocation (18).

3.2 Interleaving

So far we have analyzed the gain G obtained by using a WVQ. Now, we would like to examine the relationship between the transform size m and the coding gain. The correlation matrix $\mathbf{R}$ is a symmetrical Toeplitz matrix. In this case, the SNR gain

$$SNG = 10 \log_{10} G$$

can be explicitly expressed by the transform size m and PARCOR parameters p_i as follows [30]:

$$SNG = -10 \log_{10} \left(\prod_{i=1}^{n} (1 - p_i^2)^{\frac{m-i}{m}} \right). \tag{32}$$

It can easily be shown that the linear prediction gain approaches this SNR gain if the prediction filter size is large. This equation is useful for estimating the relationship between the performance and the transform size. Since this estimate holds for the time domain quantization procedure of (19), it is also useful for estimating the performance of these coders in relation to the length of the delay or the vector dimension.

As shown above, while a high SNR gain is expected for a large transform size m, the vector dimension must be kept small for the following practical reasons. At a fixed bitrate, computation complexity and the codebook size of the vector

quantization are exponentially proportional to the vector dimension. In order to cope with these situations, it is necessary to split the full code vector $\mathbf{c}$ into subvectors. If one splits it into J l-dimensional subvectors, SNR gain is given by

$$SNG_s = 10 \log_{10} \left[\frac{(\sum_{i=1}^{m} \lambda_i / m)}{\left(\sum_{j=1}^{J} d_j / J \right)} \right] \tag{33}$$

where d_j is the geometric mean of the weighting factors for each subvector as follows:

$$d_j = \prod_{k \in M_j} \lambda_k^{1/n}$$

M_j denotes the index set of the elements which belong to the jth subvector.

In general, $SNG_s \leq SNG$, since the denominator of (33) is the arithmetic mean of d_j while that of 18 is the geometric mean of d_j. However, equality holds if d_j is uniformly independent of j–i.e., even if the transform components are split into subvectors, SNR gain remains unchanged provided that the geometrical mean of the weighting factors for subvectors can be made equal.

Up to this point in our analysis, we have assumed that the transform used is the KLT as described earlier. The KLT is not a general transform; it is specific to a particular AR process. The TWIN-VQ algorithm, on the other hand, is meant to deal with arbitrary audio signals, and thus uses the suboptimal (but very effective) modified discrete transform (MDCT).

The complete set of MDCT coefficients passed to the VQ stage forms a very large vector, typically in the range of 256-1024 elements within the TWIN-VQ

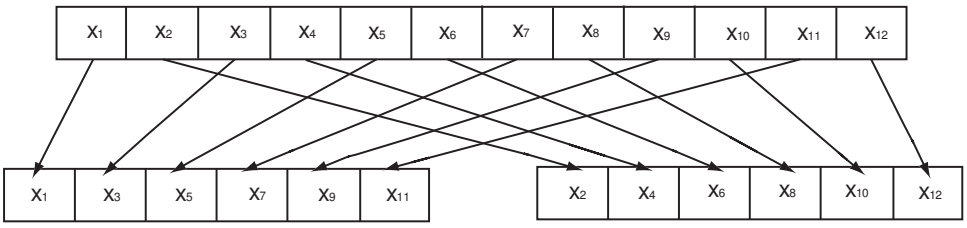

Figure 11: Interleaving a 12 dimensional vector into two 6 dimensional vectors

framework. Quantizing the whole MDCT coefficient set as a single vector is not feasible because of the high computational complexity of the VQ index search and the difficulty achieving a good design using algorithms like the generalized Lloyd algorithm that generate only locally optimal solutions. The TWIN-VQ algorithm overcomes these difficulties by splitting the large MDCT coefficient vector into smaller sub-vectors such that the geometric mean of the weighting coefficients corresponding to each sub-vector remains the same. This is done by decimating the MDCT spectrum by the number of sub-vectors to be generated. For example, if $[x_1, x_2, x_3, x_4, \ldots, x_{n-1}, x_n]^T$ is an n dimensional vector, interleaving it into two sub vectors would give the vectors $[x_1, x_3, \ldots, x_{n-1}]^T$ and $[x_2, x_4, \ldots, x_n]^T$ as illustrated in Figure 11.

3.3 Two-Channel Conjugate VQ (TC-VQ)

The final quantization step in TWIN-VQ is performed using a technique called two-channel conjugate VQ (TC-VQ). TC-VQ uses two different codebooks that in some sense are "conjugates" of each other [58]. The TC-VQ encoder selects a

codebook vector from each of the two codebooks, calculates the average, and then compares this average to a given input vector using a perceptually weighted mean square distortion measure; i.e.,

$$d^2 = \sum_{i=1}^{N} \sum_{j=1}^{N} \left(\mathbf{x} - \frac{\mathbf{y}_{1i} + \mathbf{y}_{2j}}{2} \right)^T \mathbf{W} \left(\mathbf{x} - \frac{\mathbf{y}_{1i} + \mathbf{y}_{2j}}{2} \right). \tag{34}$$

In the above equation, $\mathbf{x}$ is the input vector, $\mathbf{y}_1$ and $\mathbf{y}_2$ denote vectors from the conjugate codebooks and $\mathbf{W}$ is a diagonal matrix with the perceptual weight values along its diagonal. Indices of the pair of codebook vectors that minimize the distortion are then transmitted to the decoder. A conjugate VQ structure has much higher resolution than a normal codebook of the same size. As a simple example, consider a TC-VQ codebook with N code vectors in each conjugate codebook. The effective number of codevectors that can be represented is N^2– many more than the $2N$ codevectors that could be constructed using a simple VQ codebook with the same number of elements. The length of the corresponding channel codeword b is also reduced by half and the probability that the indices of both output vectors are corrupted in transmission is significantly reduced. In contrast, if only one codebook is used, the distortion significantly increases when a transmitted code vector is lost.

For example, the SNR performance for a Gaussian source is approximately proportional to the bitrate r per sample. The proportional constant in dB is $10 \log_{10}(4)$ or approximately 6 dB/bit. If the bitrate is reduced from r to $r/2$, the

SNR will decrease $3r$ dB. Thus, given a fixed bitrate, a two conjugate codebook system results in reduced distortion when transmission errors occur compared to a single codebook system.

3.3.1 Design of Conjugate Codebooks

Conjugate codebooks can be designed from a training set of vectors using an iterative algorithm that is similar to the generalized Lloyd algorithm [21]. In this method, both codebooks are simultaneously optimized by locally minimizing the quantization distortion. The convergence of the algorithm is guaranteed because the distortion is minimized at each iteration of the algorithm.

Any random codebook can be used as the starting point. If the improvement in distortion becomes less than a threshold, the codebooks are considered to have converged to the optimum.

1. Quantization of $\mathbf{u}_i$. For all training vectors $\mathbf{u}_i$, the best pair of intermediate reconstruction vectors $\mathbf{y}_{1m}$ and $\mathbf{y}_{2n}$ is selected so as to minimize d from given codebooks $\mathbf{Y}_1$ and $\mathbf{Y}_2$.

2. Fix codebook $\mathbf{Y}_2$ and renew codebook $\mathbf{Y}_1$. The new intermediate reconstruction vector $\mathbf{y}_{1n}$ is derived from the average distortion D_n for the old $\mathbf{y}_{1n}$. The average distortion is given by

$$D_n = \sum_{j=1}^{N} \sum_{\substack{\mathbf{u}_i \in \\ \mathbf{y}_{1n} \otimes \mathbf{y}_{2j}}} \|\mathbf{u}_i - \frac{\mathbf{y}_{1n} + \mathbf{y}_{2j}}{2}\|^2.$$

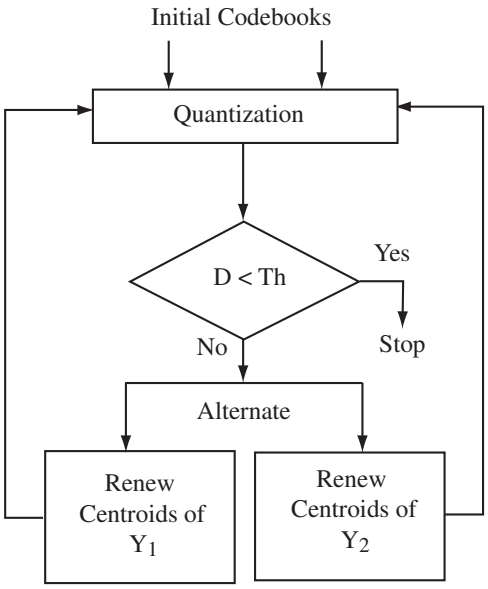

Figure 12: Conjugate codebook design algorithm.

To estimate the codebook vector in $\mathbf{Y}_1$ that minimizes the average distortion, we differentiate it by $\mathbf{y}_{1n}$ and equate to zero. The resulting expression for the new codebook vector is

$$\mathbf{y}_{1n} = \Psi^{-1} \sum_{j=1}^{N} \sum_{\substack{\mathbf{u}_i \in \\ \mathbf{y}_{1n} \otimes \mathbf{y}_{2j}}} (2\mathbf{u}_i - \mathbf{y}_{2j}),$$

where

$$\Psi = \sum_{j=1}^{N} \sum_{\substack{\mathbf{u}_i \in \\ \mathbf{y}_{1n} \otimes \mathbf{y}_{2j}}} 1.$$

3. The above step is repeated, but this time the codebook $\mathbf{Y}_1$ is fixed, and code vectors $\mathbf{y}_{2m}$ are renewed.

4. The average distortion is checked and the process is stopped if the difference in distortion falls below a particular threshold.

5. These above steps are repeated till the condition in the previous step is met. The same training set is used for each iteration.

A simple flow chart for this process is as shown in Figure 12.

3.3.2 Fast Encoding for Conjugate VQ

In conjugate VQ, one codevector is chosen from each codebook to encode an input vector. The chosen pair of codevectors should minimize the distortion. The most straight forward method of searching for the best pair is to calculate the distortion measure for all possible pairs, but this approach is not practical because of its high computational complexity. For example, for a twin codebook of 32 codevectors each, the number of distortion computations is on the order of $32^2 = 1024$. To overcome this problem, we use a fast encoding strategy which splits the encoding process into two steps: pre-selection and main-selection.

During pre-selection, a fixed number of candidate codevectors are chosen from a codebook and stored in a buffer where the number of candidates is less than the codebook size. The candidates chosen are those most likely to result in the minimum distortion and this procedure is performed separately for both the codebooks. In the main-selection process, all pairs of candidates obtained in the pre-selection process are combined, and their distortion measures are calculated. The pair giving the minimum distortion measure is chosen as the encoded output. Clearly the main selection process is actually identical to the optimal encoding process except

that it operates on a smaller set of codevectors.

The pre-selection process can be further organized by performing an area-localized pre-selection. Here, the codebook is divided into smaller sections, with the number of sections being equal to the number of candidates in the preselection. This organization of the codebook vectors within the candidate buffer simplifies the programming and reduces the search complexity.

Finally, the computation can be further reduced by reusing parts of the pre-selection process within main-selection. In the main-selection procedure, all possible pairs of pre-selection candidates are evaluated by the distortion measure, based on the following equation

$$d^2 = \|\mathbf{y}_1 + \mathbf{y}_2 - \mathbf{x}\|^2 \tag{35}$$

where, $\mathbf{y}_1$ and $\mathbf{y}_2$ are codevectors in the codebooks $\mathbf{Y}_1$ and $\mathbf{Y}$ respectively, and $\mathbf{x}$ is the input vector to be encoded. Weighting factors have been omitted in (35) for clarity, but the idea is identical for the WVQ case. Many of the computations in the above equation can be split between the pre- and main-selection processes.

The method used to split the task of computing (35) is called hit zone masking. To understand this method let us rewrite (35) as

$$d^2 = \|(\mathbf{y}_{1n} + \mathbf{y}_{1p}) + (\mathbf{y}_{2n} + \mathbf{y}_{2p}) - \mathbf{x}\|^2 \tag{36}$$

where the subscript n and p denote the normal (perpendicular) and parallel com-

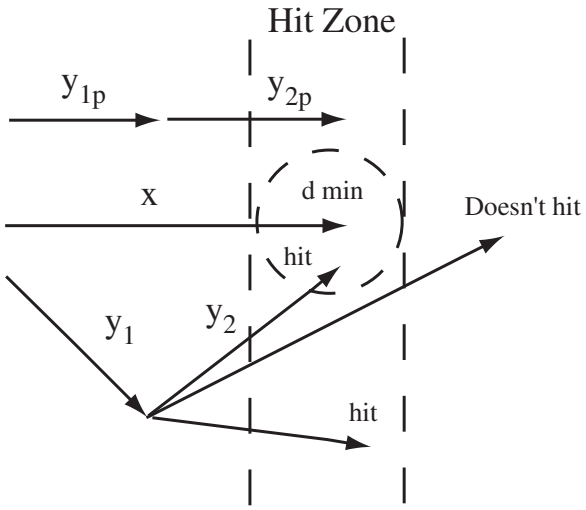

Figure 13: Hit zone masking method.

ponents of a vector. Mathematically this can be represented as

$$\mathbf{y} = \mathbf{y}_n + \mathbf{y}_p \tag{37}$$

where $\mathbf{y}_n \perp \mathbf{y}$ and $\mathbf{y}_p \| \mathbf{y}$. Given that the inner product of normal vectors is zero, (36) can be simplified to

$$d^2 = \|(\mathbf{y}_{1n} + \mathbf{y}_{2n})\|^2 + (\|\mathbf{y}_{1p}\| + \|\mathbf{y}_{2p}\| - \|\mathbf{x}\|)^2. \tag{38}$$

The first term of (38) is always positive, so the distortion measure is always greater than the second term, i.e.,

$$d^2 \geq (\|\mathbf{y}_{1p}\| + \|\mathbf{y}_{2p}\| - \|\mathbf{x}\|)^2. \tag{39}$$

The hit zone masking exploits this characteristic. Figure 13 illustrates this method with the current minimum distortion measure in the main-selection process ex-

pressed by *dmin*. The area between the parallel dashed lines is called the "hit zone". If the sum of two candidate vectors is outside the hitzone then the distortion measurement for the pair is skipped since this pair cannot minimize *dmin*. This hit-zone judgement can be determined by adding the parallel vector components and this sum must be in the range $\|\mathbf{x}\| \pm dmin$ to be in the hit zone. Parallel vectors can be added with low computational complexity because this is a scalar (i.e., element by element) operation.

The distortion measure for pre-selection within either code book is given by

$$\begin{aligned} d_p^2 &= \|2\mathbf{y} - \mathbf{x}\|^2 \\ &= 4\|\mathbf{y}\|^2 - 4\mathbf{y} \cdot \mathbf{x} + |\mathbf{x}\|^2, \end{aligned} \tag{40}$$

where d_p is the distortion measure. On the other hand, the distortion measure for main-selection as described by (35) can be written as

$$\begin{aligned} d^2 &= \|\mathbf{y}_1\|^2 + \|\mathbf{y}_2\|^2 - 2\mathbf{y}_1 \cdot \mathbf{x} \\ &-2\mathbf{y}_2 \cdot \mathbf{x} - 2\mathbf{y}_1 \cdot \mathbf{y}_2 + \|\mathbf{x}\|^2. \end{aligned} \tag{41}$$

Note that the first four terms of the above equation have already been calculated for the pre-selection distortion measure. Thus, these terms can be saved after the pre-selection step and reused during the main-selection. Furthermore, the last term $\|\mathbf{x}\|^2$ is calculated only once, and remains a constant throughout the encoding process.

The coder proposed in this work uses the fast conjugate vector quantizers described above. The fast encoder is especially useful here since we must encode each critical band separately using multiple conjugate vector quantizers. Using a

full search quantization, the proposed scalable coder would not be feasible because of the high computational complexity of its implementation.

4 REVERSE ENGINEERING THE TWIN-VQ

Developing a new, competitive audio compression algorithm is not an easy task. In this work, we modify Twin-VQ as implemented in the MPEG 4 natural audio coder reference software to create a scalable algorithm that is effective at low bit rates [56][60]. The Twin-VQ tools in the MPEG 4 reference software was developed by NTT corp., Japan. The training data used to design the VQs by NTT has not, however, been made public. Therefore, the training set required to design a scalable coder which is similar to Twin-VQ is not readily available. In our case, we need a training set to design new VQs for each of the different critical bands. In this chapter we describe a method to synthesize the required training set from the original Twin-VQ codebook itself.

Vector quantizers are used primarily for data compression to speed transmission or to reduce storage requirements. In many compression systems, operations like linear prediction, subband decomposition or wavelet transformation are carried out prior to the use of VQ. Thus, the signal that is encoded by the VQ is already represented in an efficient manner – i.e. with much of the signal energy concentrated into a few coefficients. An optimal VQ codebook contains a great deal information about an underlying data source model which can be extracted and used to design a new codec having a different structure and yet optimized for the same source model. The redesign process for a new VQ-based system involves

training the system again using either a set of collected signals or a probability density function (pdf) that models the source of the signal. Since neither the source pdf nor the original training set are available, we would normally have to create our own training set of audio sequences. However, VQ codebooks optimized for a particular training set does not necessarily work well for other training sets. A simple experiment to demonstrate this is performed in the experimental verification section. In the case of the Twin-VQ, the developers may have even formatted the training data to give a more generalized representation of the underlying source. Thus, a VQ designed over an arbitrary training set of available audio sequences may not perform as efficiently as the original, highly optimized Twin-VQ codebook.

A simple way to design a new VQ from an existing VQ is to transform the codebook vectors of the old VQ in such a way that all pre-quantization processing (e.g. transformations) are inverted. This technique works perfectly if the preprocessing operations are linear and orthogonal. In particular, if a transformation is orthogonal, the distance measure (the mean square error, MSE, for the VQ) is preserved in the transform domain [21]. In this chapter, we discuss a method to reverse engineer VQs for nonorthogonal transformations and to repartition the VQ into multiple, lower dimensional VQs, each optimal for arbitrary subspaces of the original codeword space. We then apply this method to Twin-VQ to create separate vector quantizers for each critical band and thus allow for perceptual

scalability.

Our aim is re-engineer the TWIN-VQ coder to be scalable – i.e., to have a layered quantization scheme in which each layer adds a small increment of fidelity to the reconstructed audio signal. The first step in designing such a system is to partition the VQ designed for original MDCT signal space into subspaces corresponding to the different critical bands of human hearing (e.g. the bark scale)[32]. Note that partitioning of vectors into sub vectors can be viewed as a linear transform in which distance is not preserved. Consequently, directly partitioning the original codebook into subvectors corresponding to critical bands does not lead to a good solution as we will show here. Instead, the reverse engineering scheme proposed here turns out to be far more effective.

Most current image compression systems use transforms such as the DCT (Discrete Cosine Transform) and the DWT (Discrete Wavelet Transform). These transforms are either orthogonal transforms or close to orthogonal transforms (as in the case of 9-7 or 5-3 biorthogonal wavelet transforms), so reverse engineering them is straight-forward and does not require the approach developed here. We note, however, that some of the new transforms that have been recently developed for image compression like the contourlet and curvelet transforms are not even close to orthogonal. Thus, the proposed reverse engineering scheme might be highly effective when applied to these more recent compression systems.

In practical compression systems, VQ is often applied toward the end of the

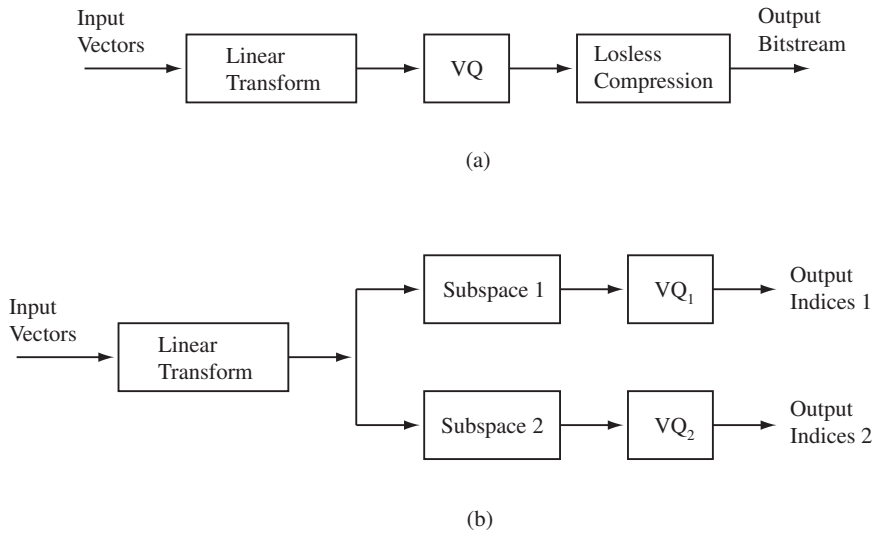

Figure 14: Block diagrams of a general VQ based compression systems. (a) system that quantizes a transformed signal using VQ. (b) a system that quantizes subspaces of the original signal separately.

encoding process and has the effect of reducing the bitrate of the signal representation dramatically. Most operations prior to the VQ are linear and deterministic and they can almost always be easily inverted. Furthermore, these operations can be identified and characterized simply by studying the decoder implementation. Therefore, if we can synthesize a training set from the VQ codebook, we can always pass each element in this set through the various inversion stages of the decoder to create a training set for the original signal space (in our case, the space containing all possible audio signals). In this chapter, we describe a method of synthesizing a training set from a VQ and using it to design new VQ codebooks for arbitrary spatial partitionings and transformations of the original vector (audio signal) space. Figure 14 shows two notional compression systems using vector quantization. In Figure 14(a) the original signal is transformed and the VQ is applied directly to the transformed signal while in Figure 14(b) the signal vector is split into two subvectors that are each fed into separate VQs, illustrating the spatial partitioning for the vector space previously mentioned.

The most commonly used VQ design approaches are random coding, pruning, pairwise nearest neighbor, splitting, and the Linde, Buzo, and Gray (LBG) or the generalized Lloyd algorithm [21][61]. The common requirement for all these algorithms is that they use a set of random samples (a training set) generated by an underlying probability density function (pdf) rather than the pdf itself since finding closed-form, optimal solutions is extremely difficult even when it is known

exactly. Therefore, the most straight forward way to reverse engineer a VQ is to synthesize a training set whose statistics match those of the original training set as closely as possible. The original codebook can be seen as a variable bin histogram representing the original training set.

4.1 Training Set Synthesis

We need an accurate estimate of the underlying signal pdf to synthesize a good training set. Furthermore, to simplify modeling on a computer the estimated pdf should be a superposition of simple functions. Many techniques have been proposed to estimate densities from training set data including nearest neighbor, Parzen's window and histograms [62][63]. The problem in our case is that the amount of data available to us has been reduced to the number of elements in the codebook by the LBG or some other clustering algorithm. The earliest density estimation techniques developed for reduced data sets use the condensed nearest neighbor rule (CNN) [64][65], and the technique is still of interest to researchers as evidenced by recent work [29][66][67]. These techniques can be broadly classified as nearest neighbor (NN) based techniques or Parzen's window-based techniques. Unfortunately, the NN-based techniques do not result in functions of known and easily generated random variables that can be used to generate training vectors. Parzen's window estimators, on the other hand, provide a representation that is a linear combination of simple pdf functions (e.g. "windows") like Gaussian or

the uniform densities. To use a Gaussian window effectively, one must be able to estimate the variance or, in the multidimensional case, the covariance matrix of each window function [67]. Unfortunately, the VQ codebook does not contain enough information to do this accurately. The obvious choice, then, is to use the uniform window function which requires only a weight and the width/spread – quantities that can be easily estimated from the polytope formed by each VQ bin. Note that this approach is similar to the way in which variable bin size histograms are designed [62]. A histogram measures the frequency of occurrence of vectors in specific cells whose sum total partition the entire vector space (as defined by the vectors of the training set), and the frequency of a particular cell is thus an estimate of the probability mass of that cell. If the cell size is reduced (resulting in an increase in the number of cells), the estimate converges asymptotically to the pdf of the training set [29]. Consequently, the histogram of a training set approximates the shape of the original pdf.

In our problem of synthesizing a representative training set, we are given only the VQ codebook vectors and, if available, the entropy codes assigned to each codebook index. To develop a synthesis methodology, we must study the VQ design process. The main aim in the design of the VQ is to find a codebook specifying the encoder that will maximize the overall performance as specified by the statistical average over a suitable distortion measure. We use here mean square error as our distortion measure. The encoder and decoder are completely

specified by the partition of the vector space into the cells $\mathbf{R}_1, \mathbf{R}_2, \ldots, \mathbf{R}_N$ and the codebook, $C = \{\mathbf{y}_1, \mathbf{y}_2, \ldots, \mathbf{y}_N\}$, respectively. Optimality for the partition satisfies the nearest neighbor (NN) condition – i.e., for a given set of output levels, $\mathbf{C}$, the optimal partition cells satisfy

$$\mathbf{R}_i \subset \{\mathbf{x} : d(\mathbf{x}, \mathbf{y}_i) \leq d(\mathbf{x}, \mathbf{y}_j)\} \tag{42}$$

and the optimal code vectors for a given partition satisfy the centroid condition given by

$$\mathbf{y}_i = cent(\mathbf{R}_i). \tag{43}$$

For the squared error or Euclidean distortion measure, the centroid of a set $\mathbf{R}_i$ is simply the minimum mean square estimate of $\mathbf{X}$ given $\mathbf{X} \in \mathbf{R}_i$, i.e.

$$\mathbf{y}_i = cent(\mathbf{R}_i) = E(\mathbf{X}|\mathbf{X} \in \mathbf{R}_i) \tag{44}$$

The conditions of (42) and (43) are the necessary but not sufficient conditions for optimality of a VQ codebook and partition. By iteratively applying the two conditions, one can obtain a VQ design that is at least locally optimal. As mentioned earlier, this VQ design procedure is similar to the problem of constructing a variable bin histogram [29]. A variable bin histogram is generated by assuming m cells $A_1, A_2, \ldots, A_m$, each characterized by the coordinate of the center x_i and the number of samples within each cell k_i. In the VQ case, cells are characterized by the VQ codebook entries and the partition rule. The only thing missing is the

number of samples within each cell. This, however, can be estimated from the entropy codes assigned to each codebook entry since the entropy code depends on the probability of the code word. Furthermore, the shape of the underlying pdf of the training set is preserved in the spacing of the cells and in their shapes, i.e., - the larger a cell, lower its probability density at any given point within it. Given these assumptions, a training set can be synthesized by generating uniformly distributed vectors for each VQ partition. This requires us to generate random variables distributed according to a constant density over the polytopal partition cell. To create such random vectors, we first generate a uniform pdf over a Cartesian grid which encloses the VQ cell. We then choose N vectors generated by this pdf which fall inside the VQ partition. The following discussion justifies this technique for generating uniformly distributed vectors within an irregularly shaped polytopal region. Let **U** be the support of a uniform pdf $p(x)$ and let **S** be the uneven partition as shown if Figure 15. Here **S** is a proper subset of **U** and **L** is the compliment of **S** with respect to **U**. The pdf $p(x)$ can then be written as

$$p(x) = P_1 p(x|x \in \mathbf{S}) + P_2 p(x|x \in \mathbf{L}) \tag{45}$$

where P_1 and P_2 are the probabilities that $x \in \mathbf{S}$ and $x \in \mathbf{L}$, respectively. The above equation can also be interpreted as a classification problem where the two classes are **S** and **L** and the classes are mutually exclusive – i.e. there is no intersection between the sets. Since the two classes are mutually exclusive, the

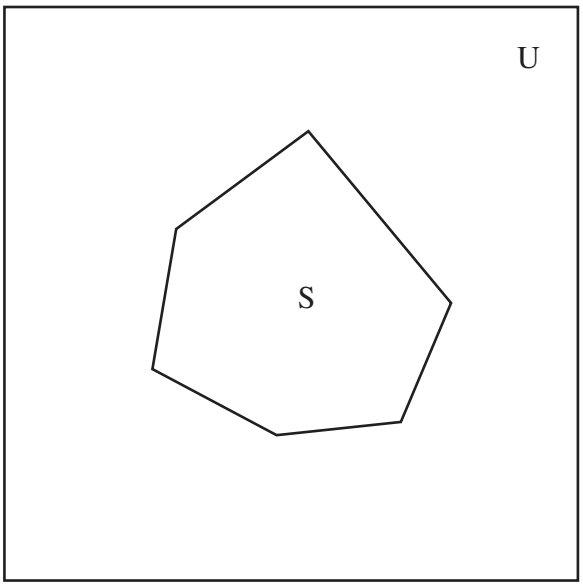

Figure 15: An irregular convex polytope S enclosed in the region of support for a uniform pdf over the region U.

underlying pdfs must also be uniform. Thus, the vectors generated by $p(x)$ within the set $\mathbf{S}$ will be uniformly distributed in $\mathbf{S}$. By synthesizing training sets for each VQ partition according to the probability of the partition and combining these sets, we generate a complete training set that has a histogram similar to that of the original training set.

The following steps outline the proposed technique for synthesizing a training set from a VQ codebook:

1. Assume that the original training set is large compared to the VQ codebook size and that the number of number of elements in it is M. If indices are entropy coded, we can estimate the probability of a codebook vector, $p(\mathbf{y}_i)$

since it is inversely proportional to the number of bits assigned to the code vector. This probability estimate multiplied with M provides the number of vectors in each partition. If an entropy coder is not used or if its parameters are unknown, we instead assume that the number of vectors in each partition cell is equal and given by $\frac{M}{k}$ where k is the number of code vectors in the codebook.

2. For a given codebook vector $\mathbf{y}_i$, random vectors are generated as described above such that they are uniformly distributed over the appropriate polytopal region.

3. The preceeding step is repeated for all the codebook vectors. The problem of generating vectors for the overload region is side-stepped by confining the problem to a finite region of support that depends on the number of partitions and their sizes.

In the above approach, we assume that the Euclidean distance metric is used in generating our training set. Euclidean distance d is defined as

$$d = (\mathbf{x}_1 - \mathbf{x}_2)^T(\mathbf{x}_1 - \mathbf{x}_2) \tag{46}$$

where $\mathbf{x}_1, \mathbf{x}_2 \in \mathbf{R}^{k\times 1}$. In many coders, weighted distance measures are used to make the VQ a more efficient. A weighted distance measure is given by

$$d = (\mathbf{x}_1 - \mathbf{x}_2)^T\mathbf{W}(\mathbf{x}_1 - \mathbf{x}_2) \tag{47}$$

where $\mathbf{W}$. A property of a distance measure is that it is always non-negative, i.e.

$$d = (\mathbf{x}_1 - \mathbf{x}_2)^T \mathbf{W} (\mathbf{x}_1 - \mathbf{x}_2) \geq 0. \tag{48}$$

This implies that $\mathbf{W}$ has to be positive semidefenite and it can thus be written as

$$\mathbf{W} = \mathbf{R}^T \mathbf{R} = \mathbf{U}^T \mathbf{\Lambda}^{T1/2} \mathbf{\Lambda}^{1/2} \mathbf{U} \tag{49}$$

where $\mathbf{U}$ is a unitary matrix with eigenvectors of $\mathbf{W}$ as its columns and is a diagonal matrix with the eigenvalues of $\mathbf{W}$ as its diagonal elements. Consequently, the weighted distance measure can be written as

$$d = (\mathbf{x}_1 - \mathbf{x}_2)^T \mathbf{R}^T \mathbf{R} (\mathbf{x}_1 - \mathbf{x}_2) \tag{50}$$

which is nothing but the Euclidean distance in the space transformed by the matrix $\mathbf{R}$. Therefore to synthesize the training set for a VQ designed using a weighted distance metric like that used in [56] or [26], we need only construct the training set as above and transform all the synthesized vectors by the matrix $\mathbf{R}^T$.

4.2 Theoretical Analysis

In the approach of the previous section, we approximate a pdf within a VQ partition cell as uniform. Here, we justify this choice. In the reverse engineering problem which motivates this work, we do not know the shape of the underlying pdf within the codebook partition. Our goal in this section is to characterize the error incurred when we use the uniform density approximation outlined above in

place of the unknown, underlying pdf. Note that this error is equivalent to the variance of the truncated pdf which describes the source distribution within the partition.

For a multidimensional pdf over a convex polytopal region, we can claim the following: (1) the mean vector is composed of the means of the marginal pdfs of the given multidimensional pdf in all dimension and (2) the variance (distortion with respect to the centroid) is the sum of the variances of the marginal pdfs. During VQ design, the partitions are formed such that the distortion in a given region is minimized. Assuming that the underlying pdf can be represented as a Gaussian Mixture Model (GMM), and that the number of codebook vectors is greater than the number of modes in the mixture, we can say that in most cases the pdf over a VQ partition is denser near the centroid (i.e. the mean). Thus, we can assume that in most partitions, the marginal density functions are either unimodal or monotonically increasing or decreasing functions. There could also be cases where the probability density is large closer to the edges of the polytope, thereby having marginal densities with minima close to the mean. These cases would be very rare, however, if we assume a reasonably large codebook size. Following the above discussion, we can thus characterize the variance (the mean square distortion in our case) of a multidimensional pdf confined to a polytopal region by characterizing the variances of the marginals.

For a given VQ codebook, we assume that the underlying pdf is smooth.

Consequently, we can further assume that the marginal pdfs are smooth and are defined over a finite interval [a, b] on the real line. Our problem then becomes one of comparing the variance of a one dimensional uniform density function to that of unimodal and monotonic density functions over a fixed interval. Seaman and Jacobson have independently shown that the variance is maximized by the uniform density for a set of unimodal functions (with some constraints)[68][69]. For the monotonic case, we first consider two examples: (1) a set of linear monotonic decreasing functions and (2) a set of truncated exponentials with varying convergence rates. For the set of linear monotonic functions, it is easily shown that the uniform density has the maximum variance. The set of linear monotonic functions can be defined as

$$f(x) = (1 + e) - 2ex \tag{51}$$

over the interval [0,1], where e is a value in the interval [0,1] and when $e = 0$, the function is the uniform density function. An example of this function is as shown in Figure 16. The variance of this function is given by

$$Var(x; f(x)) = \frac{1}{12} - \frac{e^2}{36} \tag{52}$$

and therefore

$$Var(x; u(x)) = \frac{1}{12} \geq Var(x; f(x)) \tag{53}$$

where $u(x)$ is the uniform density over the interval [0,1]. This logic can be extended to any finite interval on the real line. Considering now case (2), the pdf for the

set of truncated exponentials can be written as

$$f(x) = \left(\frac{b}{(1 - \exp(-b))} \right) \exp(-bx) \tag{54}$$

where the parameter b controls the rate of convergence of the pdf over the interval [0,1]. The interval over [0,1] is taken simply for convenience and can be easily extended to any other interval on the real line. Figure 17 shows a plot of the variance of the truncated exponential with respect to the parameter b. From this plot, we can see that the variance of the uniform pdf (the broken line in the figure) upper bounds only a certain subset of the truncated exponentials – specifically, for $0.05 < b < 4.5$. Nevertheless, we can still say that the variance of a one dimensional uniform density function (over a fixed interval) forms an upper bound with respect to the variances of a large set of unimodal and monotonic density functions defined over a common finite interval. Extending this to the multidimensional case using the marginal density argument of the previous paragraph, we can further say that the uniform density over a fixed polytopal region is likely to have higher variances and therefore form an upper bound on the distortion relative to that incurred using the true (unknown) pdf.

In the previous paragraphs, we showed that if the distortion computed using uniform density approximation over each partition provides an upper bound relative to the distortion in some common situations. Thus, the true rate distortion performance is likely to be better than the operational R-D performance esti-

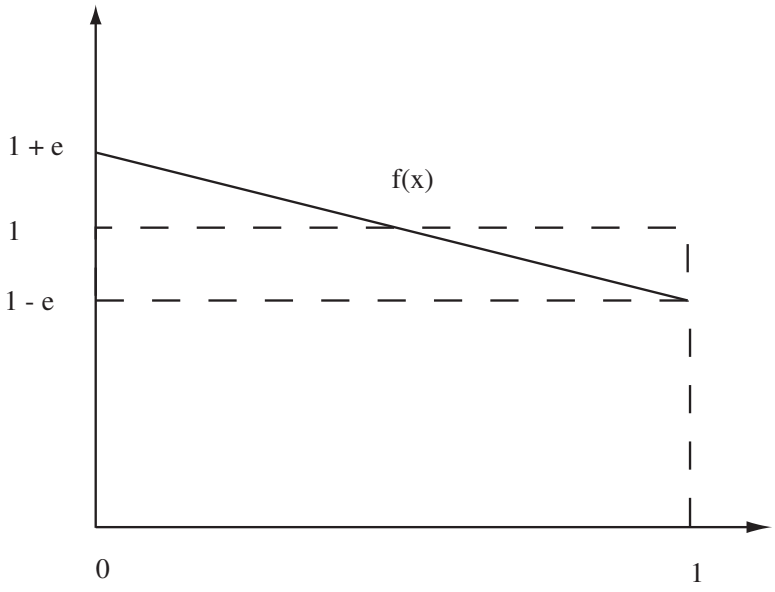

Figure 16: Plot of linear monotonically decreasing function. The parameter e controls the slope of the pdf.

mated for the synthesized training set. It has been shown that as the number of partitions is increased, the probability density in each partition approaches that of the uniform density function [70]. This implies that as the number of partitions is increased (i.e., the size of the codebook is increased), the upper bound on the distortion converges to the distortion integral of the true underlying pdf [71][72]. The rate at which this convergence occurs can be demonstrated as follows. Let $f(\mathbf{x})$ be a mixture of k Gaussian densities and $\mathbf{x} \in \mathbb{R}^n$. If we design a VQ for $f(\mathbf{x})$ assuming negligible overload distortion and k codebook vectors, an optimal VQ would very likely place a codebook vector at the mean of each Gaussian in the GMM. Each VQ cell is then a convex polytope with the mean of a Gaussian

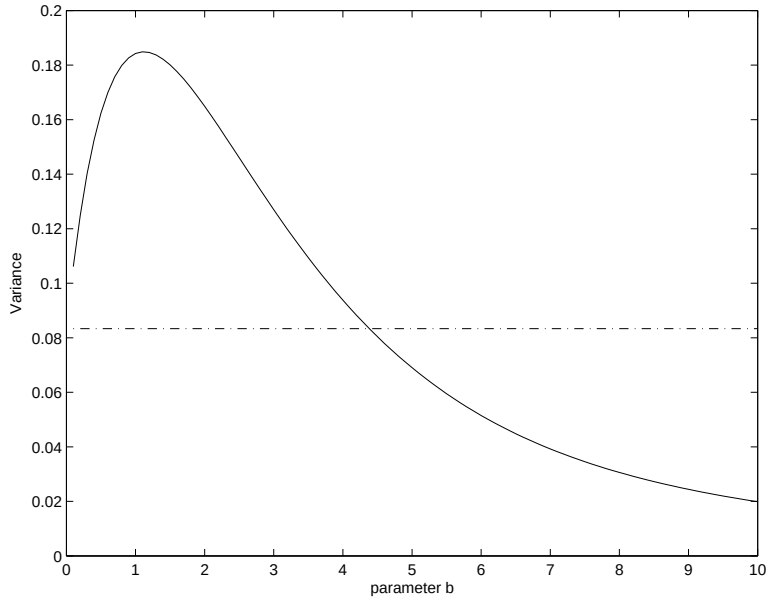

Figure 17: Plot of variance of the truncated exponential with respect to the rate parameter b. The broken line is the variance of a uniform pdf over the same interval.

element as its centroid. If we increase the number of codebook vectors, the sizes of the VQ cells at the modes of the Gaussian components decrease and new VQ cells are introduced covering the tails of the Gaussian components. Our goal is to show that if the number of VQ cells is increased then the shape of the conditional pdf over each partition rapidly approaches that of the uniform density. To do this, we first show that the conditional pdf on a VQ cell centered at the mode rapidly converges to the uniform density. Consider a one dimensional Gaussian pdf with zero mean and variance σ^2 truncated in the interval [-1, 1] and given by

$$g(x) = \frac{1}{p\sqrt{2\pi\sigma^2}} \exp\left(\frac{-x^2}{2\sigma^2}\right) \tag{55}$$

where p is a normalizing factor ensuring that $\int_{-1}^{1} g(x)dx = 1$. If $h(x)$ is a uniform pdf over the interval [-1,1], then the mean square error (MSE) between $h(x)$ and $g(x)$ is given by

$$d = \int_{-1}^{1} (g(x) - h(x))^2 dx = \int_{-1}^{1} (g^2(x) + h^2(x) - 2g(x)h(x))dx \tag{56}$$

which is found to be equivalent to

$$d = \frac{erf\left(\frac{1}{\sigma}\right)}{2\left[erf\left(\frac{1}{\sqrt{2\sigma^2}}\right)\right]} \tag{57}$$

where the erf function is the Gaussian error function. Therefore, d is a monotonically decreasing function with respect to σ. A plot of d versus the standard deviation σ is shown in Figure 18. We see from the plot that as the variance is increased, the pdf over the fixed interval rapidly converges to that of the uniform

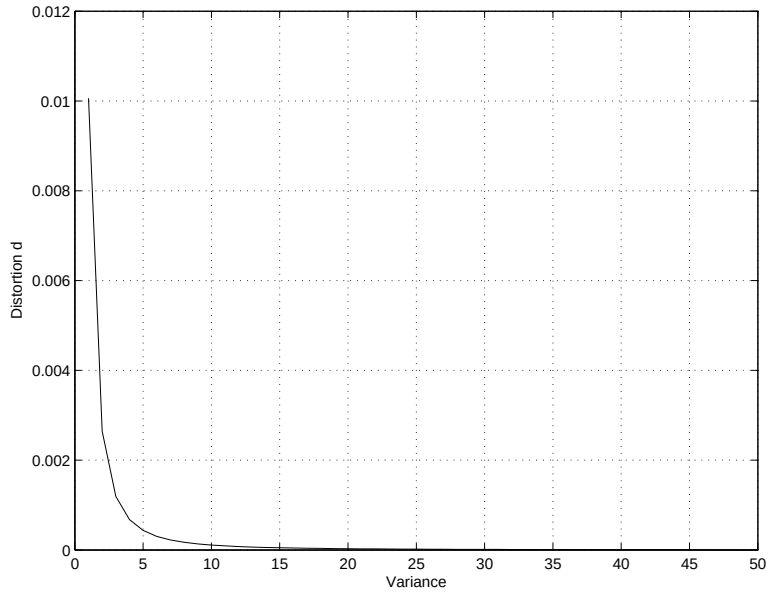

Figure 18: Plot of the mean square error between a truncated Gaussian and a uniform pdf over a fixed σ^2.

density. This analysis extends directly to multiple dimensions as follows. Let $p(x)$ be a truncated Gaussian within a polytope $\mathbf{V}$, with mean 0 and covariance matrix $\mathbf{R}$ for $\mathbf{x} \in \mathbb{R}^n$. Its density is thus given by

$$p(\mathbf{x}) = \frac{\exp\left(\frac{-\mathbf{x}^T\mathbf{R}\mathbf{x}}{2}\right)}{\int_V \exp\left(\frac{-\mathbf{y}^T\mathbf{R}\mathbf{y}}{2}\right) d\mathbf{y}} \tag{58}$$

The covariance matrix is a positive definite matrix, hence we can represent it in its spectral form as

$$\mathbf{R} = \mathbf{U}^T\mathbf{\Lambda}\mathbf{U} \tag{59}$$

where $\mathbf{U}$ is a matrix with the eigenvectors of $\mathbf{R}$ as its columns and the diagonal matrix $\mathbf{\Lambda}$ contains the eigenvalues of $\mathbf{R}$. Now, by rotating the coordinates of

the space such that the eigenvectors align with the coordinate axes, the pdf will be separable, and the diagonal elements of $\mathbf{\Lambda}$ can be viewed as the variances of the Gaussian pdfs along each coordinate axis. Clearly, as the eigenvalues of $\mathbf{R}$ increase, $\mathbf{R}^{-1} = \mathbf{U}^T\mathbf{\Lambda}^{-1}\mathbf{U}$ converges to a matrix with all its elements equal to zero. This implies that in the limit as the eigenvalues go to infinity, the pdf described in (58) goes to

$$p(x) = \frac{1}{\int_V d\mathbf{y}} = h(x) \tag{60}$$

which is the uniform distribution over the polytope V. Note that increasing the variance of the truncated Gaussian is completely analogous to reducing the size of the region of support while keeping variance constant. This is what occurs when the number of VQ partitions is increased.

4.3 Smoothed Training Set Synthesis

For a moderate to large codebook size N, the rate-distortion curves for the synthesized codebooks converge rapidly to those of the true codebooks with increasing N. For smaller values of N, however, a training set corresponding to a smooth PDF approximation should provide better performance. Such a training set can be synthesized with only small changes to proposed approach. The specific steps are as follows:

1. From the original VQ codebook, we synthesize a training set as in Section

3.2. This results in a training set that has been implicitly generated by a piecewise uniform density model.

2. To smooth the underlying piecewise uniform PDF, we use a Parzen's window function; specifically, a Gaussian window given by:

$$\varphi(\mathbf{x}) = \frac{1}{\sqrt{2\pi}} \exp\left(\frac{-\mathbf{x}^T\mathbf{R}\mathbf{x}}{2}\right) \tag{61}$$

3. To generate a training set that has a smoothed pdf we take the synthesized training set as in step 1, say $\mathbf{Y} = \{\mathbf{y}_1, \mathbf{y}_2, \ldots, \mathbf{y}_M\}$, and synthesize new training set vectors $\mathbf{X} = \{\mathbf{x}_1, \mathbf{x}_2, \ldots, \mathbf{x}_M\}$ distributed according to a PDF given by

$$\mathbf{x}_i \sim \varphi(\mathbf{x}) = \frac{1}{\sqrt{2\pi}} \exp\left(\frac{-(\mathbf{x}-\mathbf{y}_i)^T\mathbf{R}(\mathbf{x}-\mathbf{y}_i)}{2h}\right) \tag{62}$$

where h is a smoothing factor – the larger the value of h, the smoother the estimated PDF. While smoothing does not add a lot of computational complexity to training set synthesis, it does necessitate the generation of larger training sets in order to accurately represent the smooth underlying PDF.

4.4 Reverse Engineering TWIN-VQ

As detailed in chapter 3, the Twin VQ algorithm uses vector interleaving and two-channel conjugate codebooks. Thus, to obtain a training set representative of the MDCT coefficients, we need to first obtain a training set that represents the

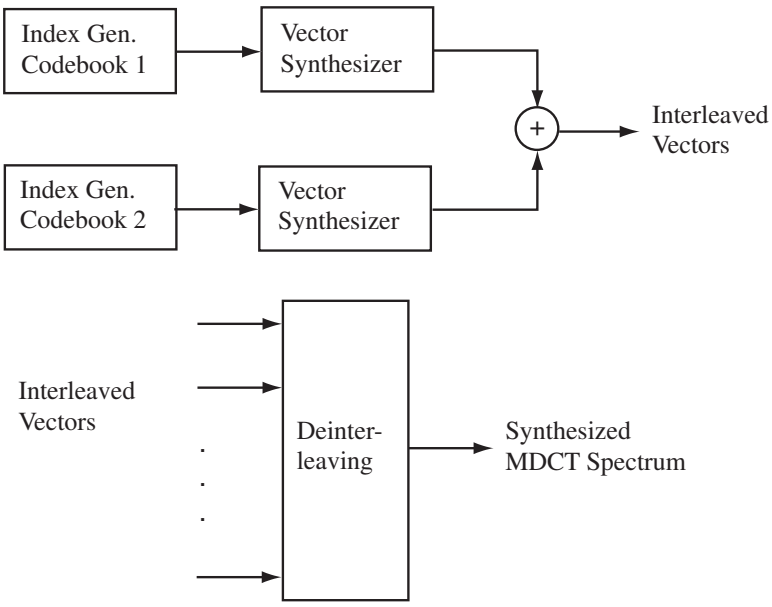

Figure 19: MDCT frame training set synthesis.

two conjugate VQs. The training sets for the conjugate VQs are then combined randomly to form the interleaved vectors, and these interleaved vectors, are deinterleaved to obtain a frame of MDCT coefficients. The two channel conjugate VQ used in the MPEG-4 Twin VQ has two codebooks of 174 codebook vectors each. Generating a training set and obtaining all the possible combinations of the training set vectors prior to deinterleaving poses a major challenge. As an example if we directly combine the conjugate VQ codebooks there are about 174×174 different combinations possible – too large a number for the synthesis procedure outlined in the previous section to handle efficiently. To overcome this difficulty, we generate the MDCT coefficient vector one at a time as discussed in the paragraphs that follow.

The block diagram as shown in Figure 19 illustrates the procedure proposed to obtain training set samples for the flattened MDCT spectrum. A random number generator first selects an index for each of the two conjugate codebooks, useing the probability information obtained from the Huffman coding tool. These indices are then passed to a vector synthesis block which generates random vectors, uniformly distributed over the quantization bin of the specified codebook vector. Combining the vectors generated for each conjugate codebook, we obtain a single interleaved vector. Since Twin VQ decomposes the 1024 size MDCT frame into 64 different interleaved subvectors, we must generate 64 different interleaved vectors as described above and then deinterleave them to obtain a single training set vector for the MDCT frame. This technique is statistically equivalent to the training set synthesis procedure mentioned in the previous section, but it saves memory space and computation by generating one MDCT spectrum vector at a time.

4.5 Experimental Verification

4.5.1 Operational Rate Distortion Curves

In this section, we present some numerical examples to demonstrate the performance of the proposed training set synthesis method. In the following experiments, we evaluate the rate distortion curves for different scenarios, comparing the original and synthesized VQs. We assume here that the underlying source pdfs are either Gaussian pdfs or mixtures of Gaussians, and we note that the distortion

integrals are calculated using the spherical invariance property of the Gaussian and a Monte Carlo technique proposed by Deak [73][74]. Figure 20 shows the operational rate-distortion (RD) curve assuming that the original source training set is generated by a symmetric 3-Dimensional Gaussian pdf. Here, the new training set is synthesized assuming that the probability of each VQ codebook vector is known (i.e. that we have access to the entropy codes). From the figure, we see that the distortion decreases with the bit-rate and that the curves for the synthesized and original designed VQ are very close together, beginning to converge at higher rates. To illustrate this more precisely, we compare in Figure 21 the two operational rate-distortion curves from Figure 20 by taking their ratio. We also plot the 95% confidence intervals. From this plot, we see that the ratio is significantly greater than one for small codebook sizes, indicating that the synthesized VQ is greatly inferior to the directly designed VQ, but we note that it tends to unity as the codebook size is increased, illustrating the expected asymptotic convergence. The same experiment is repeated for a 2-dimensional Gaussian Mixture Model with three Gaussian components, and the ratio of the RD curves for the original versus the synthesized codebooks is plotted in Figure 22. In this case, however, we plot ratios for both the smoothed and unsmoothed synthesized codebooks. As expected, smoothed training set synthesis performs considerably better than unsmoothed synthesis for smaller codebook sizes, but it performs equivalently once the codebook size exceeds 60.

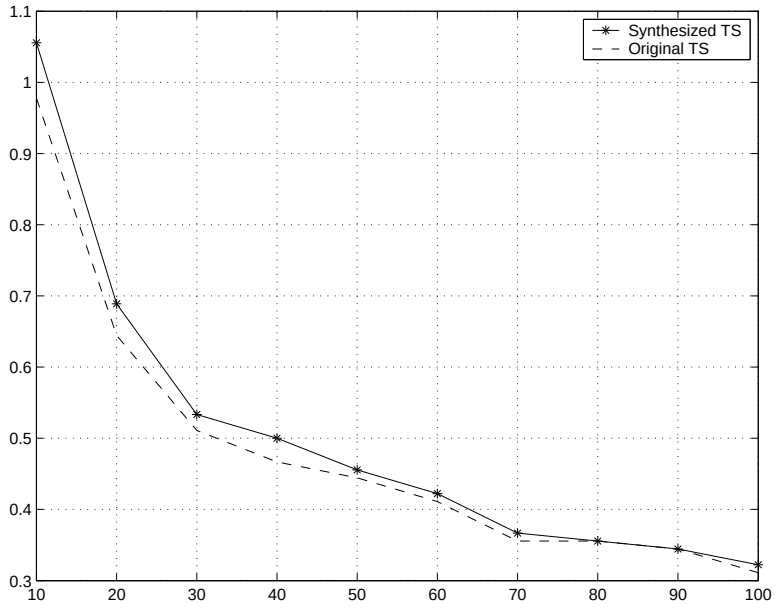

Figure 20: Plot of Rate (VQ codebook size) vs. the Distortion in Mean Squared Error for a symmetric Gaussian pdf assuming prior knowledge of the probabilities of VQ codebook vectors.

The examples above have illustrated both the utility of training set synthesis for VQ redesign and the speed with which it converges to the optimal solution as the codebook size increases. Our real interest, however, is in redesigning VQs for subspaces or transformed spaces of the original signal space – e.g., repartitioning it to describe the different subspaces formed by grouping together different elements of the original vector space. Once we have the synthesized training set, all we have to do to design the new subspace VQs is transform each of the training vectors into the appropriate space. This is much easier than directly transforming a PDF. To illustrate our approach, we perform two experiments. In the first experiment, we redesign a vector quantizer for a linearly transformed (non orthogonal) space while in the second, we create separate VQs for subspaces of the original vector space.

4.5.2 Transformed Space Vector Quantization

The contourlet transform is most commonly applied to images and is used to efficiently represent the edges within and image that have orientations other than the horizontal and vertical [75]. This contourlet transformation is implemented by first performing a pyramidal decomposition, and then applying a directional filter bank on the high frequency components of the image. In the following experiment we assume that we are already given a VQ-based scheme that encodes 512x512 grayscale images, where each vector is formed by 8x8 pixel blocks. The

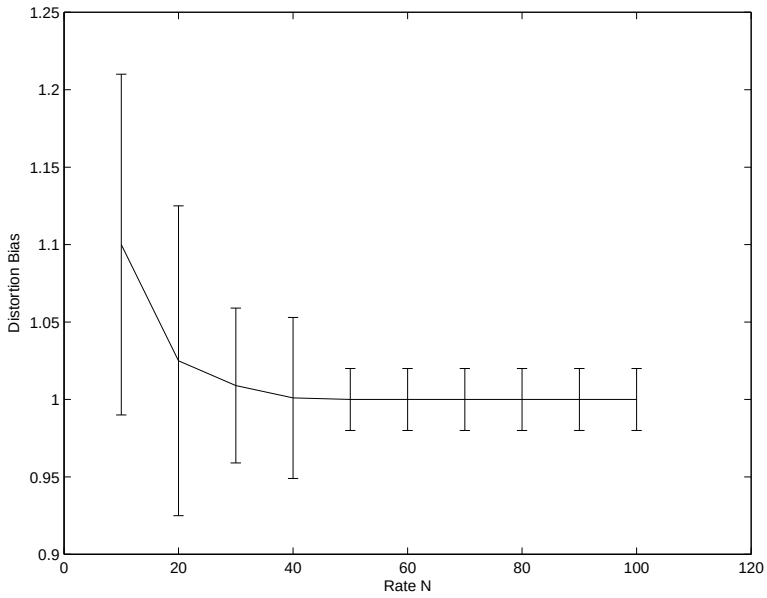

Figure 21: Plot of the rate (VQ codebook size) versus the ratio of distortion in mean squared error for a symmetric Gaussian pdf assuming prior knowledge of probabilities of VQ codebook vectors.

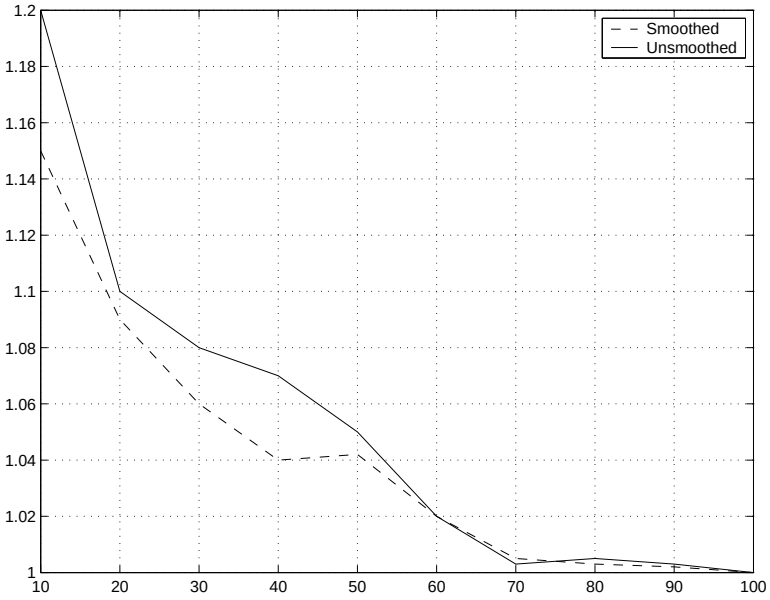

Figure 22: Plot of the rate (VQ codebook size) versus the ratio of distortion in mean squared error for a 2 dimensional Gaussian mixture assuming prior knowledge of probabilities of VQ codebook vectors. Both smoothed and unsmoothed cases are illustrated.

VQ is trained from the standard Lena, Barbara and Boats images and contains 256 codevectors. We wish to design a new image compression system that applies the contourlet transform on 8x8 pixel blocks of the original image and then uses a VQ to compress the different high frequency directional components. The simplest way to do this is to form new codebooks by directly transforming the original codebook. Let us call such a codebook the 'extracted codebook'. As an alternative, we design new codebooks from the original codebook using the proposed training set synthesis approach. To do this, we first synthesize a training set from the original codebook, transform the training set using the contourlet transformation, and finally design new codebooks for each of the transform coefficient vectors.

For the experiment presented here, the contourlet transform is performed using the Contourlet Toolbox developed by Minh Do [76]. The pyramidal filter bank and the directional filter banks are implemented using the 5-3 wavelet transform, and a three stage pyramidal transform is used to decompose the image into three different frequency subbands (one low and three high frequency subbands). The three higher frequency bands are further decomposed into 3, 8 and 16 directional subbands respectively. In the experiment presented here, we consider quantization of only the two different directional subbands obtained by doing a directional decomposition on subband-3. We label these directional subband-1 and directional subband-2. Note that the collective transform (from pyramidal filtering to

Table 1: Comparison performance (in MSE) between VQs designed using the original training set and the synthesized training set for linearly transformed data.

Directional Subbands	Optimal Redisign	Extracted Codebook	Synthesized Codebook with Probability	Synthesized Codebook without Probability
Directional Subband 1	11.32	24.82	16.28	20.92
Directional Subband 2	9.23	21.20	14.44	20.57

directional decomposition) forms a highly non-orthogonal transform – a case for which direct codevector transformation is not likely to be effective.

Given a training set, one can design VQs for any desired bit-rate. In this example, we design each of the new (lower dimensional) codebooks at the same rate as the original codebook so that the total bit-rates of both codes are the same. This results in codebooks that contain 256 code vectors each. Table 1 compares the mean square distortion for the two directional component vectors and four different cases - optimal redesign using the original training set, new codebooks that are directly extracted from the original codebook, and training set synthesis with and without entropy codes. We can see from the table that the synthesized VQ performs much better than the extracted VQ. Specifically there is 19-34% reduction in the distortion using the synthesized codebooks versus the directly extracted codebook vectors.

4.5.3 Partitioned Space Vector Quantization

In the next experiment, we design VQs for subspaces formed by repartitioning the original vector space into lower dimensional subspaces. If $\mathbf{x}$ is a vector such that $\mathbf{x} \in \mathbb{R}^n$ with elements $\mathbf{x} = [x_1, x_2, \ldots, x_n]^T$, this vector space can be repartitioned simply by regrouping its element as $\mathbf{x}_1 = [x_1, x_2, \ldots, x_l]^T$ and $\mathbf{x}_2 = [x_{l+1}, x_{l+2}, \ldots, x_n]^T$ for some integer $l < n$. Here, we generate the original training set distributed as a four dimensional, bimodal Gaussian mixture density. The location of the modes m_1, m_2 of each Gaussian density element are given by $m_1 = [0000]^T$ and $m_2 = [2321]^T$, respectively, and the covariance matrices $\mathbf{R}_1, \mathbf{R}_2$ are given by $\mathbf{R}_1 = \mathbf{I}$ (identity) and

$$\mathbf{R}_2 = \begin{bmatrix} 1 & 0.3 & 0.1 & 0 \\ 0.3 & 1 & 0.3 & 0.1 \\ 0.1 & 0.3 & 1 & 0.3 \\ 0 & 0.1 & 0.3 & 1 \end{bmatrix}$$

The first two elements of the original four dimensional vector are mapped to subspace 1 and the remaining elements to subspace 2. The VQ codebook for the full space is initially designed from the original training set using the LBG algorithm - we call this codebook the original codebook. The original training set contains 1000 vectors and the original codebook size is 20 vectors. As in the previous example, we consider two ways of designing the new codebooks: (1) directly partition the original codevectors into the required subspaces and (2) using the proposed approach to synthesize a training set, partitioning the training set into subspaces and then redesigning the codebooks for the corresponding subspaces.

Table 2: Comparison of performance (in MSE) between VQs designed using the original training set and the synthesized training sets for subspace vectors.

Subspace	Optimally Redesigned	Extracted Codebook	Synthesized With Probability	Synthesized Without Probability	Smoothed synthesis with Probability
Subspace 1	0.30	0.40	0.33	0.36	0.34
Subspace 2	0.23	0.39	0.27	0.33	0.25

We consider here both smoothed and unsmoothed training set synthesis, and we synthesize a training set containing 1000 vectors from the original codebook. After repartitioning each element of the training set into two two-dimensional vectors, new codebooks are designed for each subspace from these two synthesized sets. Finally, the codebook for each subspace contains 20 codevectors, maintaining the original code rate and allowing us to easily compare this system with that formed by directly partitioning the original codebook vectors into subvectors (labeled 'extracted codebook' in Table 2). The MSE performances are compared in Table 2. Studying the table, we note that the gain in performance achieved using training set synthesis instead of codebook extraction is significant – 9.5% to 16% for subspace 1 and 16.5% to 32% for subspace 2, depending upon the availability of code vector probabilities. Comparing smoothed and unsmoothed synthesis, we see that their relative mean squared errors are essentially the same: smoothing performs slightly worse on Subspace 1 and slightly better on Subspace 2.

We note, however, that for the results of both experiments, the performance

of training set synthesis is far below that achieved when the VQ is optimally redesigned using the original training set. With codevector probabilities, the average increase in MSE for the contourlet example is about 50% while for spatial partitioning it is about 19%. While these numbers may seem high, it is important to note that optimal redesign requires information (e.g. the original training set) which is unavailable to us. We present these comparisons here primarily to quantify how close the performance of the proposed training set synthesis approach is to that of the best possible codebook (e.g. to the upper performance bound).

4.5.4 Performance of training set synthesis within the TWIN-VQ framework

In our final experiment, our primary goal is to evaluate the performance of training set synthesis for the redesigned TWIN-VQ – we are not considering here the problem of scalable compression which will be addressed in the next chapter. Thus, for this experiment, we fix the output bitrate of the encoder to 16 kb/s. Since we have found that the most perceptually significant information lies within the first 18 critical bands or bark levels when coding at this bit rate, we design only 18 residual VQs. Each of the VQs must therefore operate at a rate of 0.5 bits per sample.

These different VQs are designed from two different training sets: (1) the training set obtained from randomly chosen audio sequences and (2) the training

Table 3: Sequences used for the TWIN-VQ experiment.

Sequence No.	Sequence Name	Genre	Duration (seconds)
1	Cliff Richards	Rock	20
2	Korn	Rock	20
3	Benetar	Rock	10
4	Erick Clapton	Rock	15
5	Beethoven 9th	Classical	20
6	Swan Lake	Classical	20
7	Nut Cracker	Classical	20
8	Cinderella	Classical	20

set synthesized by the method described in section 4.4. Specifically, we compare training set synthesis to two different training sets obtained from random audio samples. The audio sequences used for training are listed in Table 3. The first four are 20s sequences of rock music and the last four are 20s sequences of classical instrumental music. The first training set is obtained from sequences 1 and 2 and the second training set is obtained from sequences 5 and 6. Finally, the actual training vectors are obtained by applying an MDCT followed by the 2-stage TWIN-VQ prediction process using the TWIN-VQ tool of the MPEG-4 audio reference software [20]. The synthesized training set, on the other hand, is derived from the codebook of the TWIN-VQ MPEG-4 tool as described in section 4.4. All the three training sets contain 2000, 1024-dimensional vectors which are partitioned into the different critical bands. The residual VQs for each critical band are then designed from each of these different training sets and the remaining of the sequences within each genre (i.e., those not used in the VQ design

Table 4: Comparison of performance (in MSE) between TWIN-VQ systems designed using random audio data and synthesized training set from the MPEG-4 standard.

Genre	VQ designed from Seq.1 and 2	VQ designed from Seq. 5 and 6	Synthesized from MPEG-4 TWIN-VQ	Extracted Codebook
Genre 1 (Rock) Seq. 3 and 4	0.44	0.83	0.49	0.75
Genre 2 (Classical) Seq. 7 and 8	0.67	0.53	0.50	0.73

process) are encoded.

The weighted mean square error results for the VQs designed from each of the training sets are as shown in Table 4. The weighting values are calculated from the LPC spectrum and bark scale spectrum of the sequences being encoded in the same manner as in the TWIN-VQ encoder. From the first two columns, we see that the average distortion is much lower when the VQs used to encode sequences are designed using sequences of the same genre. However, the set of VQs designed by training set synthesis perform equally well for both the genres and is 36-69% better compared to the directly designed VQs when the genres are mismatched. Furthermore, training set synthesis has on the average a 33% lower MSE compared to direct codebook extraction. Clearly, the training set synthesis method results in a far more effective VQ over the unknown original training set

than the alternatives. In reality, of course, it is subjective audio quality that really matters in this application. Extensive subjective testing is presented in subsequent chapters.

5 SCALABLE TWIN-VQ CODER

Before we discuss our scalable Twin-VQ coder, we first present two important tools used in its construction: the modified discrete cosine transform and temporal noise shaping. The modified discrete cosine transform (MDCT) is used for time-frequency analysis within Twin-VQ, allowing critical bands to be extracted from the MDCT spectrum. On the other hand, non-simultaneous coding artifacts like pre-echo (described in section 5.2) are reduced by using the temporal noise shaping (TNS) tool.

5.1 Modified Discrete Cosine Transform

Cosine-modulated pseudo quadrature mirror filter banks (PQMF) have been used to create M-channel filter banks with almost perfect reconstruction properties [77][78][79]. Cosine modulated filter banks use a single lowpass, finite impulse response (FIR) prototype filter and modulate it to obtain bandpass filters. The PQMF banks have some nice properties such as, overall linear phase, uniform subband widths, low complexity of construction (one FIR filter and modulation) and critical sampling.

In the PQMF bank derivation, phase distortion is completely eliminated since by forcing the analysis and synthesis filters to satisfy the mirror image condition,

$$g_k[n] = h_k[L - 1 - n], \tag{63}$$

where $g_k[n]$ and $h_k[n]$ are the analysis and synthesis filters for the kth band. Adjacent channel aliasing is eliminating by establishing precise frequency domain positioning of the analysis and synthesis filters $H_k(z)$ and $G_k(z)$, respectively. After critical sampling, these conditions yield analysis filters given by

$$h_k[n] = 2w[n]\cos\left(\frac{\pi}{M}(k+0.5)\left(n-\frac{(L-1)}{2}\right)+\theta_k\right) \tag{64}$$

and synthesis filters given by

$$g_k[n] = 2w[n]\cos\left(\frac{\pi}{M}(k+0.5)\left(n-\frac{(L-1)}{2}\right)-\theta_k\right) \tag{65}$$

where

$$\theta_k = (-1)^k\frac{\pi}{4}$$

and $w[n]$ corresponds to an L-length, real coefficient, linear phase FIR prototype lowpass filter, with normalized cutoff frequency $\pi/2M$. Thus, the filter bank design is equivalent to designing the window $w[n]$.

The PQMF filterbank is not perfect reconstruction (PR). It is useful in audio coding applications to restrict the quantization distortion to specific frequency bands to a specific instance in time. Malvar and Vaidyanathan have independently shown that it is possible to have PR cosine modulated filterbanks [77][78]. This is done by appropriately constraining the synthesis filters $g_k[n]$, for $0 \leq k \leq M-1$. Here, we are interested in the MDCT which is a cosine modulated filterbank with $L = 2M$, where L is the length of the prototype filter and M is the number of

analysis filters. The MDCT analysis filter impulse responses are given by

$$h_k[n] = w[n]\sqrt{\frac{2}{M}}\cos\left(\frac{(2n+M+1)(2k+1)\pi}{4M}\right) \tag{66}$$

and the synthesis filters are obtained by time reversing the analysis filters, i.e,

$$g_k[n] = h_k[2M-1-n] \tag{67}$$

this is done so as to satisfy the overall linear phase constraint. While the above equations give the impulse responses of the analysis and synthesis filters for the MDCT, it is more typical to implement this transformation in a block form.

The MDCT analysis filterbank is implemented using a block transform of length $2M$ samples and is advanced by M samples. This implies that two adjacent blocks have an overlap of M samples (50%). Thus, the MDCT basis functions extend across two blocks in time, thereby virtually eliminating blocking artifacts. The MDCT is a critically sampled tranform, i.e., with a 50% overlap only M coefficients are created by the forward transform for each $2M$-sample input block. Given an input block $x[n]$, the transform coefficients $X[k]$, for $0 \leq k \leq M-1$ are given by

$$X[k] = \sum_{n=0}^{2M-1} x[n]h_k[n]. \tag{68}$$

The MDCT analysis performs a series of inner products between the M analysis filter impulse responses $h_k[n]$ and the input $x[n]$. On the other hand, the inverse MDCT obtains a reconstruction by computing a sum of basis vectors weighted

by the transform coefficients from two blocks. The first M-samples of the kth basis vectors, $h_k[n]$, for $0 \leq n \leq M-1$, are weighted by the kth coefficient of the current block, $X[k]$. Simultaneously, the second M-samples of the kth basis vector, $h_k[n]$, for $M \leq n \leq 2M-1$, are weighted by the kth coefficient of the previous block $X'[k]$. Then, the weighted basis vectors are overlapped and added at each time index n. Note that the extended basis functions require the inverse transformation to contain an M-sample memory in order to retain the previous set of coefficients. Thus, the reconstructed samples $x[n]$, for $0 \leq n \leq M-1$, are obtained by the inverse MDCT, defined as

$$x[n] = \sum_{k=0}^{M-1} \left(X[k]h_k[n] + X'[k]h_k[n+M] \right). \tag{69}$$

The analysis and synthesis filters for the MDCT are derived from a prototype FIR filter $w[n]$. The generalized PR conditions when applied to the prototype filter yields the constraints

$$\begin{aligned} w[2M-1-n] &= w[n], \text{ and} \\ w^2[n] + w^2[n+M] &= 1, \end{aligned} \tag{70}$$

for sample indexes $0 \leq n \leq M-1$. Several windows have been proposed [80][81][82][83]. The most commonly used window function for audio is the sine window, defined as

$$w[n] = \sin\left[\left(n + \frac{1}{2} \right) \frac{\pi}{2M} \right] \tag{71}$$

for $0 \leq n \leq M-1$. This window is used in standards like MPEG-1, Layer 3 (MP3), MPEG-4 AAC, and Twin-VQ.

5.2 Temporal Noise Shaping

Pre-echo distortion arises in transform coding systems which use perceptual coding rules. Pre-echoes occur when a signal with a sharp attack begins near the end of a transform block immediately following a region of low energy. Since masking thresholds are calculated and applied in the frequency domain, the quantization noise that is introduced in the frequency domain spreads evenly throughout the reconstructed block due to time-frequency uncertainty. This results in unmasked noise throughout the low energy region preceding the signal attack at the decoder.

Temporal noise shaping is a frequency domain technique to counter the effect of pre-echo distortion [84]. A linear prediction (LP) is applied across the frequency (rather than time). The parameters of a spectral LP filter $A(z)$ are estimated using the Levinson-Durbin algorithm as applied to the spectral coefficients $X(k)$. The prediction residual $e(k)$ is quantized, encoded and transmitted to the receiving end as side information. Because the convolution operation associated with the spectral domain prediction is a multiplication in the time domain, the TNS separates the time domain signal into a flat excitation signal and a multiplicative envelope corresponding to $A(z)$. This envelope is then used to shape the quantization noise introduced at the decoder so that it follows the shape of the signal's temporal power lever.

5.3 Scalable TWIN-VQ

The TWIN-VQ algorithm quantizes the flattened MDCT spectrum using interleave vector quantization and not the critical band specific quantization that would be required to achieve fidelity layering. To obtain psychoacoustic scalability within the TWIN-VQ framework, we modify the quantization and coding part as follows. Note that all of the steps of TWIN-VQ prior to quantization of the MDCT spectrum are retained. The flattened MDCT spectrum is divided into 27 sub vectors corresponding to the different critical bands of human hearing, with the size of each subvector and its corresponding frequency range shown in Table 5. These sub vectors are then quantized separately using the two-stage weighted vector quantizer shown in Figure 23, with the VQs being designed using the training set synthesis method introduced Chapter 4. For higher critical bands, the final residue signal is further encoded using a scalable lattice quantizer as described in the next section.

The residual VQ shown in Figure 23 is a two stage weighted VQ, and in each stage a two-channel conjugate VQ structure is used. The same weighting coefficients are used for both stages of the quantizer. The quantizer can be described by the unions two conjugate codebooks, $\mathbf{y} = \mathbf{y}_1 \cup \mathbf{y}_2$ and $\mathbf{z} = \mathbf{z}_1 \cup \mathbf{z}_2$ and is defined as

$$Q(\mathbf{x}) = \left(\frac{\mathbf{y}_{1i} + \mathbf{y}_{2j}}{2} \right) + \left(\frac{\mathbf{z}_{1k} + \mathbf{z}_{2l}}{2} \right) \tag{72}$$

Table 5: The size of the subband vectors per critical band and corresponding frequency range in Hz, for sampling frequency of 44.1kHz.

Critical Band	Number of Coefficients	Frequency Range (Hz)
1	4	0-86
2	4	86-172
3	4	172-258
4	4	258-344
5	4	344-430
6	4	430-516
7	4	516-603
8	4	603-689
9	8	0.69k-0.86k
10	8	0.86k-1.0k
11	8	1.0k-1.2k
12	8	1.2k-1.4k
13	16	1.4k-1.7k
14	16	1.7k-2.1k
15	16	2.1k-2.4k
16	16	2.4k-2.7k
17	32	2.7k-3.4k
18	32	3.4k-4.1k
19	32	4.1k-4.8k
20	32	4.8k-5.5k
21	64	5.5k-6.9k
22	64	6.9k-8.3k
23	64	8.3k-9.6k
24	64	9.6k-11k
25	128	11k-13.8k
26	128	13.8k-16.5k
27	256	16.5k-22k

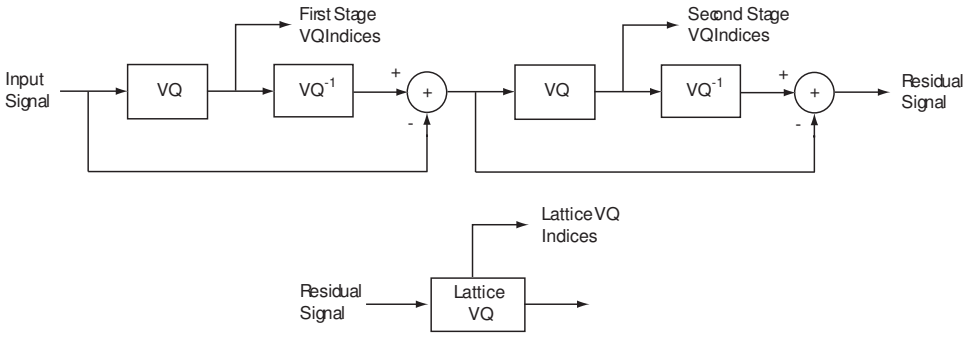

Figure 23: Two stage VQ coder followed by a lattice quantizer to generate layers of fidelity within a critical frequency band

where $Q(\mathbf{x})$ is the reconstruction value of vector $\mathbf{x}$, and i, j, k and l are indices of the codebook vectors that minimize

$$d^2 = \left[\left(\frac{\mathbf{y}_{1i} + \mathbf{y}_{2j}}{2}\right) + \left(\frac{\mathbf{z}_{1k} + \mathbf{z}_{2l}}{2}\right)\right]^T \mathbf{W} \left[\left(\frac{\mathbf{y}_{1i} + \mathbf{y}_{2j}}{2}\right) + \left(\frac{\mathbf{z}_{1k} + \mathbf{z}_{2l}}{2}\right)\right] \tag{73}$$

where $\mathbf{W}$ is a diagonal matrix containing the perceptual weighting coefficients. Note that for a two channel conjugate VQ, the reconstructed vector is represented by two codebooks. Even if only one of the codebook indices is available we can reconstruct the input signal but with reduced fidelity. Thus, a two stage residual quantizer can be viewed as having four layers of fidelity.

Perceptually transparent encoding is done by exploiting the various masking properties of the human ear, specifically the absolute threshold of hearing, simultaneous masking, and temporal masking as discussed in depth in Chapter 2. TWIN-VQ exploits absolute threshold of hearing and simultaneous masking by us-

ing the weighted VQ; our scalable TWIN-VQ does the same with both VQ stages using the same weighted distortion metric. In the original TWIN-VQ framework, forward masking issues are addressed by switching between multiple frame sizes. In our case that poses a problem since handling vectors of varying sizes would make scalability very difficult to achieve. We solve this problem by using temporal noise shaping as discussed in section 5.2.

The encoder described above quantizes each critical band with different levels of refinement; the decoder achieves fidelity scalability by reconstructing the vectors in a progressive manner. For each decoded bit rate, the bits representing the quantized coefficients are sent in a manner which maximizes the perceived improvement in audio quality, creating a perceptually layered bit stream. Note, however, that there are many ways of creating fidelity scalability using the different indices generated by the encoder, some of which are better than others.

The starting point for the scalable TWIN-VQ described above is the TWIN-VQ tool set included as part of MPEG-4 natural audio coder reference software. First, a fixed-length block of the temporal signal is transformed by the MDCT to produce a 1024 length coefficient vector. Two-stage flattening is performed using the LPC and the bark scale envelope, and the flattened MDCT coefficients are then split into subvectors corresponding to the different critical bands of human hearing as discussed in chapter 2. These subvectors are then quantized using a two-stage weighted VQ followed by a scalable lattice VQ. Thus, each critical

band is encoded by layers of indices, where each index layer signifies a level of refinement.

5.4 Lattice Quantization of the Residuals

To produce further layers of fidelity, we apply a 3 layer residual lattice quantizer to the residual signal resulting from the two previous stages of conventional vector quantization. Separate lattice quantizers are applied to the residual in each critical band in order to retain the perceptually scalable structure of the quantizer indices.

Unfortunately, it is well known that residual vector quantization becomes unproductive beyond two or three stages [21]. In our case, however, we must use another layer of VQ simply because we have so few bits available. Looking at the statistics of the final-stage residual samples, we find that they have a Laplacian-like distribution. The correlation matrix $\mathbf{R}$, calculated from the residues generated by the synthesized training set for the different subbands, indicates that the individual residual samples are largely uncorrelated. Thus, we assume here a separable multivariate Laplacian distribution underlying the residual vectors. For an n-dimensional vector $\mathbf{x} = [x_1, x_2, \ldots, x_n]$ of i.i.d Laplacian random variables x_i with zero mean and standard deviation σ, the probability density function (pdf) is given by

$$f(\mathbf{x}) = \frac{1}{(\sqrt{2}\sigma)^n} \exp\left(\frac{-\sqrt{2}}{\sigma} \sum_{i=1}^{n} |x_i|\right). \tag{74}$$

Many approaches have been used to quantize vectors generated by a Laplacian

pdf including pyramid vector quantization and piecewise uniform quantization [85][86]. In this work, we use a simple companding-based quantization scheme. Specifically, we apply a simple pdf transformation to map the Laplacian residual vector to one with a uniform distribution on the unit hypercube $[0,1]^n$ where n is the dimension of the input vector. The mapping is separable over each dimension of the input vector since (6) is separable, and it is given by:

$$y = \begin{cases} \frac{1}{2}\exp\left(\frac{\sqrt{2}x}{\sigma}\right) & \text{for } -\infty < x < 0 \\ 1 - \frac{1}{2}\exp\left(\frac{-\sqrt{2}x}{\sigma}\right) & \text{for } 0 \leq x < \infty. \end{cases} \tag{75}$$

The inverse mapping is found by inverting the above function to obtain

$$x = \begin{cases} \frac{\sigma}{\sqrt{2}}\ln 2y & \text{for } 0 \leq y \leq 0.5 \\ -\frac{\sigma}{\sqrt{2}}\ln 2(1-y) & \text{for } 0.5 \leq y \leq 1. \end{cases} \tag{76}$$

The vector that results from the mapping of (7) is then quantized using the lattice VQ.

Lattice-based VQs are generally applied to uniformly distributed sources [87][88][89], and their structure enables them to have a relatively fast encoding step. Their encoding speed has also lead to their application to quantizing nonuniformly distributed random vectors, despite their suboptimality in such cases [85][86]. Here, our primary interest is in the scalability of the bit generation process.

A lattice denoted by Λ, is a set of vectors defined by

$$\Lambda = \{\mathbf{x} : \mathbf{x} = c_1\mathbf{a}_1 + c_2\mathbf{a}_2 + \ldots + c_k\mathbf{a}_k\} \tag{77}$$

where the $\mathbf{a}_i$ are basis vectors of the lattice and c_i are integers. Thus, a lattice is a collection of vectors which can be represented as integer combinations of its

basis vectors. For the cubic (integer) lattice, the $\mathbf{a}_i$ are unit vectors orthogonal to each other. Since all integer combinations are possible, the size of the lattice is, in general, infinite. The matrix $\mathbf{G}$, composed of the row basis vectors $\mathbf{a}_i$ of lattice Λ, is called its generator matrix. The determinant of the lattice Λ is defined as

$$\det \Lambda = \left|\det \left(\mathbf{G}\mathbf{G}^T\right)\right|^{\frac{1}{2}} \tag{78}$$

where the superscript T denotes the transpose operation. The determinant of a lattice uniquely determines the volume of a Voronoi cell of the lattice. It has been shown that lattices form good representations for uniformly distributed random vectors. A practical lattice VQ is constructed by truncating the infinite lattice as (77) and scaling it to get the minimum mean square error for a given bit rate.

To obtain scalability, we use successive stages of lattice quantization. For two stages, a smooth lattice quantizer Λ_s and the coarse lattice quantizer Λ_c can be defined where

$$\Lambda_s = \left\{ \mathbf{x}_s : \mathbf{x}_s = \alpha \sum_{i=1}^{k} c_i \mathbf{a}_i,\ c_i \in \mathbf{Z} \right\} \tag{79}$$

$$\Lambda_c = \left\{ \mathbf{x}_c : \mathbf{x}_c = \sum_{i=1}^{k} c_i \mathbf{a}_i,\ c_i \in \mathbf{Z} \right\} \tag{80}$$

The smooth lattice is obtained by scaling down the coarse lattice sum by a factor $0 \leq \alpha \leq 1$. Assuming we have the same number of bits for both stages of the lattice quantizer, the codevectors will differ by only a scaling factor. In our case we use the integer lattice Z^n where the Voronoi region for each codebook vector is a hypercube of unit volume. The calculations for the scale factor for successive

quantization is simplified because the regions of integration are hypercubes. We use the techniques derived by Simon and Bosse for estimating the scale factor for a given bitrate [90]. Note that at a bit rate of 1 bit per sample, using an integer lattice is equivalent to using bit plane encoding.

6 PERCEPTUAL EMBEDDED CODING

To create a scalable coding algorithm that is truly perceptually embedded, one must carefully consider the problem of ordering the bits produced by successively quantizing the residues within and between the many critical bands. The basic situation is illustrated by the block diagram in Figure 24 in which the optimal layering of the indices I_{kj} must be determined. There are many ways of ordering the indices for example, if the ordering $(I_{11}, I_{21}, I_{31}, \ldots)$ is used then coarsely quantized coefficients are first sent in a fidelity progressive manner followed by coefficient refinements. On the other hand, the ordering $(I_{11}, I_{12}, I_{13}, \ldots)$ sends all the information about the lower frequency critical bands before information about higher frequency bands. The optimal ordering for perceptual embedding could be any one of many different orderings. To find this optimal ordering we could use one of two methods: (1) human subjective testing or (2) objective metrics. Subjective tests are generally time consuming and are impractical over such a broad range of audio fidelities; thus, objective metrics would be more appropriate here.

6.1 Objective Metrics

Many objective metrics have been proposed in literature for quantifying the perceptual quality of audio [91][92][93][94]. These objective measurement algorithms all rely on perceptual models of the human auditory system. Recently, a number

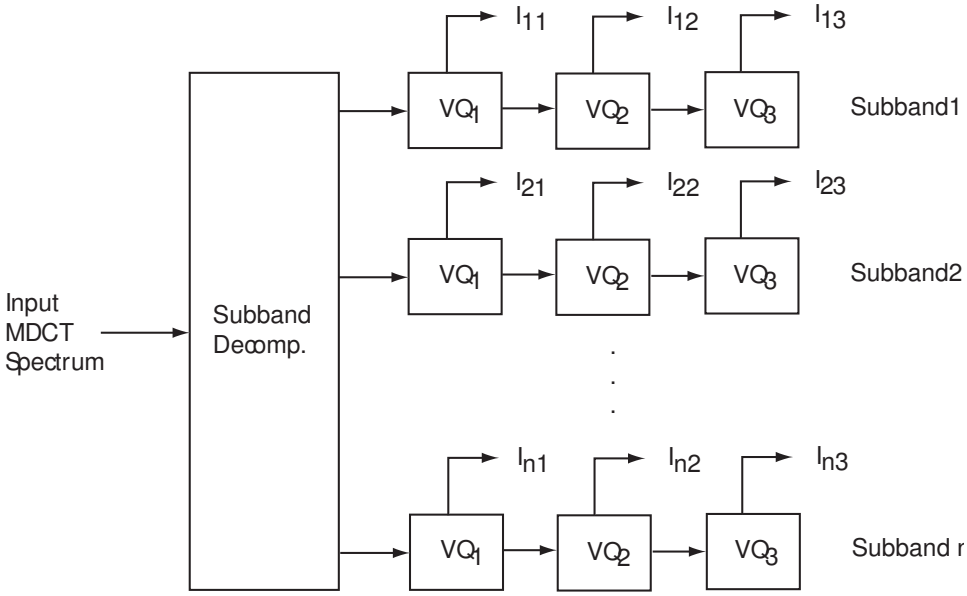

Figure 24: Block diagram showing the different index layers formed.

of these different metrics have been combined to form an objective measurement algorithm called PEAQ (perceptual evaluation of audio quality) which has been adopted by the International Telecommunication Union (ITU) as ITU-R Recommendation BS.1387-1 [95].

The final version of ITU BS.1387 includes two different quality metrics, a low complexity basic version and a more accurate, advanced version. These metrics have been optimized and validated for audio that is encoded to near-lossless quality – in other words, audio that is not significantly impaired. They have not been validated for audio that has been significantly impaired due very lossy compression [25]. Thus, these metrics are not appropriate for assessing the quality of audio that is scalably encoded for for reconstruction over a wide range of bit rates and,

consequently, audio fidelities.

6.2 Energy Equalization Approach (EEA)

A new quality assessment method for highly impaired audio was developed recently called the energy equalization approach (EEA) [25]. In this method, quantization artifacts are artificially introduced into the original audio sequence and compared with the impaired audio. A crude frequency-transform coefficient quantization method, where coefficients with magnitudes above a particular threshold T are retained and encoded, is used to introduce the impairments to the original audio sequence. The threshold T is varied until the energy of the truncated original audio signal matches that of the reconstructed audio signal. Thus, T serves as a measure of the impairment in the test signal.

To estimate the threshold, we first calculate the energy in the bandpass spectrogram of the impaired signal as follows

$$e = \sum_{i=0}^{N} \sum_{j=b_l}^{b_h} \mathbf{S}_{imp}(i,j)^2 \tag{81}$$

where $\mathbf{S}_{imp}$ is a 2-dimensional matrix containing the spectrogram of the signal being tested, i indexes the time with N time blocks and j indexes the frequency between the band limits b_l and b_h. The modified spectrum $\mathbf{S}_{mod}$ is then created by applying a threshold T to the original spectrum $\mathbf{S}_{ori}$,

$$\mathbf{S}_{mod}(i,j) = \begin{cases} \mathbf{S}_{ori}(i,j), & \text{if } |\mathbf{S}_{ori}(i,j)| \geq T \\ 0, & \text{if } |\mathbf{S}_{ori}(i,j)| < T \end{cases} . \tag{82}$$

The bandlimited energy of the modified spectrogram is thus

$$e_T = \sum_{i=0}^{N} \sum_{j=b_l}^{b_h} \mathbf{S}_{mod}(i,j)^2, \tag{83}$$

and it is compared to the energy of the impaired spectrogram given by (81). Now, to match the energies obtained by (81) and (83) an iterative optimization is performed with respect to T as follows

$$\begin{aligned} &\text{if } e_T < e_k, \text{then } T = T - \Delta \\ &\text{if } e_T > e_k, \text{then } T = T + \Delta \end{aligned} \tag{84}$$

where Δ is the step size. The threshold T^* resulting from this optimization algorithm equalizes energy given by (81) and (83).

The threshold T^* as obtained above gives us a measure of audio impairment, however, it does not give us a measurement of perceived performance. To estimate the perceptual comparisons we have to relate the threshold T^* to the subjective results obtained for the corresponding audio sequence. This is done using a linear least squares approximation method, where the subjective measures are represented as a weighted sum of estimated threshold values.

6.3 Generalized Objective Metric (GOM)

A more general objective metric (GOM) has been recently developed by Creusere, et al [96]. This metric uses the model output variables (MOVs) within the ITU standard and includes EEA as an additional MOV. Each MOV quantifies some

perceptual difference between the original audio sequence and the one reconstructed after compression. The GOM weights and linearly combines the outputs of a subset of the MOVs that is determined by a hybrid minmax/least-squares optimization procedure. MUSHRA (Multi Stimulus test with Hidden References and Anchor) subjective testing protocol, as described in the next chapter, is used for comparison. The MUSHRA protocol is accurate over a wider range of audio impairments than previous testing protocols [97].

As noted above, the ITU recommendation BS.1387 does not provide effective quality metrics over wide ranges of audio fidelity. However, the MOVs used in it measure fundamental signal qualities that are related to the perception of audio quality [91][92][93]. The GOM uses a least-squares procedure to find the optimal linear weighting for each MOV based on human subjective testing. The linear model used by the GOM to relate the MOVs and the subjective test results is given by

$$\mathbf{A}\mathbf{w} = \mathbf{p}, \tag{85}$$

where $\mathbf{p}$ is a column vector of dimension $M \times 1$ containing the average subjective scores for M audio sequences. The matrix $\mathbf{A}$ is an $M \times N$ matrix, where N is the number of MOVs used. The weight vector $\mathbf{w}$ is then determined so that the least-squares error is minimized by

$$\mathbf{w} = (\mathbf{A}^T\mathbf{A})^{-1}\mathbf{A}^T\mathbf{p}. \tag{86}$$

where $(\bullet)^T$ is the transpose operation and $(\bullet)^{-1}$ is the matrix inverse. The quality measurement of an audio sequence is thus given by

$$q = \mathbf{w}^T \mathbf{m} \tag{87}$$

where $\mathbf{m}$ is a $N \times 1$ vector containing the MOVs calculated for that sequence comparison.

The least squares solution shown above minimizes the mean square error (MSE) between the vector $\mathbf{p}$ and a vector $\mathbf{q}$ of corresponding q values as obtained by evaluating each of the M training sequences using (87). This method however, is not general and is only optimal within the training set. There is an incredible diversity of audio sequences (artists, genre, songs, etc.) and creating a training set representative of all this diversity is not feasible.

To address this issue, the GOM sacrifices performance within the training set to achieve better performance over a more general set of audio sequences. It performs a minimax optimization over a subset of MOVs but uses a linear least-squares to calculate the weights for that particular subset. The cost function used is the maximum squared error (ME) between the objective metric q and the corresponding subjective measure p. Minimizing this maximum error is like evaluating the worst case situation. To make it more robust for sequences outside the training set, the GOM considers the maximum squared error with holdout (ME-H). ME-H is calculated by finding the least square weights for the MOVs

when holding out the sequence from the training set for which the ME is being evaluated. This is done for all the sequence in the training set and the largest ME value is taken as the cost. Thus, in effect the cost is being evaluated outside the training set and the resulting weights are likely to be more robust.

The minimax algorithm can be summarized as follows:

1. A subset of MOVs is selected

2. The least-squares weight vector is calculated using (86).

3. ME is calculated over the training set as: $e = \max_{1 \leq n \leq N}(q_n - p_n)^2$ where n indexes the N test sequences while q_n and p_n are the objective and subjective metrics, respectively, of the nth audio sequence.

4. Repeat the above steps till all possible subsets of MOVs have been evaluated.

5. Choose the subset of MOVs that minimizes e.

When applied to subjective data obtained from a training set, this optimization provides better worst-case performance than the conventional linear least-squares approach. Thus, GOM forms a robust objective metric over the large range of audio impairments.

6.4 Bit Stream Optimization

The universal objective-quality metric described in the previous section is used here to find the best ordering of quantizer indices in order to obtain the optimal perceptual embedding. With respect to this metric, a greedy optimization algo-

rithm is used to perceptually layer the indices I_{kj}, starting from the lowest fidelity supported up to the highest fidelity. The objective metric compares the original and the decoded audio sequences, producing a numeric value between 0(worst possible) and 100(perfect) – the same as is used by the MUSHRA subjective test standard.

As mentioned above, there are many ways in which the indices could be layered in the encoded bitstream. We can, however, reduce the size of the optimization problem by observing a simple pattern: (1) the coarse quantization indices have to be reconstructed before the fine quantization indices and (2) given extra bits, one can either use them to refine critical bands already encoded in a coarse way or to create a coarse representation of a previously un-encoded critical band. If one represents the indices as a matrix where the rows represent the critical bands and the columns are the number of refinements for that critical band, then the optimization algorithm would proceed by layering indices from the upper left hand corner to the right and downward.

The optimization algorithm is developed as follows.

1. Within a time frame, reconstruct the coarsely encoded N frequency bands that can be supported by the lowest bitrate allowed.

2. Set Quality $Q = 0$

3. Obtain the number of bits/frame increment from a lookup table lut

4. For $i = 0$ to $i \leq N$

   (a) Refine the i^{th} band

   (b) Reconstruct the audio and evaluate the quality q

   (c) If $q >$ Q, replace Q with q and save index I_{kj} where k denotes the critical band and j denotes the bit layer

5. Reconstruct the $N + 1^{th}$ band

6. Evaluate the quality q

7. if $q >$ Q, replace Q with the current quality and save index I_{kj}

8. Add index I_{kj} to the layer ordering and bitrate = bitrate + $lut(I_{kj})$

9. Goto step (3) while the bitrate $<$ maximum bitrate

This algorithm gives us a method to obtain an effective layered embedding scheme. Obviously, it is suboptimal at any given bitrate since the layering fixed by the lower bit rates may not be optimal at the higher one. Because our goal is efficient operation over a wide range of bitrates, however this is not a concern.

7 EXPERIMENTS AND RESULTS

Seven monoaural sequences, representing a range of music types as listed in Table 6, are used to evaluate the proposed scalable encoding scheme. These sequences are sampled at 44.1 kHz with 16 bits per sample resolution. For testing of our scalable compression system, we first encode these sequences at a rate of 128 kb/s and then reconstruct the audio signals at rates of 64, 32, 24, 16 and 8 kb/s (monoaural). For comparison, we generate audio sequences using a suite of standard compression algorithms, specifically TWIN-VQ, AAC and scalable AAC-BSAC. At the reconstruction bitrate of 8 kb/s, we compare our algorithm only to the fixed-rate TWIN-VQ since it is the only standardized algorithm that can operate at this low-rate. At the rate of 16 kb/s, we compare our algorithm with both scalable AAC-BSAC (originally compressed at 64 kb/s) and with fixed-rate TWIN-VQ. Finally, at the higher bitrates of 64 and 32 kb/s we use the AAC and AAC-BSAC coders for comparison since these exhibit the best performance in this regime.

The scalable audio coder is designed as follows. At the lowest bitrate of 8 kb/s, only the first 16 critical bands are decoded. Minimum increments of 8 bits/frame can then be added to the bitstream in the optimally scalable manner as discussed in the previous chapter. For a monoaural audio sequence sampled at 44.1 kHz, this results in a bitrate resolution of 700 b/s. A lookup table with

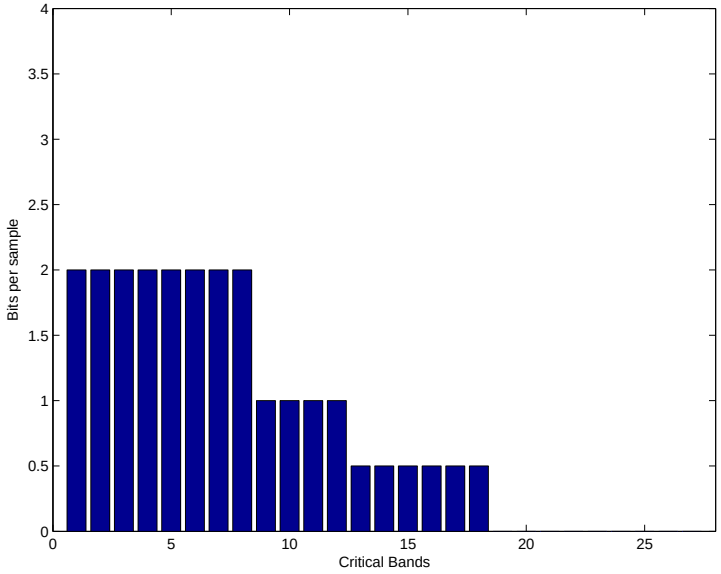

Figure 25: Bar graph showing the bits/sample allocated by the optimization program for a bitrate of 8 kb/s.

the perceptual embedding information, derived from the optimization algorithm described in the previous chapter, is used to layer the indices generated for each time frame. Bar graphs of the bit/sample allocated to each critical band by the optimization process at rates ranging from 8 – 64 kb/s is as shown in Figures 25 to 28

Human subjective testing over the different bit rates supported by our codec is performed using the state-of-the art MUSHRA (Multi Stimulus test with Hidden Reference and Anchor) testing protocol [97]. In the MUSHRA test method, a high quality reference signal is used and the systems under test are allowed to introduce significant impairments. The set of signals in a given trial consists of

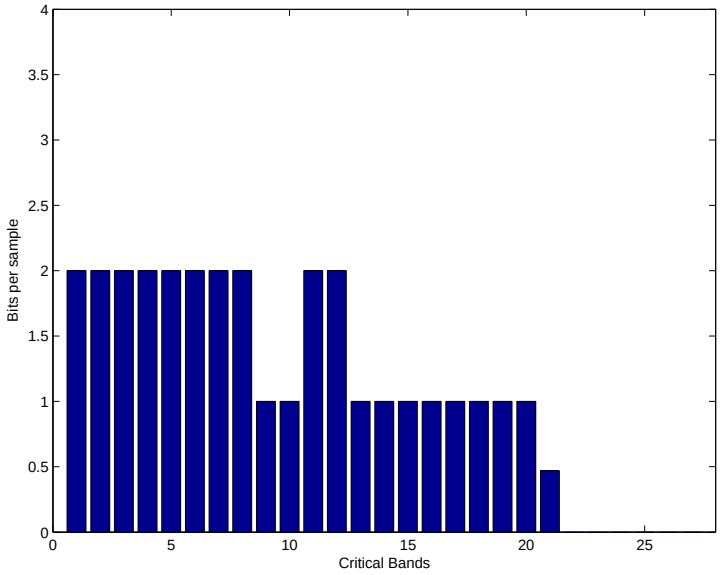

Figure 26: Bar graph showing the bits/sample allocated by the optimization program for a bitrate of 16 kb/s.

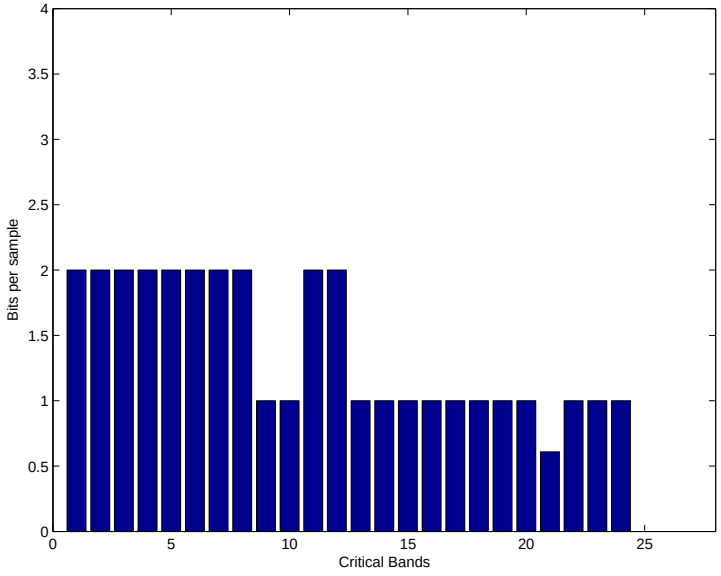

Figure 27: Bar graph showing the bits/sample allocated by the optimization program for a bitrate of 24 kb/s.

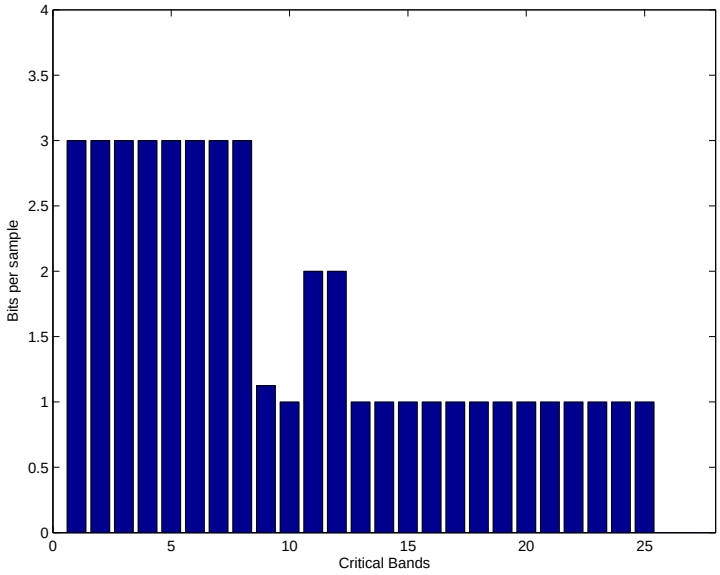

Figure 28: Bar graph showing the bits/sample allocated by the optimization program for a bitrate of 32 kb/s.

Table 6: Sequences used in subjective tests.

No.	Sequence Name	Length (seconds)	Type
1	Pat Benetar	9	Rock
2	Excalibur	24	Classical
3	Harpsichord	16	MPEG 4 test sequence
4	Quartet	23	MPEG 4 test sequence
5	Ronnie James Deo	5	Rock
6	Room with a view	15	Opera
7	2001: Space Odyssey	17	Classical

all the signals under test plus an uncompressed reference signal for comparison. A computer-controlled replay system allows the subject to instantaneously switch between the different sequences. The subjects are required to score the sequences according to the continuous quality scale (CQS), which scales from 0 to 100 with 0 as the poorest quality and 100 the best. To input the scores, a slider on an electronic display is used. The following results were obtained from 12 human test subjects. There were 27 trials per subject and each sequence was evaluated at 8, 16, 24, 32 and 64 kb/s.

Table 7: Mean scores of Scalable TWIN-VQ and fixed rate TWIN-VQ at 8kb/s.

Coder	Mean Opinion	95% Confidence Interval
Mod. TWIN-VQ	43	±11
TWIN-VQ	44	±10

Table 8: Mean scores of Scalable TWIN-VQ, AAC-BSAC and fixed rate TWIN-VQ at 16kb/s.

Coder	Mean Opinion	95% Confidence Interval
Mod. TWIN-VQ	63	±13
TWIN-VQ	71	±9
AAC-BSAC	21	±11

Table 7 compares scalable TWIN-VQ and fixed rate TWIN-VQ at a bit rate of 8kb/s averaged over all the seven sequences. From this plot, we see that the modified TWIN-VQ performs almost identically to the fixed rate TWIN-VQ at this low bitrate. The circle in the plot denotes the mean opinion score of the reconstructed audio sequences, averaged over all the different sequences and test subjects while the bars indicate the 95% confidence interval. The plot in Table 8 shows subjective test results for scalable TWIN-VQ, conventional TWIN-VQ and AAC-BSAC at 16 kb/s. From these tables we can see that the performance of

Table 9: Mean scores of Scalable TWIN-VQ, AAC-BSAC and fixed rate TWIN-VQ at 16kb/s.

Coder	Mean Opinion	95% Confidence Interval
Mod. TWIN-VQ	67	±12
AAC-BSAC	36	±9

Table 10: Mean scores for modified TWIN-VQ, AAC and AAC-BSAC at 32 kb/s.

Coder	Mean Opinion	95% Confidence Interval
Mod. TWIN-VQ	76	±11
AAC-BSAC	84	±9
AAC	93	±7

Table 11: Mean scores for modified TWIN-VQ, AAC and AAC-BSAC at 64 kb/s.

Coder	Mean Opinion	95% Confidence Interval
Mod. TWIN-VQ	82	±13
AAC-BSAC	86	±10
AAC	98	±6

the modified TWIN-VQ is close to that of fixed rate TWIN-VQ and 173% better than the scalable AAC-BSAC at the same bitrate. Table 9 compares the modified TWIN-VQ to AAC-BSAC at 24 kb/s. Here the modified TWIN-VQ performs 64% better on the average than AAC-BSAC.

At higher bitrates (32 to 64 kb/s) the scalable TWIN-VQ does not perform as well as AAC or AAC-BSAC. Tables 10 and 11 shows the mean scores and error bars associated with scalable TWIN-VQ, AAC and AAC-BSAC for a bit-rate of 32 kb/s and 64 kb/s. At these rates the AAC and AAC-BSAC perform 7-10% and 5-7% better, respectively, than scalable TWIN-VQ. Comparing Figures 8 to 11, we also note that as the bit rate increases, the quality of the audio output by the scalable TWIN-VQ improves as would that of any well-designed compression algorithm.

8 CONCLUSIONS AND FUTURE WORK

8.1 Conclusions

In the work presented here, we have modified the TWIN-VQ audio compression algorithm as described in the MPEG 4 standard to make it scalable. Subjective results show that the scalable TWIN-VQ algorithm proposed in this paper performs significantly better than scalable AAC-BSAC at bitrates of 24 kb/s or less and that it performs equivalently to the fixed rate TWIN-VQ at 8 and 16 kb/s.

We have also presented a method for reverse engineering VQs to synthesize a training set having statistics similar to those of the original training set. This synthesized training can then be used to design new VQs as is done for the scalable coder presented here. Furthermore, this technique can also approximate original source training sets for multistage systems whose final encoding stage consists of a VQ; in this case the synthesized training set need only be passed through the stages of the decoder that come after the inverse quantization stage.

The proposed encoder quantizes each critical band separately and progressively, thus creating a fine-grained scalable bit stream that is explicitly tailored to the frequency resolution of the human auditory system. By starting with the TWIN-VQ coding algorithm (long considered the best coding algorithm for non-speech audio at low bitrates), we ensure that our scalable algorithm is competitive at these low bitrates.

The major contributions of this work can be highlighted as follows:

1. We have developed a general procedure for reverse engineering vector quantizers and have used it to redesign the TWIN-VQ codebook for our new scalable coder.

2. We have developed a scalable audio coder that combines critical band-specific residual and lattice VQs to generate a fine-grained, layered bitstream specifically tailored to the frequency resolution of human auditory system.

3. We have also determined the optimal layering of the scalable bitstream using objective metrics developed to evaluate audio quality.

4. We have performed human subjective testing to rigorously quantify the performance of our scalable algorithm.

8.2 Future Work

In future work, we hope by perceptually optimizing the quantization and fidelity layering that we can create a scalable algorithm whose performance is at least equal (if not superior) to competing algorithms, both scalable and nonscalable, over a much wider range of operating bit-rates.

In addition, our scalable algorithm could be used as the basis for a joint source-channel optimized compression system. Scalability is useful since it allows the

ratio of source bits to error protection bits to be dynamically optimized to changing channel conditions. In addition, for transmission channels with fluctuating channel capacities one can use a perceptually scalable bit stream to seamlessly transition between different channel rates. Finally, one might also use the proposed coder to construct file formats that facilitate more efficient transmission of audio over heterogenous networks having differing capacities, transfer protocols and failure modes.

In the coding algorithm developed here, the perceptual optimal layering is fixed for each frame at a given bitrate. It might improve the performance if we could dynamically change the layering within each time frame to optimize the perceived audio quality. This would require the transmission of side information which could, if not properly handled, adversely affect coding performance, but such an approach could also facilitate more seamless quality transitions as the operating bit rate is dynamically adapted in real applications.

APPENDIX

Matlab codes for redesigning VQ

1. Matlab code for reverse engineering a given VQ. The following program generates a training set given a codebook.

```
function ts = tsynth(c,N,n)
%-----------------------------------------------------------
% Program to synthezie a trainig set from the VQ codebook
% Inputs: c - VQ codebook
%         N - Number of vectors/ codebook vector
%         n - nth distance measure
%-----------------------------------------------------------
[x,y] = size(c);
ts = zeros(x,0);
d = zeros(y,1);
count = 1;
ts = zeros(x,sum(N));
for i=1:y
    for j=1:y
        d(j) = sqrt((c(:,i)-c(:,j))'*(c(:,i)-c(:,j)));
    end
    d = sort(d);
    dmax = d(n);
    t = zeros(x,N(i));
    countn = 0;
    while countn~=N(i)
        rv = c(:,i)+ dmax*(rand(x,1)-0.5*ones(x,1));
        %rv = c(:,i)+ sqrt(dmax)*randn(x,1);
        for j=1:y
            drv(j) = sqrt((rv-c(:,j))'*(rv-c(:,j)));
        end
            [drvmin,index] = min(drv);
        if index == i
            countn = countn+1;
```

```
            t(:,countn) = rv;
        end
    end
    ts(:,count:count+N(i)-1) = t;
    count = count+N(i);
end
```

2. Program to synthesize the MDCT spectrum from conjugate codebooks.

```
function ts = mdct_synth(c1,c2,N,n)
%-------------------------------------------------------
% Program to synthezie a trainig vector for a 1024 point
% MDCT spectrum
% Inputs: c1 - Conjugate codebook 1
%         c2 - Conjugate codebook 2
%         n - nth distance measure
%         k - number of interleaved vectors
%-------------------------------------------------------
[x,y] = size(c1);
ts = zeros(1024,1);
d = zeros(y,1);
count = 1;
for j=1:y
    d(j) = sqrt((c1(:,i)-c1(:,j))'*(c1(:,i)-c1(:,j)));
end
d = sort(d);
dmax = d(n);

%-------------------------------------------
% Number of code vector elemtents to be read
%-------------------------------------------
cn = 1024/k;
t = zeros(cn,k);

%----------------------------
% Synthesizing the subvectors
%----------------------------
for i = 1:k
    dummy = randperm(y);
    index1 = dummy(1);
```

```
    index2 = dummy(2);
    rv1 = c1(1:cn,index1)+ dmax*(rand(cn,1)-0.5*ones(cn,1));
    rv2 = c2(1:cn,index2)+ dmax*(rand(cn,1)-0.5*ones(cn,1));
    rv = (rv1+rv2)/2;
    t(:,i) = rv;
end

%--------------------------
% Interleaving the vectors
%--------------------------
for i=1:x
    for j=1:y
        ts(count) = t(i,j);
        count = count+1;
    end
end
```

3. Program to design a VQ from a training set

```
function [c,N] = lloyd_lbg(ts,inc,tol)
%-----------------------------------------------
% Generalised Lloyd algorithm
% [new codebook] =
% lloyd_demo(training set, initial cb, tolerance);
%-----------------------------------------------
%------------
% Initialize
%------------
c = zeros(size(inc));
N = zeros(length(inc),1);

%-------------
% Distortions
%-------------
D_v = zeros(length(N),1); % Distortion in each cluster
D_t = inf; % Total Distortion
D_n = 10000000;
%-----------------
% Lloyd iteration
%-----------------
```

```
while abs(D_t - D_n) > tol | D_t - D_n < 0
    D_t = D_n;
    %--------
    % Encode
    %--------
    for i=1:length(ts)
        Di = 0; % Distortion for encoding
        Dj = inf;
        for j=1:length(inc)
            Di = (ts(:,i)-inc(:,j))'*(ts(:,i)-inc(:,j));
            if Dj>Di
                index = j;
                Dj = Di;
            end
        end
        % Nearest Neighbours
        c(:,index) = c(:,index) + ts(:,i);
        N(index) = N(index)+1;
        D_v(index) = D_v(index)+ Dj;
    end
    %----------------------
    % Empty Cell Condition
    %----------------------
    if min(N) == 0
        flag = 1;
        [v,u] = max(N);
        blah = inc(:,u);
        for k = 1:length(inc)
            if N(k)==0
                N(k) = 1;
                c(:,k) = blah + randn(size(blah));
            end
        end
    end
    [len,wid] = size(inc);
    for w = 1:len
       c(w,:) = c(w,:)./N';
    end
    inc = c;
    in = N;
    D_n = sum(D_v);
```

```
    c = zeros(size(c));
    N = zeros(size(N));
    D_v = zeros(size(D_v));
end
c = inc;
N = in;
```

4. A sample program to plot the rate distortion curves for the synthesized and original training sets

```
clear;clc;close all;
%-------------------------------------------------------------
% Program to find the rate distortion for the synthesized VQs
%-------------------------------------------------------------
N = 10:10:100;
its = 4*randn(2,400);
Do = zeros(length(N));
Dt = zeros(length(N));

for i = 1:length(N)
    [c,prob] = lloyd_lbg(its,randn(2,N(i)),0.00001);
    ts_synth = tsynth(c,prob,3);
    [c_rv,prob_r] = lloyd_lbg(ts_synth,randn(2,N(i)),0.00001);
    [blah,Do(i)] = vq_enc(4*randn(2,1000),c);
    [blah,Dt(i)] = vq_enc(4*randn(2,1000),c_rv);
end

plot(N,Do,'ro-'); hold on;
plot(N,Dt,'bx--'); hodl off; grid on;
title('Rate Distortion Comparison for
       Original and Synthesiszed VQs');
xlabel('Rate N');
ylabel('Average Distortion');
```

C programs to implement the TWIN-VQ algorithm

1. The following C function deinterleaves the input spectrum, perceptual weights.

```
 void ntt_div_vec(
  int nfr, /* Param. : block length*/
  int nsf, /* Param. : number of sub frames */
  int cb_len, /* Param. : codebook length */
  int cb_len0, /* Param.*/
  int idiv, /* Param. */
  int ndiv, /* Param. : number of interleave division */
  double target[], /* Input */
  double d_target[], /* Output */
  double weight[], /* Input */
  double d_weight[], /* Output */
  double add_signal[], /* Input */
  double d_add_signal[], /* Output */
  double perceptual_weight[], /* Input */
  double d_perceptual_weight[]) /* Output */
{
  /*--- Variables ---*/
  int  icv, ismp, itmp;
  /*--- Parameter settings ---*/
  for (icv=0; icv<cb_len; icv++) {
    /*--- Set interleave ---*/
    if ((icv<cb_len0-1) &&
    ((ndiv%nsf==0 && nsf>1) || ((ndiv&0x1)==0 && (nsf&0x1)==0)))
      itmp = ((idiv + icv) % ndiv) + icv * ndiv;
    else itmp = idiv + icv * ndiv;
    ismp = itmp / nsf + ((itmp % nsf) * nfr);

    /*--- Vector division ---*/
    d_target[icv] = target[ismp];
    d_weight[icv] = weight[ismp];
    d_add_signal[icv] = add_signal[ismp];
    d_perceptual_weight[icv] = perceptual_weight[ismp];
  }
}
```

2. Function following function normalizes the MDCT spectrum and calls the pre-

and main-selection functions.

```
void ntt_vq_pn(/* Parameters */
           int    nfr, /* block length */
           int    nsf, /* number of sub frames */
           int    available_bits, /* available bits for VQ */
           int    n_can, /* number of pre-selection candidates */
           double *codev0, /* code book0 */
           double *codev1, /* code book1 */
           int    cb_len_max, /* maximum code vector length */

           /* Input */
           double target[],
           double lpc_spectrum[], /* LPC spectrum */
           double bark_env[],     /* Bark-scale envelope */
           double add_signal[],   /* added signal */
           double gain[],
           double perceptual_weight[],

           /* Output */
           int    index_wvq[])
{
  /*--- Variables ---*/
  int    ismp, isf, idiv, ndiv, top, block_size;
  int    bits, pol_bits0, pol_bits1, cb_len, cb_len0;
  int    can_ind0[ntt_N_CAN_MAX], can_ind1[ntt_N_CAN_MAX];
  int    can_sign0[ntt_N_CAN_MAX], can_sign1[ntt_N_CAN_MAX];
  double weight[ntt_T_FR_MAX], d_weight[ntt_CB_LEN_MAX];
  double d_add_signal[ntt_CB_LEN_MAX];
  double d_target[ntt_CB_LEN_MAX];
  double d_perceptual_weight[ntt_CB_LEN_MAX];

  /*--- Parameter settings ---*/
  block_size = nfr * nsf;
  ndiv = (int)((available_bits+ntt_MAXBIT*2-1)/(ntt_MAXBIT*2));
  cb_len0 =  (int)((block_size + ndiv - 1) / ndiv);

  /*--- Make weighting factor ---*/
  for (isf=0; isf<nsf; isf++){
    top = isf * nfr;
```

```
  for (ismp=0; ismp<nfr; ismp++){
  weight[ismp+top] =
  gain[isf] * bark_env[ismp+top] / lpc_spectrum[ismp+top];
  }
}
printf("Number of ivisions = %d",ndiv);
/*--- Sub-vector division loop ---*/
for (idiv=0; idiv<ndiv; idiv++){
  /*--- set codebook lengths and sizes ---*/
  cb_len = (int)((block_size + ndiv - 1 - idiv) / ndiv);
  bits = (available_bits+ndiv-1-idiv)/ndiv;
  pol_bits0 = ((bits+1)/2)-ntt_MAXBIT_SHAPE;
  pol_bits1 = (bits/2)-ntt_MAXBIT_SHAPE;

  /*--- vector division ---*/
  ntt_div_vec(nfr, nsf, cb_len, cb_len0, idiv, ndiv,
      target, d_target,
      weight, d_weight,
      add_signal, d_add_signal,
      perceptual_weight, d_perceptual_weight);

  /*--- pre selection ---*/
  ntt_vq_pre_select(cb_len, cb_len_max, pol_bits0, codev0,
            d_target, d_weight, d_add_signal, d_perceptual_weight,
            n_can, can_ind0, can_sign0);

  ntt_vq_pre_select(cb_len, cb_len_max, pol_bits1, codev1,
            d_target, d_weight, d_add_signal, d_perceptual_weight,
            n_can, can_ind1, can_sign1);

  /*--- main selection ---*/
  ntt_vq_main_select(cb_len, cb_len_max,
             codev0, codev1,
             n_can, n_can,
             can_ind0, can_ind1,
             can_sign0, can_sign1,
             d_target, d_weight, d_add_signal,
             d_perceptual_weight,
             &index_wvq[idiv], &index_wvq[idiv+ndiv]);
}}
```

3. The following function implements the first part or the pre-selection for the fast TWIN-VQ encoding technique.

```
#define OFFSET_GAIN 1.3
void ntt_vq_pre_select(/* Parameters */
               int    cb_len, /* code book length */
               int    cb_len_max, /* maximum code vector length */
               int    pol_bits,
               double *codev, /* code book */
               /* Input */
               double d_target[],
               double d_weight[],
               double d_add_signal[],
               double d_perceptual_weight[],
               int    n_can,
               /* Output */
               int    can_ind[],
               int    can_sign[])
{
  /*--- Variables ---*/
  double xxp, xyp, xxn, xyn;
  double recp, recn;
  double pw2;
  double *p_code;
  int    icb, ismp;
  double max_t[ntt_N_CAN_MAX];
  double code_targ_tmp_p, code_targ_tmp_n, dtmp;
  double code_targ[ntt_CB_SIZE];
  int    code_sign[ntt_CB_SIZE];
  int    i_can, j_can, tb_top, spl_pnt;

  /*--- Distance calculation ---*/
  for (icb=0; icb<ntt_CB_SIZE; icb++){
    xxp=xyp=xxn=xyn = 0.0;
    code_targ_tmp_p = code_targ_tmp_n = 0.;
    p_code = &(codev[icb*cb_len_max]);
    for (ismp=0; ismp<cb_len; ismp++){
      pw2 = d_perceptual_weight[ismp] * d_perceptual_weight[ismp];

      recp =(d_add_signal[ismp] + p_code[ismp]
```

```
            * d_weight[ismp]) * OFFSET_GAIN;
      xxp = recp * recp;
      xyp = recp * d_target[ismp];
      code_targ_tmp_p +=
                pw2 * (4.0 * xyp - xxp);

      recn =(d_add_signal[ismp] - p_code[ismp]
             * d_weight[ismp]) * OFFSET_GAIN;
      xxn = recn * recn;
      xyn = recn * d_target[ismp];
      code_targ_tmp_n +=
                pw2 * (4.0 * xyn - xxn);
    }
    if ((pol_bits==1) && (code_targ_tmp_n>code_targ_tmp_p)){
      code_targ[icb] = code_targ_tmp_n;
      code_sign[icb] = 1;
    }
    else{
      code_targ[icb] = code_targ_tmp_p;
      code_sign[icb] = 0;
    }
  }

  /*--- Pre-selection search ---*/
  if (n_can < ntt_CB_SIZE){
    max_t[0] = -1.e30;
    can_ind[0] = 0;
    tb_top = 0;
    for (icb=0; icb<ntt_CB_SIZE; icb++){
      dtmp = code_targ[icb];
      if (dtmp>max_t[tb_top]){
    i_can = tb_top; j_can = 0;
    while(i_can>j_can){
      spl_pnt = (i_can-j_can)/2 + j_can;
      if (max_t[spl_pnt]>dtmp){
        j_can = spl_pnt + 1;
      }
      else{
        i_can = spl_pnt;
      }
    }
```

```
    tb_top = ntt_min(tb_top+1, n_can-1);
    for (j_can=tb_top; j_can>i_can; j_can--){
      max_t[j_can] = max_t[j_can-1];
      can_ind[j_can] = can_ind[j_can-1];
    }
    max_t[i_can] = dtmp;
    can_ind[i_can] = icb;
      }
    }
    /*--- Make output ---*/
    for (i_can=0; i_can<n_can; i_can++){
      can_sign[i_can] = code_sign[can_ind[i_can]];
    }
  }
  else{
    for (i_can=0; i_can<n_can; i_can++){
      can_ind[i_can] = i_can;
      can_sign[i_can] = code_sign[i_can];
    }
  }
}
```

4. The second part or the main-selection part of the fast TWIN-VQ encoding algorithm.

```
void ntt_vq_main_select(/* Parameters */
            int    cb_len,       /* code book length */
            int    cb_len_max,   /* maximum code vector length */
            double *codev0,      /* code book0 */
            double *codev1,      /* code book1 */
            int    n_can0,
            int    n_can1,
            int    can_ind0[],
            int    can_ind1[],
            int    can_sign0[],
            int    can_sign1[],
                        /* Input */
            double d_target[],
            double d_weight[],
```

```
            double d_add_signal[],
            double d_perceptual_weight[],
            /* Output */
            int    *index_wvq0,
            int    *index_wvq1)
{
  /*--- Variables ---*/
  int    ismp, i_can, j_can;
  int    index0, index1, i_can0, i_can1;
  double dist_min, dist;
  double *codev0_p, *codev1_p;
  double pw2, sign0, sign1, reconst;

  /*--- Best codevector search ---*/
  dist_min = 1.e100;
  for (i_can=0; i_can<n_can0; i_can++){
    codev0_p = &(codev0[can_ind0[i_can]*cb_len_max]);
    sign0 = 1. - (2. * can_sign0[i_can]);
    for (j_can=0; j_can<n_can1; j_can++){
      codev1_p = &(codev1[can_ind1[j_can]*cb_len_max]);
      sign1 = 1. - (2. * can_sign1[j_can]);
      dist = 0.;
      for (ismp=0; ismp<cb_len; ismp++){
    pw2 = d_perceptual_weight[ismp]
          * d_perceptual_weight[ismp];

    reconst = d_add_signal[ismp]
      + 0.5 * d_weight[ismp] *
        (sign0 * codev0_p[ismp] + sign1 * codev1_p[ismp]);

    dist += pw2 * (d_target[ismp] - reconst)
                * (d_target[ismp] - reconst);
      }
      if (dist < dist_min){
    dist_min = dist;
    i_can0 = i_can;
    i_can1 = j_can;
    index0 = can_ind0[i_can0];
    index1 = can_ind1[i_can1];
      }
    }
```

```
  }

  /*--- Make output indexes ---*/
  *index_wvq0 = index0;
  *index_wvq1 = index1;
  if(can_sign0[i_can0] == 1)
    *index_wvq0 += ((0x1)<<(ntt_MAXBIT_SHAPE));
  if(can_sign1[i_can1] == 1)
    *index_wvq1 +=  ((0x1)<<(ntt_MAXBIT_SHAPE));
}
```

5. The main TWIN-VQ quantize program

```
#include "ntt_conf.h"
#include "ntt_encode.h"
#include "all.h"

void ntt_tf_quantize_spectrum(
  double spectrum[], /* Input : spectrum*/
  double lpc_spectrum[], /* Input : LPC spectrum*/
  double bark_env[], /* Input : Bark-scale envelope*/
  double pitch_sequence[], /* Input : periodic peak components*/
  double gain[], /* Input : gain factor*/
  double perceptual_weight[], /* Input : perceptual weight*/
  ntt_INDEX *index) /* In/Out : VQ code indices */
{
  /*--- Variables ---*/
  int    ismp, nfr, nsf, n_can, vq_bits;
  double add_signal[ntt_T_FR_MAX];
  double *sp_cv0, *sp_cv1;
  int    cb_len_max;

  /*--- Parameter settings ---*/
  switch (index->w_type){
  case ONLY_LONG_WINDOW:
  case LONG_SHORT_WINDOW:
  case SHORT_LONG_WINDOW:
  case LONG_MEDIUM_WINDOW:
  case MEDIUM_LONG_WINDOW:
```

```
  /* available bits */
  vq_bits = ntt_VQTOOL_BITS;
  /* codebooks */
  sp_cv0 = (double *)ntt_codev0;
  sp_cv1 = (double *)ntt_codev1;
  cb_len_max = ntt_CB_LEN_READ + ntt_CB_LEN_MGN;

  /* number of pre-selection candidates */
  n_can = ntt_N_CAN;
  /* frame size */
  nfr = ntt_N_FR;
  nsf = ntt_N_SUP;
  /* additional signal */
  for (ismp=0; ismp<ntt_N_FR*ntt_N_SUP; ismp++){
    add_signal[ismp] = pitch_sequence[ismp] / lpc_spectrum[ismp];
  }
  break;
  case ONLY_SHORT_WINDOW:
  /* available bits */
  vq_bits = ntt_VQTOOL_BITS_S;
  /* codebooks */
  sp_cv0 = (double *)ntt_codev0s; sp_cv1 = (double *)ntt_codev1s;
  cb_len_max = ntt_CB_LEN_READ_S + ntt_CB_LEN_MGN;
  /* number of pre-selection candidates */
  n_can = ntt_N_CAN_S;
  /* number of subframes in a frame */
  nfr = ntt_N_FR_S;
  nsf = ntt_N_SUP * ntt_N_SHRT;
  /* additional signal */
  ntt_zerod(ntt_N_FR*ntt_N_SUP, add_signal);
  break;
default:
  fprintf(stderr,"ntt_sencode(): %d:
          Window mode error", index->w_type);
  exit(1);
}

/*--- Vector quantization process ---*/
ntt_vq_pn(nfr, nsf, vq_bits, n_can,
      sp_cv0, sp_cv1, cb_len_max,
      spectrum, lpc_spectrum, bark_env, add_signal, gain,
```

```
        perceptual_weight,
        index->wvq);
}
```

6. Residual quantization including scalar quantization

```
void sri_vq_coder(
   int cb_len_max,
   double *codev0, /*codebook 0*/
   double *codev1, /*codebook 1*/
   /* Input */
   double target[],
   double weight[],
   double add_signal[],
   double perceptual_weight[],
   /* Output Index */
   int *sri_vq_index)
{
   int i,j;
   int sri_can_ind0[6], sri_can_ind1[6],
       sri_can_sign0[6], sri_can_sign1[6];
   int sri_n_bands = 18, cumulant = 0;
   int sri_band_size[18] =
       {4,4,4,4,4,4,4,4,8,8,8,8,16,16,16,16,32,32};

   int mask, index0, index1, pol0, pol1; /* Reconstructing VQ */

   /* Residual quantizing */
   double delta, sri_temp;

   double sri_d_target[32], sri_d_weight[32], sri_d_add_signal[32];
   double sri_d_perceptual_weight[32];
   double sri_reconst[1024];
   for(i=0;i<1024;i++)
      sri_reconst[i] = 0.0;

   delta = 6000.0/128.0;

   mask = (0x1 << ntt_MAXBIT_SHAPE) - 1;
```

```
/* Split bands and quantize */
for(i=0;i<sri_n_bands;i++)
{
   for(j=0;j<sri_band_size[i];j++)
   {
       sri_d_target[j] = target[cumulant+j];
       sri_d_weight[j] = weight[cumulant+j];
       sri_d_add_signal[j] = add_signal[cumulant+j];
       sri_d_perceptual_weight[j]
                    = perceptual_weight[cumulant+j];
   }


   /* Quantize Spectrum */
   /* pre-select */
   ntt_vq_pre_select(
                sri_band_size[i], cb_len_max,
                1, codev0, sri_d_target,
                sri_d_weight, sri_d_add_signal,
                sri_d_perceptual_weight,
                6, sri_can_ind0, sri_can_sign0);

   ntt_vq_pre_select(
                sri_band_size[i], cb_len_max, 1, codev1,
                sri_d_target, sri_d_weight, sri_d_add_signal,
                sri_d_perceptual_weight,
                6, sri_can_ind1, sri_can_sign1);

   /* Main Selection */
   ntt_vq_main_select(
                sri_band_size[i], cb_len_max,
                codev0, codev1,6,6,
                sri_can_ind0, sri_can_ind1,
                sri_can_sign0, sri_can_sign1,
                sri_d_target, sri_d_weight,
                sri_d_add_signal,
                sri_d_perceptual_weight,
                sri_vq_index+sri_ind_c,
                sri_vq_index+sri_ind_c+1);

   /****   Sri Reconstruct   ****/
```

```
      index0 =
         (sri_vq_index[sri_ind_c]) & mask;
      index1 =
         (sri_vq_index[sri_ind_c+1]) & mask;
      pol0 = 1 - 2*((sri_vq_index[sri_ind_c]
             >> (ntt_MAXBIT_SHAPE)) & 0x1);
      pol1 = 1 - 2*((sri_vq_index[sri_ind_c+1]
             >> (ntt_MAXBIT_SHAPE)) & 0x1);
      for(j=0;j<sri_band_size[i];j++)
      {
         sri_reconst[cumulant+j] =
                     (pol0*codev0[index0*cb_len_max+j]
                     +pol1*codev1[index1*cb_len_max+j])*0.5;
      }

      sri_ind_c = sri_ind_c+2;
      cumulant = cumulant+sri_band_size[i];
   }
   for(i=0;i<1024;i++)
   {
      sri_temp = ((target[i]-add_signal[i])
                 /weight[i])-sri_reconst[i];
      if(sri_temp < 0)
      {
         sri_temp = (-1.0)*sri_temp;
         if(sri_temp > 6000.0)
            sri_temp = 6000.0;
         sri_residue[sri_frame_n*1024+i]
             = (int) sri_temp/delta;
      }
      else
      {
         if(sri_temp > 6000.0)
            sri_temp = 6000.0;
         sri_residue[sri_frame_n*1024+i]
             = (int)sri_temp/delta + 128;
      }

   }
   sri_frame_n++;
}
```

7. Main frame by frame time frequency encoder. This program has been modified to read in the new codebooks and save the residual quantization indices.

```
#ifndef MONO_CHAN
#define MONO_CHAN 0
#endif

/* ---------- Variable for Sri Coder --------*/

char sri_out_file[100];

/*double sri_codebook[512][1024];
int *sri_index;
int sri_ind;
int sri_frame;
int sri_no_of_bands = 27;
int sri_bits_per_band[] =
9,9,9,9,9,9,9,9,9,9,9,9,9,9,9,9,9,9,9,9,9,9,9,9,9,9,9;
int b;
int fr_cnt=0;
int sri_frame_count=0;
int id_cnt=0;
int sri_reconst_flag=0;
int sri_band_size[28] =
              0,
            256,
            384,
            512,
            576,
            640,
            704,
            768,
            800,
            832,
            864,
            896,
            912,
            928,
            944,
            960,
```

```
            968,
            976,
            984,
            992,
            996,
            1000,
            1004,
            1008,
            1012,
            1016,
            1020,
            1024;*/

double sri_max = 0., sri_min = 0.;
void sri_init(int);
void sri_save(int);
int *sri_vq_index;
int sri_ind_c = 0;
int sri_frame, sri_frame_n = 0;
int sri_reconst_flag = 0;
int sri_nbands = 18;
int *sri_residue;

/* ---------- functions ---------- */

/* Encode() */
/* Encode audio file and generate bit stream. */
/* (This function evaluates the global
    xxxDebugLevel variables !!!) */

static int Encode (
  char *audioFileName, /* in: audio file name */
  char *bitFileName, /* in: bit stream file name */
  char *codecMode, /* in: codec mode string */
  float bitRate, /* in: bit rate [bit/sec] */
  int varBitRate, /* in: variable bit rate */
  int bitReservSize, /* in: bit reservoir size [bit] */
  int bitReservInit, /* in: initial bit reservoir bits */
  char *encPara, /* in: encoder parameter string */
  char *info, /* in: info string for bit stream */
  int noHeader, /* in: disable bit stream header */
```

```
  char *magicString, /* in: bit stream magic string */
  float regionStart, /* in: start time of region */
  float regionDurat, /* in: duration of region */
  int numChannelOut,
  /* in: number of channels (0 = as input) */
  float fSampleOut)
  /* in: sampling frequency (0 = as input) */
  /* returns: 0=OK  1=error */
{
  int mode;         /* enum MP4Mode */
  float fSample;
  long fileNumSample;
  long totNumSample;
  int numChannel;
  int frameNumSample,delayNumSample;
  int frameMinNumBit,frameMaxNumBit;
  long fSampleLong,bitRateLong;
  BsBitBuffer *bitBuf;
  float **sampleBuf;
  BsBitStream *bitStream;
  AudioFile *audioFile;
  BsBitBuffer *bitHeader;
  FILE *tmpFile;
  int startupNumFrame,startupFrame;
  int numSample;
  int frameNumBit,frameAvailNumBit,usedNumBit;
  int headerNumBit;
  int padNumBit;
  long totDataNumBit,totPadNumBit;
  int minUsedNumBit,maxUsedNumBit;
  int minPadNumBit,maxPadNumBit;
  int minReservNumBit,maxReservNumBit;
  long totReservNumBit;
  int ch,i;
  long startSample;
  long encNumSample;
  int numChannelBS;
  long fSampleLongBS;
  ENC_FRAME_DATA* frameData=NULL;

  FIR_FILT *lowpassFilt = NULL;
```

```
  int downsamplFac = 1;
  float *tmpBuff;

  /* init */
  if (mainDebugLevel >= 3) {
   printf("Encode:\ n");
   printf("audioFileName=%s\ n",audioFileName);
   printf("bitFileName=%s\ n",bitFileName);
   printf("codecMode=%s\ n",codecMode);
   printf("bitRate=%.3f\ n",bitRate);
   printf("varBitRate=%d\ n",varBitRate);
   printf("bitReservSize=%d\ n",bitReservSize);
   printf("bitReservInit=%d\ n",bitReservInit);
   printf("encPara=%s\ n",encPara?encPara:"(NULL)");
   printf("info=%s\ n",info);
   printf("noHeader=%d\ n",noHeader);
   printf("magicString=%s \ n",magicString);
   printf("regionStart=%.6f\ n",regionStart);
   printf("regionDurat=%.6f\ n",regionDurat);
  }

  BsInit(0,bitDebugLevel);
  AudioInit(getenv(MP4_ORI_RAW_ENV), /* headerless file format */
        audioDebugLevel);

  mode = 0;
  do
    mode++;
  while (mode < MODE_NUM &&
  strcmp(codecMode,MP4ModeName[mode]) != 0);
  if (mode >= MODE_NUM)
    CommonExit(1,"Encode: unknown codec mode %s",codecMode);

/* Sri: mycode */
{
char *temp_p;
strcpy(sri_out_file, audioFileName);
temp_p = strstr(sri_out_file, ".wav");
strcpy(temp_p, ".idx");
}
```

```
/* check audio file */
if ((tmpFile=fopen(audioFileName,"rb"))==NULL) {
  CommonWarning("Encode:
  error opening audio file %s",audioFileName);
  return 1;
}
fclose(tmpFile);

/* open audio file */
audioFile = AudioOpenRead(audioFileName,&numChannel,&fSample,
              &fileNumSample);
if (audioFile==NULL)
  CommonExit(1,"Encode: error opening audio file %s "
         "(maybe unknown format)",
         audioFileName);

startSample = (long)(regionStart*fSample+0.5);
if (regionDurat >= 0)
  encNumSample = (long)(regionDurat*fSample+0.5);
else
  if (fileNumSample == 0)
    encNumSample = -1;
  else
    encNumSample = max(0,fileNumSample-startSample);

/* init encoder */
bitHeader = BsAllocBuffer(BITHEADERBUFSIZE);
bitRateLong = (long)(bitRate+0.5);
fSampleLong = (long)(fSample+0.5);
numChannelBS =
  (numChannelOut==0) ? numChannel : numChannelOut;
fSampleLongBS =
  (fSampleOut==0) ? fSampleLong : (long)(fSampleOut+0.5);

if ((strstr(encPara, "-aac_sys") != NULL) ||
   (strstr(encPara, "-aac_sys_bsac") != NULL)) {
  frameData= &encFrameData;
  frameData->od= &objDescr;
}

switch (mode) {
```

```
case MODE_PAR:
  EncParInit(numChannel,fSample,bitRate,encPara,
         &frameNumSample,&delayNumSample,bitHeader);
  break;
case MODE_LPC:
  EncLpcInit(numChannel,fSample,bitRate,encPara,
         &frameNumSample,&delayNumSample,bitHeader);
  break;
case MODE_G729:
  bitRate=8000;
  bitRateLong = (long)bitRate;
  if (fSample == 48000){
    lowpassFilt=initFirLowPass(48000/4000,120)  ;
    downsamplFac=6;
  }
  EncG729Init(numChannel,fSample/downsamplFac,bitRate,encPara,
              &frameNumSample,&delayNumSample,bitHeader);
  frameNumSample=frameNumSample*downsamplFac;
  break;
case MODE_G723:
  bitRate=6400;
  bitRateLong =   (long) bitRate;
  if (fSample == 48000){
    lowpassFilt=initFirLowPass(48000/4000,120)  ;
    downsamplFac=6;
  }
  EncG723Init(numChannel,fSample/downsamplFac,
         bitRate,encPara,encNumSample,
        &frameNumSample,&delayNumSample,bitHeader);
  frameNumSample=frameNumSample*downsamplFac;
  break;
case MODE_TF:
  EncTfInit(numChannel,fSample,bitRate,
            encPara,quantDebugLevel,
            &frameNumSample,&delayNumSample,
            bitHeader,frameData);
  sri_frame = (int)(encNumSample/frameNumSample)+1;
  sri_init(sri_frame);
  break;
}
```

```
frameNumBit = (int)(bitRate*frameNumSample/fSample+0.5);
/* variable bit rate: minimum 8 bit/frame (1 byte) */
/*  to allow end_of_bitstream detection in decoder */

frameMinNumBit = varBitRate ? 8 : frameNumBit;
frameMaxNumBit = frameNumBit+bitReservSize;

if (mainDebugLevel >= 3) {
  printf("mode=%d\ n",mode);
  printf("fSample=%.3f Hz  (
  int=%ld)\ n",fSample,fSampleLong);
  printf("bitRate=%.3f bit/sec  (
  int=%ld)\ n",bitRate,bitRateLong);
  printf("bitReservSize=%d bit  (%.6f sec)",
     bitReservSize,bitReservSize/bitRate);
  printf("bitReservInit=%d bit",bitReservInit);
  printf("frameNumSample=%d  (%.6f sec/frame)",
     frameNumSample,frameNumSample/fSample);
  printf("delayNumSample=%d  (%.6f sec)",
     delayNumSample,delayNumSample/fSample);
  printf("frameNumBit=%d",frameNumBit);
  printf("frameMinNumBit=%d",frameMinNumBit);
  printf("frameMaxNumBit=%d",frameMaxNumBit);
  printf("bitHeaderNumBit=%ld",BsBufferNumBit(bitHeader));
  printf("fileNumSample=%ld  (%.3f sec  %.3f frames)",
     fileNumSample,fileNumSample/fSample,
     fileNumSample/(float)frameNumSample);
  printf("startSample=%ld",startSample);
  printf("encNumSample=%ld  (%.3f sec  %.3f frames)",
     encNumSample,encNumSample/fSample,
     encNumSample/(float)frameNumSample);
}

/* allocate buffers */
bitBuf = BsAllocBuffer(frameMaxNumBit);
if ((sampleBuf
      =(float**)malloc(numChannel*sizeof(float*)))==NULL)
  CommonExit(1,"Encode: memory allocation error");
for (ch=0; ch<numChannel; ch++)
  if ((sampleBuf[ch]
```

```
     =(float*)malloc(frameNumSample*sizeof(float)))==NULL)
    CommonExit(1,"Encode: memory allocation error");
if ((tmpBuff
     =(float*)malloc(frameNumSample*sizeof(float)))==NULL)
  CommonExit(1,"Encode: memory allocation error");

/* if we have aac_raw ,
we should treat it, as with no header ,
if we have scaleable aac the header
is will be written in aacScaleableEncode*/

if ((strstr(encPara, "-aac_raw") != NULL)
   ||(strstr(encPara, "-aac_sca") != NULL))
  noHeader=1;
if ((strstr(encPara, "-aac_sys") != NULL)
   || (strstr(encPara, "-aac_sys_bsac") != NULL))
  noHeader=0;


/* open bit stream file */
if (!noHeader)
  bitStream =
     BsOpenFileWrite(bitFileName,magicString,info);
else
  bitStream =
     BsOpenFileWrite(bitFileName,NULL, NULL);

if (bitStream==NULL)
  CommonExit(1,"Encode:
       error opening bit stream file %s",bitFileName);

/* write bit stream header */
if ((strstr(encPara, "-aac_sys") == NULL)
     && (strstr(encPara, "-aac_sys_bsac") == NULL)) {
  if (!noHeader)
    if (BsPutBit(bitStream,MP4_BS_VERSION,16) ||
        BsPutBit(bitStream,numChannelBS,8) ||
        BsPutBit(bitStream,fSampleLongBS,32) ||
        BsPutBit(bitStream,bitRateLong,32) ||
        BsPutBit(bitStream,frameNumBit,16) ||
        BsPutBit(bitStream,frameMinNumBit,16) ||
```

```
        BsPutBit(bitStream,bitReservSize,16) ||
        BsPutBit(bitStream,bitReservInit,16) ||
        BsPutBit(bitStream,mode,8) ||
        BsPutBit(bitStream,BsBufferNumBit(bitHeader),16))
      CommonExit(1,"Encode:
              error writing bit stream header (frame)");
  if (BsPutBuffer(bitStream,bitHeader))
    CommonExit(1,"Encode:
              error writing bit stream header (core)");
  BsFreeBuffer(bitHeader);

  headerNumBit = BsCurrentBit(bitStream);
} else {
  /* write object descriptor  length */
  int length= BsBufferNumBit(bitHeader)/8;
  int align = 8 - BsBufferNumBit(bitHeader)% 8;
   if (align == 8) align = 0;
   if (align != 0) {
     length += 1;
   }
  BsPutBit(bitStream,length,32);
  if (BsPutBuffer(bitStream,bitHeader))
    CommonExit(1,"Encode:
          error writing bit stream header (core)");
  BsPutBit(bitStream,0,align);

  BsFreeBuffer(bitHeader);
  headerNumBit = BsCurrentBit(bitStream);
}
if (mainDebugLevel >= 3)
  printf("headerNumBit=%d",headerNumBit);

/* num frames to start up encoder due to delay compensation */
startupNumFrame =
   (delayNumSample+frameNumSample-1)/frameNumSample;

/* seek to beginning of first (startup)
frame (with delay compensation) */
AudioSeek(audioFile,
      startSample+delayNumSample
       -startupNumFrame*frameNumSample);
```

```
if (mainDebugLevel >= 3)
  printf("startupNumFrame=%d",startupNumFrame);

/* process audio file frame by frame */
frame = -startupNumFrame;
totNumSample = 0;
totPadNumBit = 0;
frameAvailNumBit = bitReservInit;
minUsedNumBit = minPadNumBit
              = minReservNumBit = frameMaxNumBit;
maxUsedNumBit = maxPadNumBit = maxReservNumBit = 0;
totReservNumBit = 0;

do
{
  if (mainDebugLevel >= 1 && mainDebugLevel <= 3) {
    printf("frame %4d ",frame);
    fflush(stdout);
  }
  if (mainDebugLevel > 3)
    printf("frame %4d",frame);

  /* check for startup frame */
  startupFrame = frame < 0;

  /* read audio file */
  numSample = AudioReadData(audioFile,sampleBuf,
              frameNumSample);
  totNumSample += numSample;
  if (numSample != frameNumSample && encNumSample == -1)
    encNumSample = totNumSample;


  /* encode one frame */
  if (!startupFrame) {
    /* variable bit rate: don't exceed bit reservoir size */
    if (frameAvailNumBit > bitReservSize)
  frameAvailNumBit = bitReservSize;

    if (frameData!=NULL){
```

```
    frameAvailNumBit +=
    frameNumBit-(18* (frameNumBit/(250*8)+1) + 7) ;
    /* minus flexmux overhead: 18 bits per
     flexmux packet plus max 7 align bits*/
  }else
  {
    frameAvailNumBit += frameNumBit;
  }
  if (mainDebugLevel >= 5)
printf("frameAvailNumBit=%d",frameAvailNumBit);
}

switch (mode) {
case MODE_PAR:
  EncParFrame(sampleBuf,
      startupFrame ? (BsBitBuffer*)NULL : bitBuf,
      startupFrame ? 0 : frameAvailNumBit,
      frameNumBit,frameMaxNumBit);
  break;
case MODE_LPC:
  EncLpcFrame(sampleBuf,
      startupFrame ? (BsBitBuffer*)NULL : bitBuf,
      startupFrame ? 0 : frameAvailNumBit,
      frameNumBit,frameMaxNumBit);
  break;
case MODE_G729:
  /* I'd suggest just to use frameNumSample! */
  /* numSample is for internal
     purposes only ...   HP 970630 */
  if (numSample !=frameNumSample)
break;
  if (downsamplFac!=0 && lowpassFilt!=NULL){
firLowPass(sampleBuf[MONO_CHAN],tmpBuff,
           numSample, lowpassFilt );
subSampl(tmpBuff,sampleBuf[MONO_CHAN],
         downsamplFac,&numSample);
  }
  EncG729Frame(sampleBuf,
      startupFrame ? (BsBitBuffer*)NULL : bitBuf,
      startupFrame ? 0 : frameAvailNumBit,
      frameNumBit,frameMaxNumBit,numSample);
```

```
  break;
case MODE_G723:
  /* I'd suggest just to use frameNumSample! */
  /* numSample is for internal
     purposes only ...   HP 970630 */
  if (numSample !=frameNumSample)
break;
  if (downsamplFac!=0 && lowpassFilt!=NULL){

firLowPass(sampleBuf[MONO_CHAN],tmpBuff,
         numSample, lowpassFilt );
subSampl(tmpBuff,sampleBuf[MONO_CHAN],
         downsamplFac,&numSample);
  }
  EncG723Frame(sampleBuf,
      startupFrame ? (BsBitBuffer*)NULL : bitBuf,
      startupFrame ? 0 : frameAvailNumBit,
      frameNumBit,frameMaxNumBit,numSample);
  break;
case MODE_TF:
  EncTfFrame(sampleBuf,
      startupFrame ? (BsBitBuffer*)NULL : bitBuf,
      startupFrame ? 0 : frameAvailNumBit,
      frameNumBit,frameMaxNumBit,
      bitRateLong,fSampleLong,frameData);
  break;
}

if (!startupFrame) {
  usedNumBit = BsBufferNumBit(bitBuf);

  if (mainDebugLevel >= 5)
printf("usedNumBit=%d",usedNumBit);

  /* write bit stream */
  if (usedNumBit > frameAvailNumBit)
CommonExit(1,"Encode:
    more bits used than available in frame+buffer");
  if (BsPutBuffer(bitStream,bitBuf))
CommonExit(1,"Encode: error writing bit stream data");
  frameAvailNumBit -= usedNumBit;
```

```
    if (frameData==NULL){
      /* write padding bits */
      padNumBit = 0;
      if (frameAvailNumBit
         -frameNumBit+frameMinNumBit > bitReservSize) {
        padNumBit = frameAvailNumBit
           -frameNumBit+frameMinNumBit-bitReservSize;

        if (mainDebugLevel >= 5)
          printf("padNumBit=%d",padNumBit);

        for (i=0; i<padNumBit; i++)
          if (BsPutBit(bitStream,0,1))
            CommonExit(1,"Encode:
                error writing bit stream padding bits");
        frameAvailNumBit -= padNumBit;
        totPadNumBit += padNumBit;
      }
    }
    if (minUsedNumBit > usedNumBit)
  minUsedNumBit = usedNumBit;
    if (maxUsedNumBit < usedNumBit)
  maxUsedNumBit = usedNumBit;
    if (minPadNumBit > padNumBit)
  minPadNumBit = padNumBit;
    if (maxPadNumBit < padNumBit)
  maxPadNumBit = padNumBit;
    if (minReservNumBit > frameAvailNumBit)
  minReservNumBit = frameAvailNumBit;
    if (maxReservNumBit < frameAvailNumBit)
  maxReservNumBit = frameAvailNumBit;
    totReservNumBit += frameAvailNumBit;

  }

  frame++;

}
/*while(encNumSample < 0 || (long)frame*frameNumSample
< (long)frameNumSample);*/
```

```
while(encNumSample < 0 ||
frame*(long)frameNumSample < encNumSample);

if (mainDebugLevel >= 1 && mainDebugLevel <= 3)
  printf(" ");

totDataNumBit =
   BsCurrentBit(bitStream)-headerNumBit-totPadNumBit;

if (frameData==NULL){
  /* write last frame and bit reservoir padding bits */
  /* required also in case of variable bit rate */
  /* to allow end_of_bitstream detection in decoder */
  for (i=0; i<frameAvailNumBit; i++)
    if (BsPutBit(bitStream,0,1))
      CommonExit(1,"Encode:
      error writing bit reservoir padding bits");
}

if (mainDebugLevel >= 3) {
  printf("totNumFrame=%d",frame);
  printf("encNumSample=%ld  (%.3f sec  %.3f frames)",
     encNumSample,encNumSample/fSample,
     encNumSample/(float)frameNumSample);
  printf("totNumSample=%ld",totNumSample);
  printf("totNumBit=%ld",BsCurrentBit(bitStream));
  printf("totDataNumBit=%ld  (%.3f bit/frame  %.3f bit/sec)",
     totDataNumBit,totDataNumBit/(float)frame,
     totDataNumBit/(float)frame*fSample/frameNumSample);
  printf("totPadNumBit=%ld",totPadNumBit);
  printf("lastPadNumBit=%d",frameAvailNumBit);
  printf("minUsedNumBit=%d",minUsedNumBit);
  printf("maxUsedNumBit=%d",maxUsedNumBit);
  printf("minPadNumBit=%d",minPadNumBit);
  printf("maxPadNumBit=%d",maxPadNumBit);
  printf("minReservNumBit=%d",minReservNumBit);
  printf("maxReservNumBit=%d",maxReservNumBit);
  printf("avgReservNumBit=%.1f",
  totReservNumBit/(float)frame);
}
```

```
  /* free encoder memory */
  switch (mode) {
  case MODE_PAR:
    EncParFree();
    break;
  case MODE_LPC:
    EncLpcFree();
    break;
  case MODE_TF:
    EncTfFree();
    sri_save(sri_frame);
    break;
  }

  /* close audio file */
  AudioClose(audioFile);

  /* close bit stream file */
  if (BsClose(bitStream))
    CommonExit(1,"Encode: error closing bit stream file");

  /* free buffers */
  if (numChannel>1)
    for (ch=0; ch<numChannel; ch++)
      free(sampleBuf[ch]);
  free(sampleBuf);
  free(tmpBuff);
  BsFreeBuffer(bitBuf);

  return 0;
}



/* ---------- main ---------- */

int main (int argc, char *argv[])
{
  char *progName = "<no program name>";
  int result;
  char oriFileName[STRLEN],bitFileName[STRLEN];
```

```
char infoDate[STRLEN];
int i,j,len;
int fileIdx;
char *info,*infoTail;
time_t curTime;

/* evaluate command line  */
CmdLineInit(0);
result = CmdLineEval(argc,argv,paraList,
switchList,1,&progName);
if (result) {
  if (result==1) {
    printf("%s: %s",progName,PROGVER);
    CmdLineHelp(progName,paraList,switchList,stdout);
    EncParInfo(stdout);
    EncLpcInfo(stdout);
    EncTfInfo(stdout);
    EncG729Info(stdout);
    EncG723Info(stdout);
    exit (1);
  }
  else
    CommonExit(1,"command line error ("-h" for help)");
}

if (mainDebugLevel >= 1)
  printf("%s: %s",progName,PROGVER);
if (mainDebugLevel >= 2) {
  printf("CVS Id: %s",CVSID);
  printf("%s",EncParInfo(NULL));
  printf("%s",EncLpcInfo(NULL));
  printf("%s",EncTfInfo(NULL));
  printf("%s",EncG723Info(NULL));
  printf("%s",EncG729Info(NULL));
}

CmdLineInit(cmdDebugLevel);

/* calc variable default values */
if (!bitReservInitUsed)
  bitReservInit = bitReservSize;
```

```
if (!regionDuratUsed)
  regionDurat = -1;
if (!oriPathUsed)
  oriPath = getenv(MP4_ORI_PATH_ENV);
if (!bitPathUsed)
  bitPath = getenv(MP4_BIT_PATH_ENV);
if (!oriExtUsed)
  oriExt = getenv(MP4_ORI_FMT_ENV);
if (oriExt==NULL)
  oriExt = MP4_ORI_EXT;

/* check command line options */
if (bitRate <= 0)
  CommonExit(1,"bit rate <= 0");
if (bitReservSize < 0)
  CommonExit(1,"bit reservoir size < 0");
if (bitReservInit < 0)
  CommonExit(1,"bit reservoir initial bits < 0");
if (bitReservInit > bitReservSize)
  CommonExit(1,"bit reservoir initial bits > size");
if (regionDuratUsed && regionDurat < 0)
  CommonExit(1,"duration of region < 0");
if (outFileNameUsed && varArgIdx[0]>=0 && varArgIdx[1]>=0)
  CommonExit(1,"only one input file allowed when using -o");
if (varArgIdx[0]<0)
  CommonExit(1,"no input file specified");

if( strstr( encPara, "-aac_sca" ) ) {
  if (bitReservSize<6000)
    bitReservSize=6000 ;
  bitReservInit=0;
  varBitRate=1;
}

/* generate info string for bit stream */
len = 1;
curTime = time((time_t*)NULL);
len += strftime(infoDate,STRLEN,
"%Y/%m/%d %H:%M:%S UTC",gmtime(&curTime));
len += strlen(PROGVER);
j = 0;
```

```
for (i=0; i<argc; i++)
  if (varArgIdx[j] == i)
    j++;
  else
    len += strlen(argv[i])+1;
len += 2*STRLEN;
len += 5*7+1;
if ((info=(char*)malloc(len))==NULL)
  CommonExit(1,"memory allocation error");
strcpy(info," ");
strcat(info,"date: ");
strcat(info,infoDate);
strcat(info," ");
strcat(info,"prog: ");
strcat(info,PROGVER);
strcat(info," ");
strcat(info,"para:");
j = 0;
for (i=0; i<argc; i++) {
  if (varArgIdx[j] == i)
    j++;
  else
  {
    strcat(info," ");
    strcat(info,argv[i]);
  }
}
strcat(info,"");
infoTail = info+strlen(info);

/* process all files on command line */
fileIdx = 0;
while (varArgIdx[fileIdx] >= 0) {

  /* compose file names */
  if (ComposeFileName(argv[varArgIdx[fileIdx]],
      0,oriPath,oriExt,oriFileName,
          STRLEN))
    CommonExit(1,"composed file name too long");
  if (outFileNameUsed) {
    if (ComposeFileName(outFileName,
```

```
          0,bitPath,bitExt,bitFileName,
              STRLEN))
    CommonExit(1,"composed file name too long");
    }
    else
      if (ComposeFileName(argv[varArgIdx[fileIdx]],1,bitPath,bitExt,
              bitFileName,STRLEN))
    CommonExit(1,"composed file name too long");

    /* complete info string */
    *infoTail = '\ 0';
    strcat(infoTail,"ori: ");
    strcat(infoTail,oriFileName);
    strcat(infoTail," ");
    strcat(infoTail,"bit: ");
    strcat(infoTail,bitFileName);
    strcat(infoTail," ");

    /* encode file */
    if (mainDebugLevel >= 1)
      printf("encoding %s -> %s",oriFileName,bitFileName);

    if (Encode(oriFileName,bitFileName,codecMode,bitRate,varBitRate,
           bitReservSize,bitReservInit,encPara,
           (char *)(noInfo ? "" : info),noHeader,magicString,
           regionStart,regionDurat,numChannelOut,fSampleOut))
      CommonWarning("error encoding audio file %s",oriFileName);

    fileIdx++;
  }

  CmdLineEvalFree(paraList);

  if (mainDebugLevel >= 1)
    printf("%s: finished",progName);

  return 0;
}

void sri_init(int frame)
{
```

```
  int i,j;
  int sri_no_of_bands = 18;
  int sri_nsf = 1024;
/*  double sample;
  FILE *sri_bk;

  sri_bk = fopen("frame_cb","r");
  if(sri_bk == NULL)
  {
     puts("Cannot open file");
  }
  for(i=0;i<512;i++)
  {
     for(j=0;j<1024;j++)
     {
        fread(&sample,sizeof(sample),1,sri_bk);
    sri_codebook[i][j] = sample;
     }
  }
  fclose(sri_bk);*/

  printf("INIT: malloc (%dx%d)", frame,2* sri_no_of_bands);

  sri_vq_index = (int*)malloc(frame*2*sri_no_of_bands*sizeof(int));
  if(sri_vq_index==NULL)
  {
     printf("Memory allocation failed");
  }

  printf("INIT: malloc (%dx%d)", frame, sri_nsf);

  sri_residue = (int*)malloc(frame*sri_nsf*sizeof(int));
  if(sri_residue == NULL)
     printf("Memory allocation failed ");

}

void sri_save(int frame)
{
   int i, sri_nsf = 1024;
   FILE *sri_idx;
```

```
   FILE *sri_sample;
   int sri_no_of_bands = 18;
   printf("sri_frame = %d",frame);

   /* open index file */
   sri_idx = fopen("sri_idx","w");
   if(sri_idx == NULL)
   {
      puts("Cannot open index file");
   }
   fwrite(&frame,sizeof(frame),1,sri_idx);
   fwrite(&sri_no_of_bands, sizeof(sri_no_of_bands),1,sri_idx);
   for(i=0;i<(frame*2*sri_no_of_bands);i++)
   {
      fwrite(&sri_vq_index[i],sizeof(int),1,sri_idx);
   }

  /* open file to store mdct coeff */
   sri_sample = fopen("sri_residue","w");
   if(sri_sample == NULL)
   {
      puts("sri_save: Cannot open file sri_residue");
   }
   for(i=0;i<(frame*sri_nsf);i++)
   {
      fwrite(&sri_residue[i],sizeof(int),1,sri_sample);
   }
   fclose(sri_idx);
   fclose(sri_sample);
}
```

8. Scalable decoder for TWIN-VQ

```
/* External variables for sri decoder */
extern int sri_frame;
extern int sri_reconst_flag;
extern int *sri_vq_index;
extern int sri_nbands;
extern int *sri_residue;
```

```
int sri_bit_alloc[27] =
{16,16,16,16,16,16,16,16,16,16,
16,16,16,16,16,16,16,16,0,0,0,0,0,0,0,0,0};

void sri_vq_dec(int*,int*,int*,
                double*,double*,
                int,int,double*);

void ntt_tf_requantize_spectrum(/* Input */
                ntt_INDEX *indexp,
                /* Output */
                double flat_spectrum[])
{
  int    vq_bits, n_sf, cb_len_max;
  double *sp_cv0, *sp_cv1;

  int i;

  /*--- Parameter settings ---*/
  switch(indexp->w_type){
  case ONLY_LONG_WINDOW:
  case LONG_SHORT_WINDOW:
  case SHORT_LONG_WINDOW:
  case LONG_MEDIUM_WINDOW:
  case MEDIUM_LONG_WINDOW:
    /* available bits */
    vq_bits = ntt_VQTOOL_BITS;
    /* codebooks */
    sp_cv0 = (double *)ntt_codev0;
    sp_cv1 = (double *)ntt_codev1;
    cb_len_max = ntt_CB_LEN_READ + ntt_CB_LEN_MGN;
    /* number of subframes in a frame */
    n_sf = ntt_N_SUP;
    break;
  case ONLY_MEDIUM_WINDOW:
  case MEDIUM_SHORT_WINDOW:
  case SHORT_MEDIUM_WINDOW:
    /* available bits */
    vq_bits = ntt_VQTOOL_BITS_M;
    /* codebooks */
    sp_cv0 = (double *)ntt_codev0m; sp_cv1 = (double *)ntt_codev1m;
```

```
    cb_len_max = ntt_CB_LEN_READ_M + ntt_CB_LEN_MGN;
    /* number of subframes in a frame */
    n_sf = ntt_N_SUP * ntt_N_MID;
    break;
  case ONLY_SHORT_WINDOW:
    /* available bits */
    vq_bits = ntt_VQTOOL_BITS_S;
    /* codebooks */
    sp_cv0 = (double *)ntt_codev0s; sp_cv1 = (double *)ntt_codev1s;
    cb_len_max = ntt_CB_LEN_READ_S + ntt_CB_LEN_MGN;
    /* number of subframes in a frame */
    n_sf = ntt_N_SUP * ntt_N_SHRT;
    break;
  default:
    fprintf(stderr, "ntt_tf_requantize_spectrum():
        %d: No such window type.",
        indexp->w_type);
    exit(1);
  }
  if(sri_reconst_flag == 0)
  {
     ntt_vex_pn(indexp->wvq,
            sp_cv0, sp_cv1, cb_len_max,
            n_sf, ntt_N_FR*ntt_N_SUP,
            vq_bits,
            flat_spectrum);
  }
  else
  {
     sri_vq_dec((sri_vq_index+sri_frame*36),
                (sri_residue+sri_frame*1024),
                sri_bit_alloc,
                sp_cv0, sp_cv1, cb_len_max,
                ntt_N_FR*ntt_N_SUP,
                flat_spectrum);
     sri_frame++;
  }

}

void sri_vq_dec(int *index,
```

```
                int *index_res,
                int *bit_alloc,
                double *sp_cv0,
                double *sp_cv1,
                int cv_len_max,
                int block_size,
                double *signal)
{
   int mask,i,vq_c,band_c;
   int pol0, pol1, index0, index1;
   int residue_bits, residue_bits_sample;
   int bands[27] = {4,4,4,4,4,4,4,4,8,8,8,8,
                    16,16,16,16,32,32,32,32,
                    64,64,64,64,128,128,256};
   int band_pos[27];
   int quant1, quant2;
   double delta, delta_orig, out;

   band_pos[0] = 0;
   for(i=0;i<26;i++)
      band_pos[i+1] = band_pos[i]+bands[i];

   mask = (0x1 << ntt_MAXBIT_SHAPE) - 1;
   vq_c = 0;
   for(band_c=0;band_c<27;band_c++)
   {
      pol0 = 0;
      pol1 = 0;
      index0 = 0;
      index1 = 0;
      residue_bits = bit_alloc[band_c];

      if(band_c<18)
      {
         if(residue_bits >= 8)
         {
            index0 = (index[vq_c]) & mask;
            pol0 =
            1 - 2*((index[vq_c] >>
            (ntt_MAXBIT_SHAPE)) & 0x1);
            residue_bits = residue_bits - 8;
```

```
            }
            if(residue_bits >= 8)
            {
               index1 = (index[vq_c+1]) & mask;
               pol1 =
               1 - 2*((index[vq_c+1] >>
               (ntt_MAXBIT_SHAPE)) & 0x1);
               residue_bits = residue_bits - 8;
            }
            vq_c = vq_c+2;
         }
         residue_bits_sample =
          (int)(residue_bits/bands[band_c])-1;
         if(residue_bits_sample < 0)
            residue_bits_sample = 0;

         delta = 6000.0/pow(2,residue_bits_sample);
         delta_orig = 6000.0/128;

         for(i=0;i<bands[band_c];i++)
         {
            signal[band_pos[band_c]+i] =
            (pol0*sp_cv0[index0*cv_len_max+i]
            + pol1*sp_cv1[index1*cv_len_max+i])*0.5;
            quant1 = index_res[band_pos[band_c]+i];
            if(quant1 > 127)
            {
               quant2 = (int)((quant1-128)*delta_orig/delta);
               out = (double)(quant2*delta);
            }
            else
            {
               quant2 = (int)(-1*quant1*delta_orig/delta);
               out = (double)(quant2*delta);
            }
            signal[band_pos[band_c]+i] =
            signal[band_pos[band_c]+i] + out;
         }
      }
   }
```

```
/*--- Sri Variables ---*/
int sri_frame = 0;
int sri_reconst_flag = 0;
int *sri_vq_index;
int sri_nbands;
void sri_dec_init(void);
int *sri_residue;

void sri_dec_init()
{
   int i,j, idly;
   int nframes, nbands;
   double idly1;
   //double sample;
   FILE *sri_idx, *sri_res, *sri_bit;

   printf("Coder type: 0 - for original decoder\ n
                       1 - for new decoder\ n");
   scanf("%d",&sri_reconst_flag);

   /*sri_bk = fopen("frame_cb","r");
   if(sri_bk == NULL)
   {
      printf("Cannot open file\ n");
   }
   for(i=0;i<512;i++)
   {
      for(j=0;j<1024;j++)
      {
         fread(&sample,sizeof(sample),1,sri_bk);
     sri_codebook[i][j] = sample;
      }
   }*/

   sri_idx = fopen("sri_idx","r");
   if(sri_idx == NULL)
   {
      printf("Cannot open index file\ n");
   }

   fread(&idly,sizeof(idly),1,sri_idx);
```

```
nframes = idly;
fread(&idly,sizeof(idly),1,sri_idx);
nbands = idly;

sri_nbands = nbands;

printf("INIT: malloc (%dx%d)\ n", nframes, 2*nbands);
sri_vq_index = (int*)malloc(nframes*2*nbands*sizeof(int));
if(sri_vq_index==NULL)
{
   printf("Memory allocation failed\ n");
}
for(i=0;i<nframes*2*nbands;i++)
{
   fread(&idly,sizeof(idly),1,sri_idx);
   sri_vq_index[i] = idly;
}

sri_residue = (int*)malloc(nframes*1024*sizeof(int));
if(sri_vq_index==NULL)
   printf("Memory allocation failed\ n");

sri_res = fopen("sri_residue","r");
if(sri_res == NULL)
{
   printf("Cannot open residue index file \ n");
}
for(i=0;i<nframes*1024;i++)
{
   fread(&idly,sizeof(idly),1,sri_res);
   sri_residue[i] = idly;
}

/* sri_bit = fopen("bit_alloc","r");
if(sri_bit == NULL);
{
   printf("Cannot open bit allocation file \ n");
}
for(i=0;i<27;i++)
{
   fread(&idly,sizeof(int),1,sri_bit);
```

```
      sri_bit_alloc[i] = idly;
   }
   fclose(sri_bit); */

   /* temporary goofy fix */

   fclose(sri_idx);
   fclose(sri_res);
}
```

C and Matlab programs to implement the greedy bit allocation

1. The following C program performs the greedy bit allocation as described in Chapter 6.

```
  /*********************************************/
 /*            Greedy Bit Allocation           */
/*********************************************/

/* This program calculates the bit allocation
   for the sequence bene.wav. The bit allocation
   can be calculated for any given sequence or
   collection of sequences                     */

# include <stdio.h>
# include <stdlib.h>
# include <math.h>

int main(void)
{
   int i,j,k,N;
   int bit_inc = 8;
   int bit_alloc_table[82][27];
   int bit_alloc[27] = {4,4,4,4,4,4,4,
                        4,4,4,4,4,8,8,
                        8,8,8,8,0,0,0,
                        0,0,0,0,0,0};
   int bit_alloc_new[27] = {4,4,4,4,4,4,4,4,
                            4,4,4,4,8,8,8,8,
                            8,8,0,0,0,0,0,0,
                            0,0,0};

   double max_q = 0, quality; /* Quality metric */

   FILE *qp, *bap, *batp;

   for(i=0;i<82;i++)
   {
      for(j=0;i<27;i++)
      {
```

```
   if(bit_alloc[i] == 0){
      N = i;
      break;
   }
}

/* Lower frequency bands refinement */

for(j=0;j<N;j++)
{
   bit_alloc_new[j] = bit_alloc[j] + bit_inc;

   /* Write the new bit allocation into file */

   bap = fopen("alloc","w");
   for(k=0;k<27;k++)
   {
      fprintf(bap,"%d",bit_alloc_new[k]);
   }
   fclose(bap);

   system("./mp4dec bene.mp4");
   system("matlab < q_test.m");

   qp = fopen("quality","r");
   fscanf(qp,"%lf",&quality);
   fclose(qp);

   if(quality > max_quality)
   {
      max_quality = quality;
      for(k=0;k<27;k++)
      {
         bit_alloc_table[i][k] = bit_alloc_new[k];
      }
   }
}

/* Higher frequency band coarse refinement */

bit_alloc_new[N] = bit_alloc[N] + bit_inc;
```

```
   /* Write the new bit allocation into file */

   bap = fopen("alloc","w");
   for(k=0;k<27;k++)
   {
      fprintf(bap,"%d",bit_alloc_new[k]);
   }
   fclose(bap);

   system("./mp4dec bene.mp4");
   system("matlab < q_test.m");

   qp = fopen("quality","r");
   fscanf(qp,"%lf",&quality);
   fclose(qp);

   if(quality > max_quality)
   {
      max_quality = quality;
      for(k=0;k<27;k++)
      {
         bit_alloc_table[i][k] = bit_alloc_new[k];
      }
   }

   for(j=0;j<27;j++)
      bit_alloc[j] = bit_alloc_table[i][k];
}

/* Write the bit allocation table into file */

batp = fopen("bit_allocation_table","w");
for(i=0;i<82;i++)
{
   for(j=0;j<27;j++)
   {
      fprintf(batp,"%d",bit_allocation_table[i][j]);
   }
}
fclose(batp);
```

```
   return(0);
}
```

2. The Matlab program below estimates the quality of a decoded audio sequence using the qmetric.m program written by Charles D. Creusere (ccreuser@nmsu.edu). Quality of an audio sequence is given by a number between 0 (poor quality) to 100 (best quality).

```
%--------------------------------------------------
% Program to find the qualtiy of two audio sequences
% This program is meant to be used by greedy.c
% program for the greedy bit allocation.
%--------------------------------------------------
clear;clc;close all;

[x,fs,N] = wavread('../original/bene.wav');
[x2,fs1,N1] = wavread('../decoded/bene.wav');

if fs != fs1
   disp('The sampling rates do not match');
   exit;
end

quality = qmetric(x,x2);

save quality -ASCII
exit
```

REFERENCES

[1] T. Moriya, N. Iwakami, A. Jin, and T. Mori, "A design of lossy and lossless scalable audio coding," in *Proceedings. 2000 IEEE International Conference on Acoustics, Speech, and Signal Processing, 2000 ICASSP '00*, vol. 2.

[2] R. Yu, S. Rahardja, L. Xiao, and C. C. Ko, "A fine granular scalable to lossless audio coder," *IEEE transactions on Audio, Speech and Language processing*, vol. 14, no. 4, July 2006.

[3] R. Geiger, G. Schuller, and T. Sporer, "Fine grain scalable perceptual and lossless coding based on intmdct," in *IEEE workshop on applications of signal processing to audio and acoustics*, Oct. 2003.

[4] J. Zhou, Q. Zhang, Z. Xiong, and W. Zhu, "Error resilient scalable audio coding (ersac) for mobile applications," in *IEEE Fourth Workshop on Multimedia Signal Processing, 2001*, Oct. 2001.

[5] F. Riera-Palou, A. den Brinker, and A. Gerrits, "A hybrid parametric-waveform approach to bit stream scalable audio coding," vol. 2, Nov. 2004.

[6] R. Mohan, J. R. Smith, and C.-S. Li, "Adapting multimedia internet content for universal access," *IEEE Trans. Multimedia*, vol. 1, no. 1, p. 104114, Mar. 1999.

[7] C. Dorize, J.-M. Muller, and D. Sereno, "Detailed description of the mvat audio candidate to mpeg-4," *ISO/IEC/JTC1/SC29/WG11, MPEG95/0412*, Nov. 1995.

[8] J. Herre *et al.*, "The integrated filterbank based scalable mpeg-4 audio coder," in *105 th Convention of the audio engineering society*, Preprint 4810.

[9] D. Sinha and C. Sundberg, "Unequal error protection (uep) for perceptual audio coders," in *Proc. International Conference on Acoustics, Speech and Signal Processing*, Phoenix, Arizona, Apr. 1999.

[10] A. Jin *et al.*, "Scalable audio coder based on quantizer units of mdct coefficients," in *Proc. ICASSP'99*, 1999, pp. 897–900.

[11] J. Li, "Embedded audio coding (eac) with implicit auditory masking," *ACM Multimedia*, Dec. 2002.

[12] P. Chou and Z. Miao, "Rate-distortion optimized streaming of packetized media," 2001. [Online]. Available: citeseer.ist.psu.edu/chou01ratedistortion.html

[13] S. Ye, H. Ai, and C. Kuo, "A progressive approach for perceptual audio coding," in *Proc. 2000 IEEE International Conference on Multimedia and Expo*, vol. 2, pp. 815–818.

[14] A. Scheuble and Z. Xiong, "Scalable audio coding using the nonuniform modulated complex lapped transform," in *Proc. 2001 IEEE International Conference on Acoustics, Speec, and Signal Processing*, vol. 5, pp. 3257–3260.

[15] Real producer basic 8.51. [Online]. Available: http://www.realnetworks.com/

[16] Windows media technologies 8.0. [Online]. Available: http://www.microsoft.com/

[17] C. Dunn. Winsac 1.0. [Online]. Available: http://www.scalatech.co.uk/

[18] R. Vafin and W. B. Kleijn, "Rate-distortion optimized quantization in multistage audio coding," *IEEE Transactions on Audio, Speech and Language Processing*, vol. 14, no. 1, pp. 311–320, Jan. 2006.

[19] J. Shapiro, "Embedded image coding using zerotrees of wavelet coefficients," *IEEE Transactions on Signal Processing*, vol. 41, no. 12, pp. 3445–3462, 1993.

[20] (1998(E)) Mpeg-4 standards document iso/iec fcd 14496 - 3 subpart 4. [Online]. Available: http://www.chiariglione.org/mpeg/

[21] A. Gersho and R. Gray, *Vector Quantization and Signal Compression.* MA 02061, USA: Kluwer Academic Publishers, 1992.

[22] K. Brandenburg, O. Kunz, and A. Sugiyama, "Mpeg-4 natuaral audio coding," *Signal Processing: Image Communication*, vol. 15, no. 1, Jan. 2000.

[23] P. Chu, "Quadrature mirror filter design for an arbitrary number of equal bandwidth channels," vol. 33, Feb. 1985.

[24] A. Jin, "Scalable audio coder based on quantizer units of mdct coefficients," in *Conf. Rec., Audio Engineering Society Convention*, San Francisco, CA, Oct. 1992, pp. 897–900.

[25] C. Creusere, "Understanding perceptual distortion in mpeg scalable audio coding," *IEEE transactions on Acoustics Speech and Signal Processing*, vol. 15, no. 3, pp. 422–431, May 2005.

[26] N. Iwakami and T. Moriya, "Transform domain weighted interleaved vector quantization (twin vq)," in *Proc. 101st convention of the audio engineering society*, p. preprint 4810.

[27] S. Kandadai and C. Creusere, "Reverse engineering vector quantizers using training set synthesis," in *Proc. of the European Signal Processing Conference*, Vienna, Austria, Sept. 2004, pp. 789–792.

[28] ——, "Reverse engineering vector quantizers for repartitioned vector spaces," in *39th Asilomar Conference on Signals, Systems and Computers*, Asilomar, CA, Nov. 2005.

[29] K. Fukunaga, *Introduction To Statistical Pattern Recognition.* NY 10003: Academic Press Inc.

[30] T. Quatieri, *Discrete-Time Speech Signal Processing: Principles and Practice.* New Jersey, USA: Prentice Hall PTR, 2001.

[31] L. Rabiner and R. Schafer, *Digital Processing of Speech Signals.* New Jersey, USA: Prentice Hall PTR, 1978.

[32] T. Painter and A. Spanias, "Pereceptual coding of digital audio," *Proceedings of the IEEE*, vol. 88, no. 4, Apr. 2000.

[33] J. Johnston, "Estimation of perceptual entropy using noise masking criteria," in *Proc. ICASSP-88*, May 1988, pp. 2524–2527.

[34] E. Zwicker and H. Fastl, *Psychoacoustics Facts and Models.* Berlin, Germany: Springer-Verlag, 1990.

[35] E. Terhardt, "Calculating virtual pitch," *Hearing Res.*, vol. 1, pp. 155–182, 1979.

[36] D. Greenwood, "A cochlear frequency position function for several species," *Journal of Acoustic Society of America*, vol. 87, pp. 2592–2605, 1990.

[37] B. Moore, "Masking in the human auditory system," *Collected papers on digital audio bit-rate reduction*, pp. 9–19, 1996.

[38] B. Scharf, "Critical bands," *Foundations of Modern Auditory Theory.*

[39] R. Hellman, "Assymetry of masking between noise and tone," *Percep. Psychphys.*, vol. 11, pp. 241–246, 1972.

[40] J. Hall, "Auditory psychophysics of coding applications," *The Digital Signal Processing Handbook*, pp. 39.1–39.25, 1998.

[41] H. Fletcher and W. Munson, "Relation between loudness and masking," *Journal of the Acoustic Society of America*, vol. 9, pp. 1–10, 1937.

[42] J. Egan and H. Hake, "On the masking pattern of simple auditory stimulus," *Journal of the Acoustic Society of America*, vol. 22, pp. 622–630, 1950.

[43] G. Miller, "Sensitivity to changes in the intensity of white noise and its relation to masking and loudness," *Journal of the Acoustic Society of America*, vol. 19, pp. 609–619, 1947.

[44] J. Hall, "Asymmetry of masking revisited: Generalization of masker and probe bandwidth," *Journal of the Acoustic Society of America*, vol. 101, pp. 1023–1033, 1997.

[45] S. B. W. Jesteadt and J. Lehman, "Forward masking as a function of frequency, masker level and signal delay," *Journal of the Acoustic Society of America*, vol. 71, pp. 950–962, 1982.

[46] B. Moore, "Psychophysical tuning curves measured in simultaneous and forward masking," *Journal of the Acoustic Society of America*, vol. 63, pp. 524–532, 1978.

[47] K. Brandenburg, "Perceptual coding of high quality digital audio," *Applications of Digital Signal Processing to Audio and Acoustics*, 1998.

[48] J. Johnston, "Transform coding of audio signals using perceptual noise criteria," *IEEE Journal on Selected Areas in Communications*, vol. 6, pp. 314–23, Feb. 1988.

[49] H. Fuchs, "Improving joint stereo audio coding by adaptive inter channel prediction," in *Proceedings 1993 IEEE ASSP Workshop Apps. of Signal Processing to Aud. and Acoustics*, 1993.

[50] ——, "Improving mpeg audio coding by backward adaptive linear stereo prediction," in *Proceedings 99th Conv. Aud. Eng. Soc.*, Oct. 1995.

[51] P. Noll, "Wideband speech and audio coding," *IEEE Communications Magazine*, pp. 34–44, Nov. 1993.

[52] ——, "Digital audio coding for visual communications," *Proceedings of IEEE*, vol. 83, pp. 925–943, June 1995.

[53] S. Quackenbush, "Noiseless coding of quantized spectral components in mpeg-2 advance audio coder," in *IEEE Workshop Applications of Signal Processing to Audio and Acoustics*, 1997.

[54] D. Schulz, "Improving audio codecs by noise substitution," *J. Audio Eng. Soc.*, pp. 593–598, July 1996.

[55] S. Park, Y. Kim, S. Kim, and Y. Seo, "Multi-layer bit-sliced bit-rate scalable audio coding," *103rd AES Convention*, 1997.

[56] N. Iwakami, T. Moriya, , and S. Miki, "High quality audio coding at less than 64 kbits/s by using transform domain weighted interleave vector quantization (twinvq)," in *Proc. of the Internation Conf. on Acoustics Speech and Signal Processing*, May 1995, pp. 3095–3098.

[57] T. Moriya and M. Honda, "Tranform coding of speech using a weighted vector quantizer," vol. 6, no. 2, Feb. 1988.

[58] T. Moriya, "Two-channel conjugate vector quantization for noisy channel speech coding," vol. 10, no. 5, June 1995.

[59] ——, "Design of robust conjugate vector quantizer for noisy channel speech coding," in *Proc. ISIT*, p. 164.

[60] S. Kandadai and C. Creusere, "Perceptually-weighted audio coding that scales to extremely low bitrates," in *Proceedings Data Compression Conference*, Mar. 2006.

[61] Y. Linde, A. Buzo, and R. M. Gray, "An algorithm for vector quantizatizer design," *IEEE Transactions on Communications*, vol. 25, pp. 84–95, 1980.

[62] E. Parzen, "On estimation of a probability density function and mode," *Annals of Mathematical Statistics*, vol. 33, no. 3, pp. 1065–1076, 1962.

[63] R.O.Duda, P.E.Hart, and D.G.Stork, *Pattern Classification*. New York, USA: John Wiley and Sons, Inc., 2001.

[64] B. Dasarathy, *NN Pattern Classification Techniques*. IEEE Computer Society Press, 1991.

[65] P. Hart, "The condensed nearest neighbor rule," *IEEE Transaction on Information Theory*, vol. 14, no. 3, May 1968.

[66] P. Mitra, C. Murthy, and S. Pal, "Density-based multiscale data condensation," *IEEE Transactions on Pattern Analysis and Machine Intelligence*, vol. 24, no. 6, June 2002.

[67] M. Girolami and C. He, "Probability density estimation from optimally condensed data samples," *IEEE Transactions on Pattern Analysis and Machine Intelligence*, vol. 25, no. 10, Oct. 2003.

[68] J. Seaman and P. Odell, "Variance upper bounds," *Encyclopedia of Statistical Sciences*, vol. 9, pp. 480–484, 1988.

[69] "The maximum variance of restricted unimodal distribution," *The annals of Mathematical Statistics*, vol. 40, no. 5, pp. 1746–1752, Oct. 1969.

[70] A. Gersho, "Asymptotically optimal block quantization," *IEEE trans. On Information Theory*, vol. 25, no. 4, July 1979.

[71] P. Zador, "Asymptotic quantization error of continous signal and the quantization dimension," *IEEE trans. Inform. Theory*, vol. 28, no. 2, Mar. 1982.

[72] J. A. Bucklew and G. L. Wise, "Multidimensional asymptotic quantization theory with rth power distortion measures," *IEEE trans. On Information Theory*, vol. 28, no. 2, Mar. 1982.

[73] I. Deak, "Probabilities of simple n-dimensional sets for the normal distribution," *IIE Transactions*, vol. 35, pp. 285–293, 2003.

[74] K.-T. Fang, *Symmetric Multivariate and Related Distributions, Monographs on Statistics and Applied Probability 36.* Chapman and Hall, 1987.

[75] M. N. Do and M. Vetterli, "Contourlets: a directional multiresolution image representation," *IEEE International Conference on Image Processing*, Sept. 2002.

[76] M. N. Do. Contourlet tool box. [Online]. Available: http://www.ifp.uiuc.edu/ minhdo/software/

[77] P. Vaidyanathan, *Multirate Systems and Filterbanks.* Prentice Hall PTR, 1993.

[78] H. S. Malvar, *Signal Processing with Lapped Transforms.* Artech House Publishers, 1992.

[79] M. Vetterli and J. Kovacevic, *Wavelets and Subband Coding.* Prentice Hall PTR, 1995.

[80] J. Princen and A. Bradley, "Analysis/synthesis filter bank design based on time domain aliasing cancellation," *IEEE Trans. Acoust., Speech, Signal Processing*, vol. ASSP - 34, pp. 1153–1161, Oct. 1986.

[81] H. Malvar, "Lapped transforms for efficient transform/subband coding," *IEEE Trans. Acoust., Speech, Signal Processing*, vol. 38, pp. 969–978, June 1990.

[82] S. Cheung and J. Lim, "Incorporation of biorthogonality into lapped transforms for audio compression," in *Proc. Int. Conf. Acoustics, Speech, and Signal Processing (ICASSP-95)*, pp. 3079–3082.

[83] J. Princen, J. Johnson, and A. Bradley, "Subband/transform coding using filterbank design based on time domain aliasing cancellation," in *Proc. Int. Conf. Acoustics, Speech, and Signal Processing (ICASSP-87)*, May 1987, pp. 50.1.1–50.1.4.

[84] J. Herre and J. Johnston, "Enhancing the performance of perceptual audio coders by using temporal noise shaping (tns)," in *Proc. of 101st Convention of the Audio Engineering Society*, 1993.

[85] T. Fischer, "A pyramid vector quantizer," *IEEE Transactions on Information Theory*, vol. 32, no. 4, pp. 568–583, 1986.

[86] D. Jeong and J. Gibson, "Uniform and peicewise uniform lattice vector quantization for memoryless gaussian and laplacian sources," *IEEE Transactions on Information Theory*, vol. 38, no. 3, pp. 786–804, May 1993.

[87] J. Conway and N. Sloane, "Voronoi regions of lattices, second moments of polytopes, and quantization," *IEEE Transactions on Information Theory*, vol. 28, 1982.

[88] ——, "Fast quantizing and decoding algorithms for lattice quantizers and codes," *IEEE Transactions on Information Theory*, vol. 28, pp. 227–232, 1982.

[89] ——, *Spheres Packing, Lattices and Groups*. NY 10010, USA: Springer - Verlag NY Inc.

[90] S. Simon and L. Bosse, "Design of successive approximation lattice vector quantizers," in *IEEE Int. Conf. on Acoustics, Speech, and Signal Processing (ICASSP'97)*, 1997, pp. 2697–2700.

[91] T. Thiede and E. Kabot, "New perceptual quality measure for the bitrate reduced audio," *Preprint 4280, Copenhagen, Denmark*, 1996.

[92] J. Beerends and J. Stemerdink, "A perceptual audio quality measure based on psychoacoustic sound representation," *Journal of the Audio Engineering Society*, vol. 40, Dec. 1992.

[93] S. Morissette, B. Paillard, P. Mabilleau, and J. Soumagne, "Perceval: Perceptual evaluation of the quality of audio signals," *Journal of the Audio Engineering Society*, vol. 40, pp. 21–31, January/February 1992.

[94] "Method for objective measurements of perceived audio quality," in *Recommendation ITU-R BS.1387-1, Geneva, Switzerland*, 1998-2001.

[95] (1998-2001) Methods for objective measurement of perceived audio quality, recommendation itu-r bs.1387-1. [Online]. Available: http://www.itu.int/

[96] C. D. Creusere, R. Vanam, and K. Kallakuri, "A universal objective metric of human subjective audio quality," *IEEE Trans. Acoust. Speech and Signal Processing*, 2006.

[97] "Method for subjective assesment of intermediate quality levels of coding systems," *Recommendation IRU-R BS.1534-1,(Question ITU-R 220/10).*